Structural and biochemical characterization of marburgvirus VP35 and its role in immune evasion

by

Parameshwaran Ramanan

A thesis submitted to the graduate faculty

in partial fulfillment of the requirements for the degree of

DOCTOR OF PHILOSOPHY

Major: Biochemistry

Program of Study Committee:

Gaya K. Amarasinghe, Co-major Professor
Richard B. Honzatko, Co-major Professor
Michael Shogren-Knaak
Mark S. Hargrove
Drena L. Dobbs

Iowa State University

Ames, Iowa

2012

TABLE OF CONTENTS

LIST OF FIGURES

LIST OF TABLES

LIST OF ABBREVIATIONS

Activator protein-1	AP-1
Antigen presenting cell	APC
Baculovirus inhibitor of apoptosis protein repeat domain	BIR
C-type lectin receptor	CLR
Carbohydrate recognition domain	CRD
Caspase activation and recruitment domain	CARD
Central basic patch	CBP
DC-associated C-type lectin	DECTIN
DC-specific ICAM3-grabbing nonintegrin	DC-SIGN
Death domain	DD
Dendritic cell	DC
Double-stranded RNA	dsRNA
double-stranded RNA binding domain	dsRBD
dsRNA dependent protein kinase	PKR
Ebolavirus	EBOV
Endosomal sorting complex required for transport	ESCRT
First basic patch	FBP
Heteronuclear single quantum coherence	HSQC
Iκβ kinase	IKK
Immunoreceptor tyrosin-based activation motif	ITAM
In-vitro transcription	IVT
Interferon	IFN
Interferon inhibitory domain	IID

Interferon regulatory factor	IRF
Interferon stimulated gene	ISG
Interleukin-1 receptor associated kinase	IRAK
Isothermal titration calorimetry	ITC
Laboratory of genetics and physiology 2	LGP2
Leucine-rich repeat	LRR
Lipopolysaccharide	LPS
Macrophage mannose receptor	MMR
Macrophage-inducible C-type lectin	MINCLE
Marburgvirus	MARV
Melanoma differentiation associated gene 5	MDA5
Mitogen activated protein kinase	MAPK
Myeloid C-type lectin-like receptor	MICL
Natural killer cell	NKC
Neuronal apoptosis inhibitory protein	NAIP
Newcastle disease virus	NDV
NFκβ essential modulator	NEMO
NOD-like receptor	NLR
Nuclear factor kappa-light-chain-enhancer of activated B cells	NFκβ
Nuclear magnetic resonance	NMR
Nucleotide-binding and oligomerization domain	NOD
Pathogen associated molecular pattern	PAMP
Pattern recognition receptor	PRR
PKR activator	PACT
Pyrin domain	PYD

Respiratory syncytial virus	RSV
Reston *Ebolavirus*	REBOV
Retinoic acid induced gene-I	RIG-I
RIG-I like receptor	RLR
Selenomethionine	SeMet
Sendai virus	SeV
Signal transducer and activator of transcription	STAT
Spleen tyrosine kinase	SYK
T-cell immunoglobulin mucin domain-1	TIM-1
TAK-1 binding protein	TAB
TAR RNA-binding protein	TRBP
TIR domain-containing adaptor protein inducing IFN-β	TRIF
TIR-domain containing adapter protein	TIRAP
Toll-like receptor	TLR
Toll/Interleukin-1 receptor	TIR
TRAF family member-associated NFκβ activator binding kinase-1	TBK
Transforming growth factor beta activated kinase -1	TAK-1
TRIF-related adaptor molecule	TRAM
Untranslated region	UTR
Vesicular stomatitis virus	VSV
Zaire *Ebolavirus*	ZEBOV

ABSTRACT

Filoviruses are among the most deadly pathogens that cause acute disease in humans. *Ebolavirus* (EBOV) and *marburgvirus* (MARV) are the two members of this family, which have been documented to cause infrequent but severe outbreaks of hemorrhagic fever in humans. The severe pathogenesis and high lethality associated with filoviral infections, is in part, due to the suppression of host innate immune responses by virus-encoded proteins. Hence, structural and biochemical studies of filoviral proteins, to uncover the immune evasion mechanisms employed by filoviral proteins are an intense area of investigation. Previous studies on EBOV, have shown that one of the viral proteins called VP35 plays a key role in virus replication by functioning as a cofactor in the viral replication complex, and immune suppression by antagonizing the type I interferon (IFN) pathway. The C-terminal region of EBOV VP35 was implicated in dsRNA binding and IFN antagonism, although the mechanisms for immune evasion remained poorly defined. Recent work from our lab has resulted in crystal structures of Zaire *ebolavirus* (ZEBOV) and Reston *ebolavirus* (REBOV) VP35 C-terminal domain, and ZEBOV VP35 C-terminal domain bound to dsRNA. These studies gave new insights into the role of conserved basic residues in the C-terminal domain in both viral replication and immune evasion functions of VP35. These studies also established that mutation of residues mediating dsRNA binding also resulted in diminished IFN-inhibition using *in vivo* assays. In addition, the dsRNA bound structure suggested a potential mechanism by which EBOV VP35 hides viral dsRNA from detection by host RIG-I like receptors (RLRs). Studies addressing immune evasion mechanisms by *filoviruses* have predominantly been done on ZEBOV, and functions of MARV proteins are largely

uncharacterized and are inferred through homology to EBOV. Moreover recent reports on MARV proteins have shown that there are important differences in cell entry, host tropism, replication complex formation, and immune evasion mechanisms between the two viruses. The goal of my thesis work was to develop a comparative understanding of EBOV and MARV VP35, by characterizing MARV VP35 mediated immune evasion mechanisms using structural, biochemical, and cell biological studies. During the course of this study, we solved the crystal structure of MARV VP35 interferon inhibitory domain (IID) bound to dsRNA. This structure revealed several similarities with ZEBOV VP35 IID, but importantly there are several striking differences. Similar to ZEBOV, mutation of residues involved in dsRNA contacts in the MARV VP35 IID-dsRNA structure results in diminished dsRNA binding and IFN inhibition *in vivo*. While both MARV and ZEBOV VP35 IID bind to dsRNA in a sequence independent manner, MARV VP35 IID binds long(er) dsRNA compared to ZEBOV. We did not observe any interactions of MARV VP35 IID with the dsRNA blunt-ends, as in the case ZEBOV VP35. We biochemically validated these structural differences by *in vitro* dsRNA binding assays and show that MARV VP35 IID binds preferentially to longer dsRNA. Moreover MARV VP35 IID is insensitive to the presence of 5' or 3' overhangs in dsRNA, whereas ZEBOV VP35 IID binds preferentially to blunt-end dsRNA compared to overhang containing dsRNA. In this study, for the first time, using *in vitro* ATPase assays, we show that while both MARV and ZEBOV VP35 IID can inhibit RIG-I activation by overhang containing dsRNA, only ZEBOV VP35 IID can inhibit RIG-I activation by short blunt-end dsRNA. In addition we show that both MARV and ZEBOV VP35 IID can inhibit MDA5 activation by poly I:C, a long dsRNA mimic, mediated ATPase activation. The results from this study supports a model based on both structural and

biochemical data, in which MARV and ZEBOV VP35 IID inhibit host immune responses by sequestration of overlapping (double-strandedness) and distinct (blunt-ends) RNA PAMPs from being detected by host RIG-I like receptors. This work provides new insight into the structure and function of MARV VP35 IID, and advances our understanding of the structural basis for dsRNA binding by MARV VP35 IID and its role in IFN antagonism and immune evasion.

CHAPTER 1. HOST INNATE IMMUNITY

1.1 Introduction

The immune system allows host cells to combat constant challenges by pathogen invasion. Even single-celled prokaryotic organisms such as bacteria have a rudimentary immune system in the form of proteins and restriction enzymes that can fight bacteriophage infections (Bikard & Marraffini, 2012). Eukaryotic organisms including plants, invertebrates and vertebrate animals, have evolved extremely complex immune systems to survive and counteract infections by pathogens. In higher eukaryotes such as vertebrates, once the pathogens are able to cross the physical barriers such as the epithelial and mucosal layers of external organs, the immune systems kicks in and is able to detect the breach in defenses very quickly and efficiently in order to prevent infection and clear the pathogen. The immune system of higher eukaryotes has two components – innate and adaptive immunity. Innate immunity is a quick, inherent, broad response to a variety of pathogens and serves as the first line of defense for the host (Akira et al, 2006). Innate immunity is mediated though the production of variety of chemicals such as chemokines, cytokines and other proteins that can counteract the pathogen (Newton & Dixit, 2012). Host immune mechanisms, whether simple or complex have a fundamental purpose: to recognize self from non-self. The innate immune system consists of specialized proteins called pattern recognition receptors (PRRs), which act as surveillance mechanisms to detect pathogen infections by detecting unique molecular

signatures called pathogen associated molecular patterns (PAMPs) (Olive, 2012). There are different classes of PRRs, which detect components from a variety of pathogens such as bacterial cell wall components, carbohydrates like lipopolysaccharide, mannose, peptidoglycans, bacterial peptides, fungal glycans and viral genomes such as DNA and RNA (Takeuchi & Akira, 2010). This triggers an inflammatory response mediated through an intricate network of protein-protein interactions, which results in the production of interferons (IFNs) and other chemokines, cytokines involved in clearing the infection.

Adaptive or acquired immunity is mediated by the production of antibodies by T and B cells against specific antigens from pathogens presented to the immune system by specialized set of cells called antigen-presenting cells (APCs) such as dendritic cells (DCs) and macrophages (Bonilla & Oettgen, 2010). The adaptive immune response is highly tailored to respond to a specific pathogen. Acquired immunity also confers immunological memory to the host, allowing it to remember specific antigens and prevent future infections by mounting a strong, specific response to recurring infections. The activation of innate immunity is a required and necessary step for the activation of acquired immunity (Iwasaki & Medzhitov, 2010). Hence the two pathways are tightly coupled and regulated by host cells in order to modulate the overall response to infection by fine-tuning the signaling processes that leads to inflammation. This complexity has allowed host cells to detect and counteract a variety of different pathogens such as bacteria, fungi, viruses, and sometimes even endogenous stress signals from toxic chemicals that may be produced in the host. Pathogens interfere with these signaling processes, by hijacking one or more host components, resulting in attenuation or dysregulation of the immune response, leading to disease.

Pattern recognition receptors (PRRs) serve as the starting point for triggering host innate and adaptive immune responses through its ability to detect pathogens. Their varied cellular location and the ability to detect various types of molecular signatures, allow them to readily detect the presence of a broad range of pathogens and mobilize the innate immune cells. It is important to understand the mechanisms involved in PAMP recognition and signal transduction and how pathogens interfere with this process. This will allow us to develop strategies for better therapeutics, since PAMP recognition is a key early step in immune activation.

1.2 Pattern recognition receptors

Pattern recognition receptors (PRRs) are surveillance proteins, which detect pathogen associated molecular patterns (PAMPs) and initiate the innate immune responses (Takeuchi & Akira, 2010). The host cell is equipped to detect PAMPs at different stages of pathogen invasion and in different cellular compartments, since PRRs are expressed in many different cell types and both at the cell surface, cytosol and endosomal vesicles (Kumar et al, 2011). There are four major classes of PRRs, each detecting distinct molecular signatures from a variety of different pathogens – Toll-like receptors (TLRs), C-type lectin receptors (CLRs), NOD-like receptors (NLRs), and RIG-I like receptors (RLRs). The TLRs and CLRs help detect pathogens at the cell surface or in the endosome, whereas the NLRs and RLRs are cytoplasmic receptors (Takeuchi & Akira, 2010). All of these different PRRs trigger innate

and adaptive immune responses through an intricate network of distinct and overlapping pathways. There is also a significant level of crosstalk among these pathways, which serves to fine tune the immune response depending on the severity and the variety of pathogens that the host cell encounters (Crozat et al, 2009).

1.3 Toll-like receptor signaling

The TLRs are integral membrane proteins, which can be located either in the plasma membrane or the endosomal compartment. The TLRs recognize a variety of PAMPs such as single-stranded and double-stranded RNA and DNA. TLRs recognize their ligands through an ectodomain and transduce the signal through their cytoplasmic domains to downstream adapter proteins to initiate the production of chemokines and cytokines that help combat the infection (Figure 1-1). TLRs consist of a cytoplasmic Toll/Interleukin-1 receptor (TIR) domain and an extracellular receptor domain composed of 19-25 leucine-rich repeats (LRRs) (Gay & Gangloff, 2007) (Figure 1-2A). Of the different members of this family of proteins, TLR1, 2, 4, 5, 6 are expressed at the plasma membrane where they detect a broad range of PAMPs from bacteria, fungi and protozoans such as lipopolysaccharide (LPS), flagellin, peptidoglycans, unmethylated CpG, lipophosphoglycan (LPG) (Gay & Gangloff, 2007; Langefeld et al, 2009; Sorbara & Philpott, 2011). TLRs 3, 7, 8 and 9 are found in endosomal membranes and play critical roles in the context of recognizing viral infections by recognizing viral nucleic acids. Of these TLR3 is specific for viral double-stranded RNA (dsRNA)

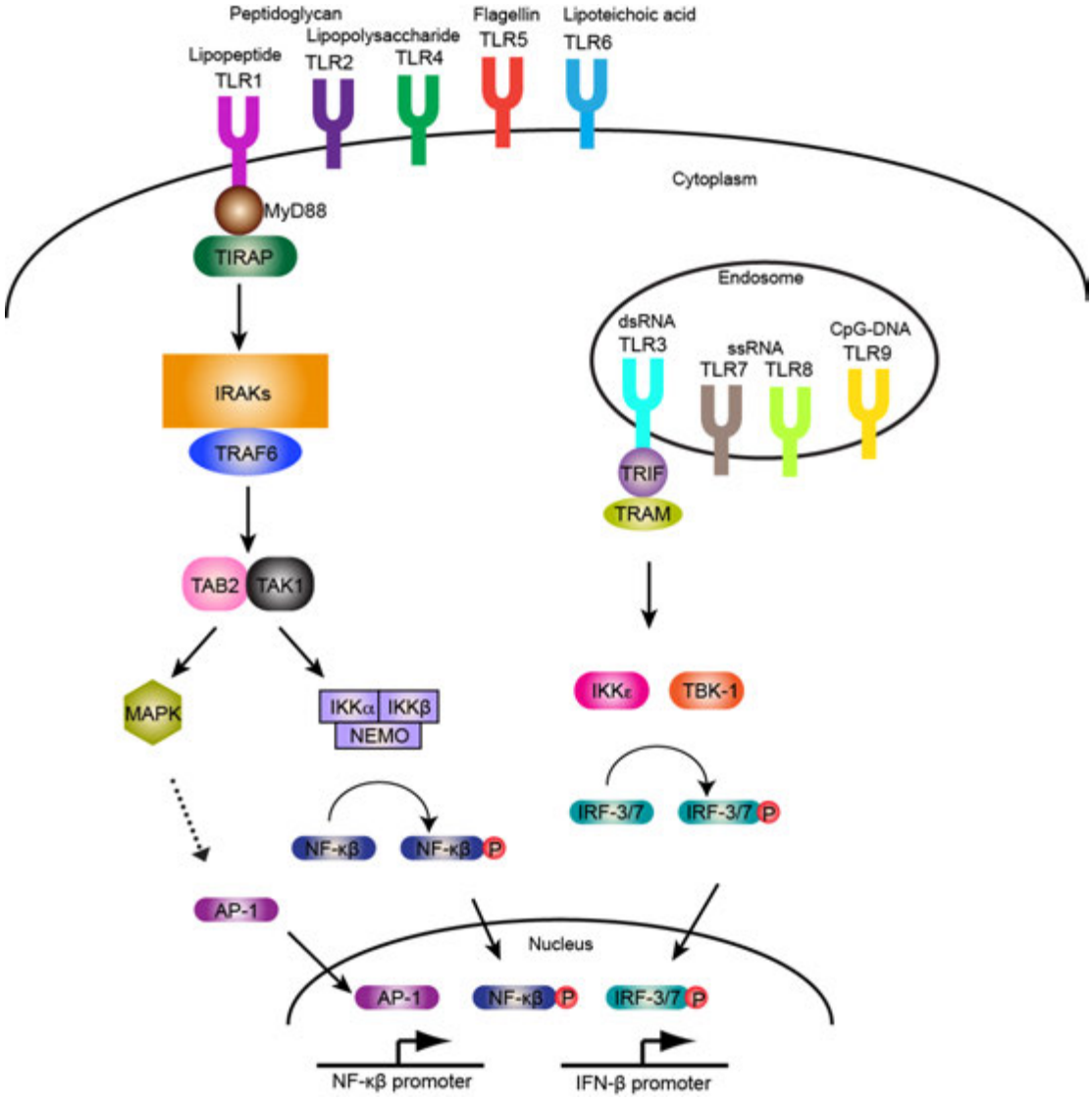

Figure 1-1. TLR mediated signaling.

TLRs are activated by a wide range of bacterial, fungal and viral PAMPs. Ligand induced dimerization of TLRs trigger signaling through MyD88-dependent and independent pathways to activate NF-κβ and IRF-3/7 transcription factors which turn transcription of genes under the control of NF-κβ and IFN-β promoters respectively. In addition TLRs can also activate the AP-1 transcription factor through the MAP kinase pathway.

and poly I: C, TLR7, 8 recognize viral single-stranded RNA (ssRNA), while TLR9 recognizes viral genomic DNA (Akira & Takeda, 2004; Barton & Medzhitov, 2003).

TLR3 is of specific importance in the detection of viral infections, since it recognizes dsRNA, a viral PAMP. Its localization at the endosomal membrane allows it to detect RNA genome containing virus, which is internalized into the cell through endocytosis. The ectodomain or receptor domain of TLRs including TLR3, contain a series of leucine-rich repeats with the consensus sequence XLXXLXLXXNXLXXLXXXXFXXLX, where X represents any amino acid (Bell et al, 2005). The length and post-translational modifications, most commonly N-linked glycosylation, of the LRRs differ among the different classes of TLRs. These LRR motifs enforce a distinct solenoid structure bent into a horseshoe shape with each LRR sequence making up one turn of the solenoid (Figure 1-2B) (Bell et al, 2006; Bell et al, 2005). The hydrophobic leucine residues all point inwards into the concave surface of this horseshoe structure forming a hydrophobic core. In most TLRs, ligand binding occurs through this concave surface of the ectodomain (Bell et al, 2005). Similar to other TLRs, the TLR3 ectodomain is highly glycosylated with atleast 15 proposed N-linked glycosylation sites (Botos et al, 2011; Sun et al, 2006). The residues that get glycosylated are distributed throughout the structure. The ectodomain also has specific motifs, which cap the N and the C-terminus called LRR-NT and LRR-CT respectively, the structures of which differ among the different TLRs (Bell et al, 2006; Botos et al, 2011). The crystal structure of TLR3 bound to 46bp dsRNA gave new insight into the nature of ligands that TLR3 binds and the conformation of the TLR3 dimer, which serves as the active signaling entity. Two molecules of TLR3 ectodomains bind to the 46bp dsRNA, to form an M-shaped structure, where the dsRNA binds near the N and the C-terminus of both molecules (Figure 1-2C). The two TLR3

molecules interact with each other through their respective LRR-CT regions (Gay & Gangloff, 2007; Liu et al, 2008; Kang & Lee, 2011). This explains why a minimum length of 45bp dsRNA is required to activate TLR3, because all of the above interactions are required to form the active signaling complex. The dsRNA interactions are only the phosphodiester backbone and hence it is a sequence independent mode of recognition. Of specific note are four histidine residues in TLR3, which bind to the phosphate groups of dsRNA, and regulate the pH dependent binding of TLR3 to dsRNA. TLR3 only interacts with dsRNA at the endosomal pH of near 6.5, since the imidazole rings of the histidine would be deprotonated at physiological pH (Liu et al, 2008). Upon ligand binding, the TLR ectodomain dimerization (Figure 1-2C) drives the cytoplasmic TIR domains of two TLR molecules to come into close contact with each other. The TIR domains are protein-protein interaction motifs containing the signature death domain (DD) fold (Figure 1-1D) (Barton & Medzhitov, 2003; Botos et al, 2009; Leonard et al, 2008).

This dimerization allows it to recruit adapter proteins such as myeloid differentiation primary-response protein 88 (MyD88) and TIR-domain containing adapter protein (TIRAP) (Figure 1-2) (Liu et al, 2008; Takada et al, 2007). MyD88 also contains a TIR domain and helps recruit other death domain fold containing members of the signaling complex through protein-protein interactions (Botos et al, 2009; de Bouteiller et al, 2005; Leonard et al, 2008). For example MyD88 is known to recruit the interleukin-1 receptor associated kinases (IRAKs) through protein-protein interactions mediated by

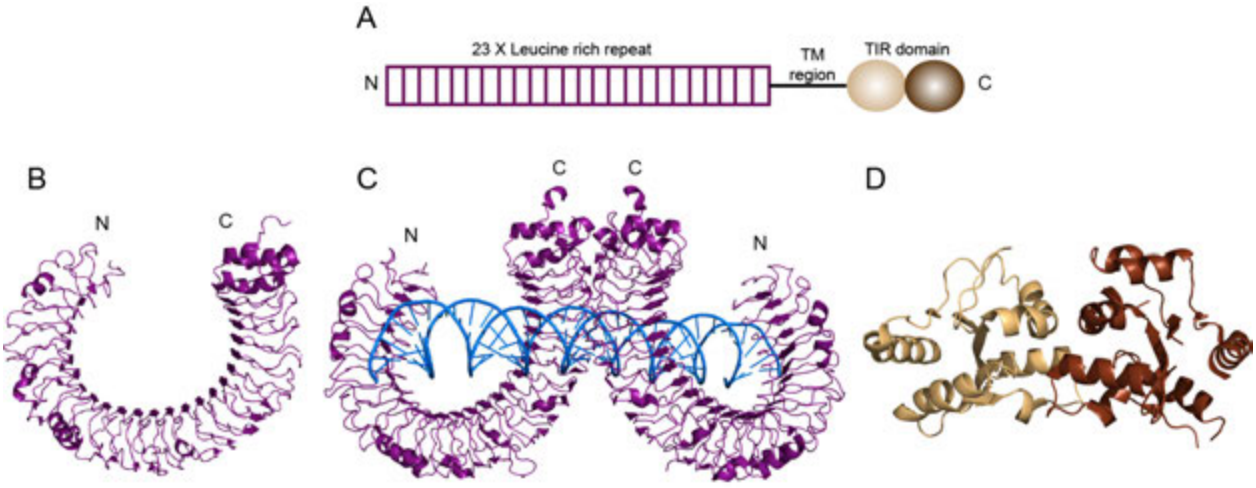

Figure 1-2. Structural basis for dsRNA recognition by TLR3.

(A) The domain organization of representative TLR member TLR-3. The extracellular receptor domain at the N-terminus region has a tandem LRR rich domain connected to the cytoplasmic signaling TIR domain through a transmembrane region. (B) Crystal structure of the receptor domain of TLR-3 (purple) shows the signature horseshoe shaped solenoid structure (PDB 3CIG) (Liu et al, 2008). (C) Crystal structure of TLR3 bound to dsRNA (blue) shows the ligand induced dimerization of the receptor domain (PDB 3CIY) (Liu et al, 2008). (D) The C-terminal TIR domain of TLR10 shows the canonical death domain fold containing two alpha helical subdomains (light and dark brown) (PDB IT3G) (Khan et al, 2004).

their death domains. Upon assembling the different IRAKs, they undergo autophosphorylation and trans-phosphorylation, which results in binding of and tumor necrosis factor receptor-associated factor 6 (TRAF6) to the IRAKs (Figure 1-2). The IRAKs-TRAF6 complex associates with another protein complex consisting of the transforming growth factor beta activated kinase (TAK1) and TAK1-binding proteins (TABs). The activated TAK1 complex phosphorylates both mitogen activated protein kinases (MAPK) and the IKK complex (Barton & Medzhitov, 2003; Jenkins & Mansell; Verstak et al, 2009). The phosphorylation of MAPK leads to activation of transcription factors such as activator protein-1 (AP-1). The TAK1 complex also phosphorylates and activates the IKK complex which is composed of three subunits – IKK-α, IKK-β and IKK-γ which is also called as NF-κβ essential (NEMO) (Figure 1-2). The function of this IKK complex is to regulate the transcription factor NF-κβ, which is a protein complex composed of homo or heterodimers of one of several proteins – REL-A, REL-B, REL, p50, p52 and p65 (Brasier, 2006; Gilmore, 1999). These dimers are held in an inactive conformation in the cytoplasm by the inhibitor of NF-κβ kinase (IκB). TAK1 activation of the IKK complex, leads to phosphorylation of IκB, which leads to its poly-ubiquitination and proteasomal degradation thus activating the NF-κβ dimer (Karin & Ben-Neriah, 2000). The activation of the transcription factors such as AP-1 and NF-κβ result not only in the production of the type I IFNs such as IFN-β, which is a key component of the innate immune response, but also serves as a necessary step for the activation of the adaptive immune response by producing chemokines (such as IL-6, IL-1β and IL-12), chemokine receptors, cell-adhesion molecules and other co-stimulatory molecules (Iwasaki & Medzhitov, 2004). In addition to the MyD88/TIRAP dependent

signaling and activation of NF-κβ, some members of the TLRs such as TLR3 and 4, activate the transcription factors called interferon regulatory factors (IRF) 3 and 7, which stimulate IFN-β production. This is mediated by another pathway, which is dependent on recruitment of another set of adaptor proteins called TIR domain-containing adaptor protein inducing IFN-β (TRIF) and TRIF-related adaptor molecule (TRAM) (Akira & Takeda, 2004; Kawai & Akira, 2010). These two adapter proteins result in the autophosphorylation and activation of the IFN kinases IKK-ε and TRAF family member associated NF-κβ activator (TANK)-binding kinase-1 (TBK-1) (Kawai & Akira, 2007). These kinases then phosphorylate and activate IRF-3 and IRF-7, which dimerize and localize to the nucleus where they turn on the transcription of type I interferons (Figure 1-1). Thus TLR mediated signaling can activate the production of cytokines, chemokines (such as IL-6, IL-1β and IL-12), chemokine receptors through multiple pathways and serves not only to trigger the innate immune response but also acts as a necessary precursor for the activation of the adaptive immune response.

1.4 C-type lectin receptor signaling

The CLRs are a class of membrane bound PRRs which recognize carbohydrate motifs in various pathogens. These proteins contain a conserved carbohydrate recognition domain (CRD) through which it detects various ligands in a calcium-dependent manner (Geijtenbeek & Gringhuis, 2009; Hollmig et al, 2009). CLRs are expressed in a variety of cells including macrophages, natural killer (NK) cells and dendritic cells (DCs) (McGreal et al, 2005), which are antigen-presenting cells and play a critical role in modulating the adaptive immune response by activating multiple signaling cascades in a carbohydrate-specific manner

(Geijtenbeek & Gringhuis, 2009). CLRs recognize a wide variety of PAMPs such as mannose, fucose, N-acetyl glucosamine, and β-glucans (Weis et al, 1998). In addition CLRs also regulate migration, adhesion and antigen uptake and presentation in DCs (Figdor et al, 2002). Structural studies on DC-SIGN and mannose receptors have given insights into the specificity and mechanism of ligand recognition by the carbohydrate recognition domains of these proteins (Feinberg et al, 2000; Feinberg et al, 2009). The CRDs of both DC-SIGN and mannose receptors adopt the typical C-type lectin fold (Figure 1-3A). In the case of DC-SIGN, both the terminal N-acetyl glucosamine and an internal mannose residue of the oligosaccharide interacts both directly and through the calcium ion via hydrogen bonds and hydrophobic interactions (Figure 1-3A). The CRD of mannose receptor has a similar fold to DC-SIGN but binds only to the terminal N-acetyl glucosamine moiety of the oligosaccharide, while the rest of the ligand points away from the protein (Figure 1-3B).

CLRs can be divided into two major types – group I and group II. The group I CLRs contain multiple carbohydrate recognition domains (CRDs) (Figure 1-3B) in the N-terminus, whereas the group II members contain a single CRD in the C-terminus (Weis et al, 1998). The macrophage mannose receptor (MMR), DEC-205 and related family of proteins belong to the group I CLRs. The asialoglycoprotein receptor family of proteins which include DC-associated C-type lectin-1, 2 (DECTIN-1, 2), macrophage-inducible C-type lectin (MINCLE), dendritic cell-specific ICAM3-grabbing nonintegrin (DC-SIGN), DC immunoreceptor (DCIR), myeloid C-type lectin-like receptor (MICL) and

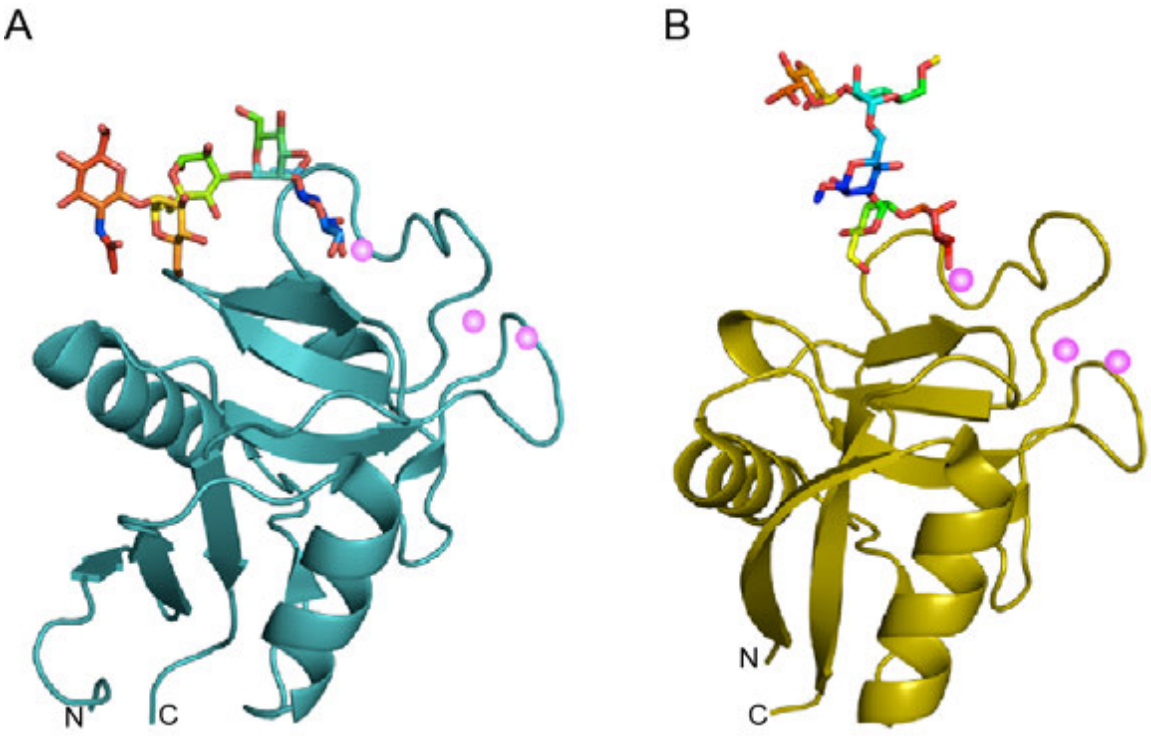

Figure 1-3. Structural basis for carbohydrate recognition by CLRs.

(A) The carbohydrate recognition domain (CRD) of DC-SIGN receptor (cartoon representation) bound to a pentasaccharide (stick representation) (PDB 1K9J) (Feinberg et al, 2001). Magenta spheres represent the three calcium ions bound to the protein. (B) CRD of rat mannose receptor (cartoon representation) (2IT5) bound to high mannose oligosaccharide (stick representation) (Feinberg et al, 2000). Magenta spheres represent the three calcium ions bound to the protein.

DC NK lectin group receptor-1 (DNGR-1) belong to group II (Brown et al, 2007; Hollmig et al, 2009). Recent studies have shown that there are two major pathways that the CLR mediated signaling triggers host immune responses. CLRs such as DC-SIGN, DCIR and MICL mediate signaling by phosphorylation and activation of the Ser/Thr kinase called RAF1 (Figure 1-4) (Gringhuis et al, 2009; Gringhuis et al, 2007). RAF1 subsequently phosphorylates the p65 subunit of the NF-κβ complex, which results in activation and nuclear retention of the complex. The alternate pathway involving the DECTIN-1, 2 and MINCLE receptors involves interactions with immunoreceptor tyrosin-based activation motif (ITAM) containing adaptor molecules such as Fc receptor γ-chain (FcRγ) (Kerrigan & Brown). This activates the spleen tyrosine kinase (SYK), which mediates NF-κβ and AP-1 activation by targeting multiple downstream effector proteins (Figure 1-4) (Gringhuis et al, 2009; Gringhuis et al, 2007; Kerrigan & Brown; Kingeter & Lin). In addition there is cross-talk between the SYK and the RAF1 pathways to negatively regulate TLR mediated signaling to modulate NF-κβ activation in response to extracellular cues (Geijtenbeek & Gringhuis, 2009; Hollmig et al, 2009). Taken together, all of these data suggest that CLRs play a very important role in the functioning of the immune system, especially due to their expression on the surface of antigen presenting cells such as dendritic cells. Although the exact signaling mechanisms triggered by CLR ligand recognition is unclear, it is becoming increasingly apparent that it likely involves networking with the other innate immune receptors, especially TLRs.

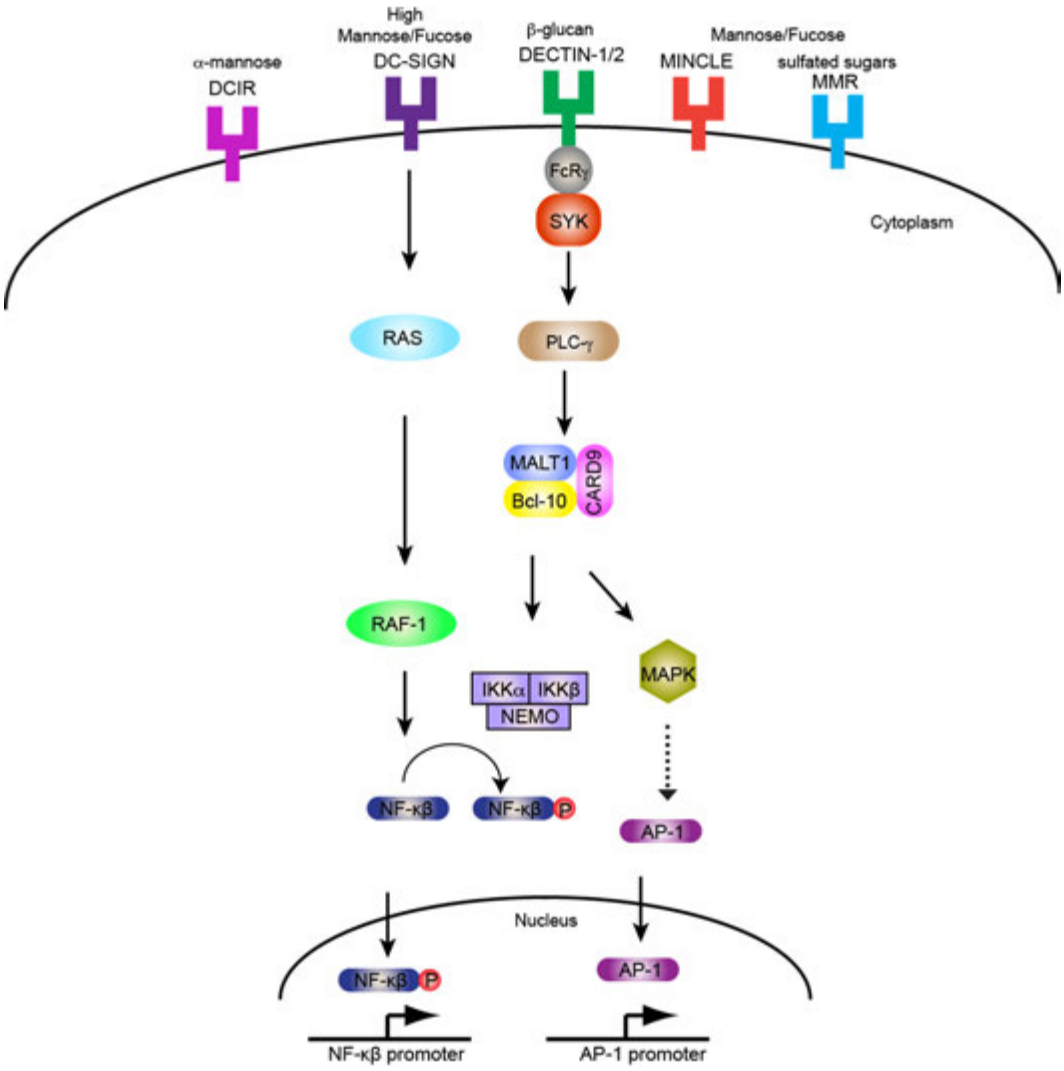

Figure 1-4. CLR mediated signaling.

CLRs are activated by a broad range of bacterial and fungal carbohydrate PAMPs. Ligand induced dimerization of TLRs trigger signaling through two independent pathways, one mediated through RAF-1 kinase and the other through the SYK kinase. These pathways lead to the activation of activate NF-κβ and AP-1 transcription factors resulting in inflammatory response.

1.5 NOD-like receptor signaling

The nucleotide-binding oligomerization domain (NOD)-like receptors are cytoplasmic proteins, which detect a broad range of microbial PAMPs including peptidoglycans from bacterial cell wall and viral PAMPs such as RNA (Franchi et al, 2006). The common feature among the different NLRs is the tripartite domain organization. They are classified into different types based on the different N-terminal effector domains such as caspase activation and recruitment domain (CARD), Pyrin domain (PYD) or baculovirus inhibitor repeat (BIR) domain (Franchi et al, 2006; Sirard et al, 2007). All NLRs share a central nucleotide-binding and oligomerization domain and a C-terminal receptor domain characterized by leucine-rich repeats (LRRs). The NLRs are in an autoinhibited conformation in which the receptor domain interacts with the NOD domain and upon recognition of PAMPs by the LRR, the NLRs undergo conformational changes resulting in oligomerization and downstream signaling mediated by the NOD domain (Langefeld et al, 2009; Proell et al, 2008). Recent structural work on NLRX1, a family member of NLRs present in the mitochondria has resulted in the crystal structure of the C-terminal ligand-binding domain (Hong et al, 2012) (Figure 1-5). The C-terminal domain of NLRX1 shows the typical arrangement of the tandem LRRs arranged in a curved, crescent shape with the concave hydrophobic core pointing inwards (Figure 1-5A). There are 8 LRR sequences in NLRX1 and they are capped at the N- and the C-terminus by alpha-helical LRR-NT and LRR-CT motifs (Hong et al, 2012; Moore et al, 2008; Ye & Ting, 2008). The crystal structure shows that this domain of the protein forms a dimer through extensive interactions between the LRR-CT motifs (Figure 1-5A). Positively charged patches identified via the structure and

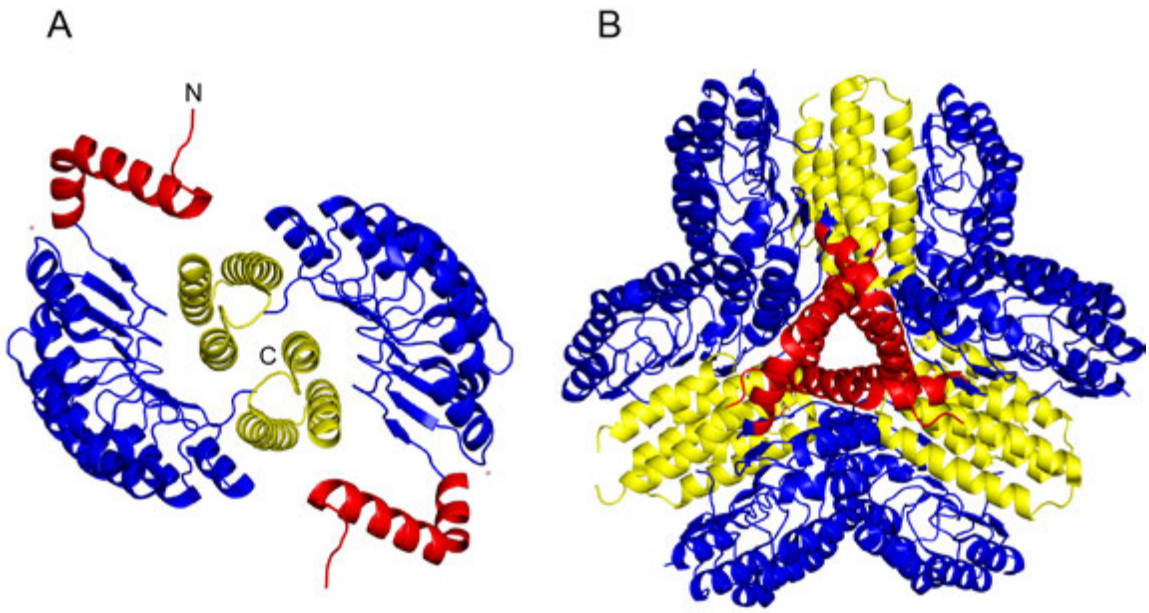

Figure 1-5. Structure of the ligand binding domain of NOD-like receptor.

(A) Cartoon representation of the C-terminal ligand binding domain of NLRX1 shows the three typical regions – the LRR-NT cap region (red), the LRR region (blue) containing eight tandem LRR motifs, and the LRR-CT region (yellow) (PDB 3UN9) (Hong et al, 2012). The dimerization of the ligand-binding domain is mediated through the LRR-CT region. (B) The hexameric ring-like arrangement of the ligand-binding domain of NLRX1 as a result of the trimerization mediated by the LRR-NT region (red) (PDB 3UN9) (Hong et al, 2012).

mutational analysis has been shown to be important for NLRX1 binding to single-stranded and double-stranded RNA (Hong et al, 2012). Also the NLRX1 C-terminal domain dimer trimerizes through the LRR-NT, resulting in a hexameric ring-like arrangement, that lends support to the hypothesis that upon ligand binding, NLRX1 may assemble into a ring-like structure and helps to recruit downstream effector proteins (Figure 1-5B).

Upon ligand binding, the CARD domains of NLRs interacts with downstream CARD containing Ser/Thr kinase receptor-interacting kinase 2 (RIP2) (Figure 1-6) (Kufer, 2008; Langefeld et al, 2009; Shaw et al). Activation of RIP2, results in phosphorylation and activation of the IKK complex, which in turn activates NF-κβ by phosphorylating and targeting Iκβ for degradation (Brasier, 2006; Gilmore, 1999; Kufer, 2008). In addition RIP2 also activates the MAPK pathway resulting in the activation of AP-1. The PYD containing NLRs are called NALPs and they detect a variety of bacterial components including flagellin (Proell et al, 2008).

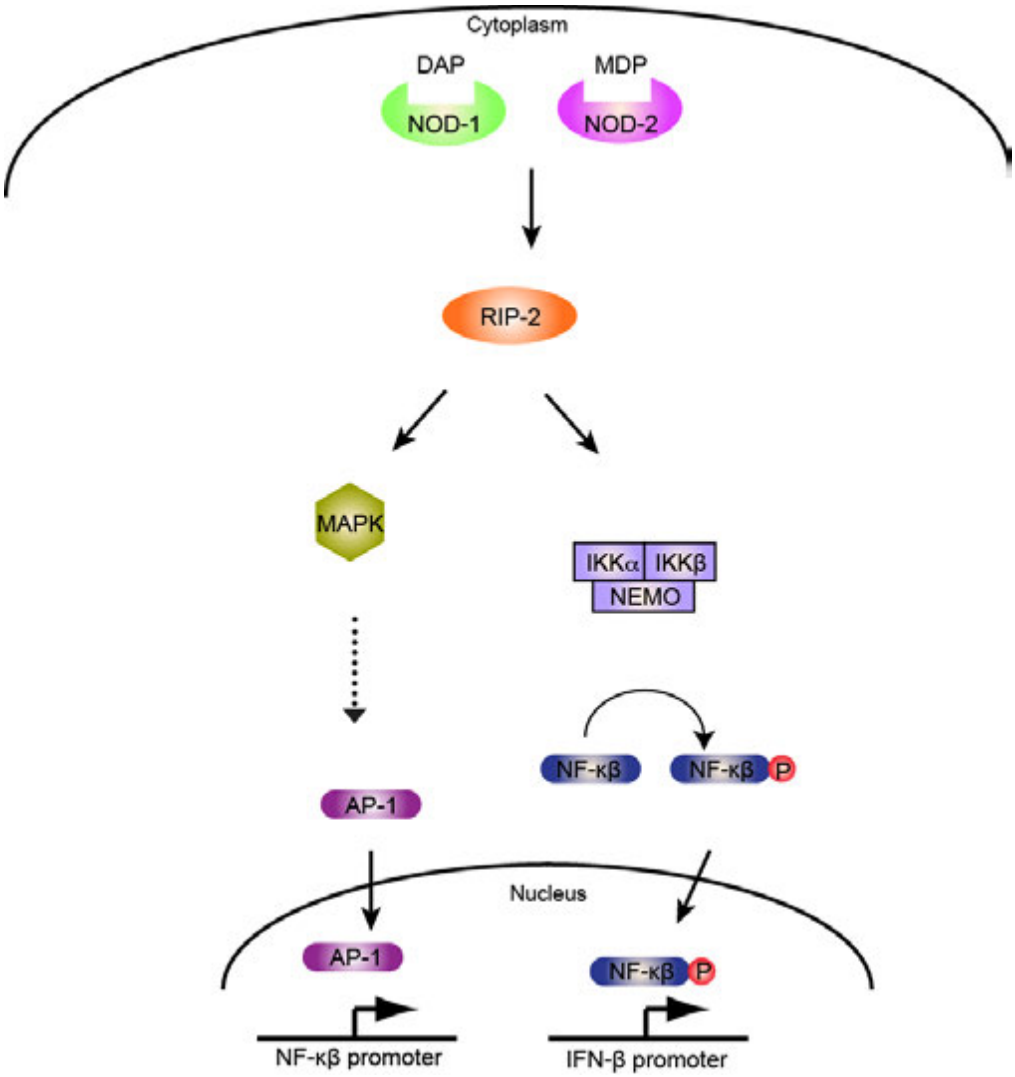

Figure 1-6. NLR mediated signaling.

NLRs are cytoplasmic PRRs activated by bacterial PAMPs such as DAP and MDP. Ligand binding leads to activation of NLRs which signal through the adaptor protein RIP-2 to activate both the IKK complex and MAPK pathways to trigger nuclear translocation of AP-1 and NF-κβ transcription factors.

Upon detection, they undergo conformational change and oligomerization and recruit the downstream adapter protein called ASC, which has a PYD and CARD. The NALPs interact with ASC through a PYD-PYD interaction, while a CARD-CARD interaction helps recruit and activate Caspase 1. Assembly of this multi-protein complex called the inflammasome leads to the recruitment of several Caspase 1 molecules and leads to proteolytic processing and maturation of IL-1β and IL-18 (Shaw et al; Williams et al). These cytokines are then secreted to induce the type II interferons and NK cell activation. The BIR domain containing NLRs are called neuronal apoptosis inhibitory proteins (NAIPs) and also assemble inflammasomes leading to Caspase 1 recruitment and activation upon ligand binding. Thus NLR activation leads to signaling cascades, which link the innate and the adaptive immune responses (Shaw et al; Williams et al).

1.6 RIG-I-like receptor signaling

The retinoic acid-inducible gene I (RIG-I)-like receptor family of proteins are cytoplasmic PRRs, which play a key role in host antiviral responses by detecting viral PAMPs, especially viral dsRNA (Fairman-Williams et al, 2010). The RLRs have three members RIG-I, melanoma differentiation associated gene 5 (MDA5) and laboratory of genetics and physiology 2 (LGP2). RIG-I and MDA5 contain two tandem N-terminal caspase activation and recruitment domains (CARDs), which are protein-protein interaction motifs and are essential for signaling (Leung et al, 2012; Loo & Gale, 2011). It has been shown that over-expression of the CARD domains of RIG-I serves as a constitutive activator of type I

IFN, suggesting that the CARD domains are required and sufficient for downstream signaling (Binder et al, 2011; Loo & Gale, 2011). LGP2 lacks the CARD domains and cannot take part in signaling; hence may play a role in negative regulation of RIG-I and MDA5 (Rothenfusser et al, 2005; Yoneyama et al, 2005). All three proteins consist of a central tripartite DEX/DH domain called helicase domains 1 and 2 (Hel1 and 2) and a helicase insertion domain (Heli) in addition to a C-terminal RNA binding domain (RBD). RIG-I and MDA5 are known to be activated by distinct and overlapping RNA ligands (Kato et al, 2006; Loo et al, 2008; Yoneyama et al, 2005). RIG-I has been shown to be activated by RNA containing a 5-triphosphate cap and short double-stranded regions whereas MDA5 has been linked to the recognition of longer dsRNA and its synthetic analogue poly I:C (Leung & Amarasinghe, 2012; Leung et al, 2012; Lu et al, 2010; Yoneyama et al, 2004). Correspondingly some viruses trigger RIG-I or MDA5 selectively and some viruses trigger both. For example, members of the single-stranded negative sense RNA genome viruses such as rabies virus, vesicular stomatitis virus (VSV), Sendai virus (SeV), influenza virus, Newcastle disease virus (NDV), respiratory syncytial virus (RSV) have been shown to selectively trigger RIG-I mediated immune responses. On the other hand, long dsRNA genome containing viruses such as picornaviruses trigger MDA5 mediated responses (Loo et al, 2008; Yoneyama et al, 2005). Recent structural and functional studies on RIG-I have resulted in a model for the mechanism of activation by dsRNA (Jiang et al, 2011; Kageyama et al, 2011; Kowalinski et al, 2011; Lu et al, 2010; Luo et al, 2011). Crystal structures of full length RIG-I in the absence of dsRNA suggests that the helicase insert domain is engaged in intramolecular protein-protein interactions with the CARD domains keeping RIG-I in a closed, autoinhibited conformation by masking the CARD domains (Figure 1-7A). RIG-I

dsRNA complex structures show that upon dsRNA binding, RIG-I undergoes a conformation change, in which the helicase and the C-terminal domains are engaged in protein-RNA

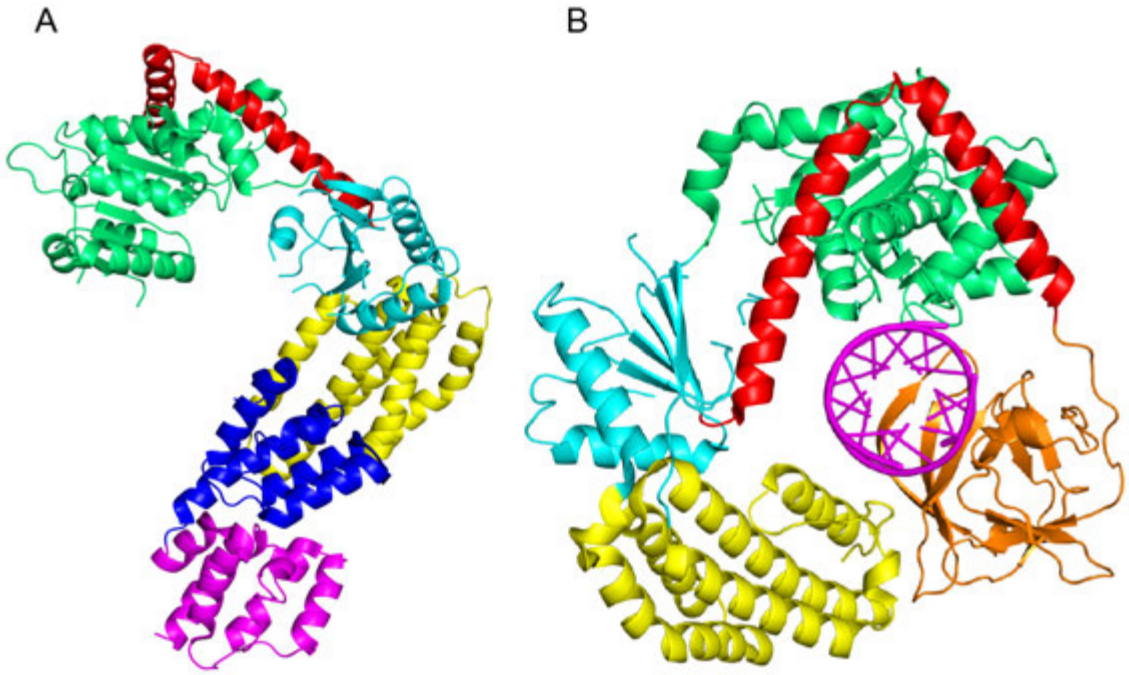

Figure 1-7. Structure of autoinhibited and dsRNA-bound RIG-I.

(A) Cartoon representation of the autoinhibited conformation of full-length duck RIG-I showing the first N-terminal CARD domain (magenta), second CARD domain (blue), helicase insert domain (yellow), helicase-2 domain (cyan), regulatory pincer domain (red) and helicase-1 domain (green) (PDB 4A2W) (Kowalinski et al, 2011). (B) Cartoon representation of RIG-I-dsRNA complex structure showing the helicase domains (same coloring scheme as figure A) and the C-terminal RNA binding domain (orange) bound to dsRNA (magenta) (PDB 2YKG) (Luo et al, 2011)

contacts and the N-terminal CARD domains are free to interact with downstream CARD containing proteins like IPS-1 (Figure 1-7B) (Cui et al, 2008; Kowalinski et al, 2011; Leung & Amarasinghe, 2012; Luo et al, 2011; Weis et al, 1998; Yoneyama & Fujita, 2009). Thus the C-terminal and the helicase domains act as regulatory elements of RIG-I and MDA5 by keeping the CARD domains masked until ligand recognition occurs. In addition crystal structures of the RD of RIG-I in complex with dsRNA has shown that this domain is responsible for the recognition of the 5'-triphosphate cap of dsRNA through a network of hydrogen bonds and base-stacking interactions mediated by conserved hydrophobic and basic residues, although it can also bind to blunt end dsRNA (Gringhuis et al, 2009; Li et al, 2009; Lu et al, 2011; Lu et al, 2010). A number of recent studies have also studied the implications of MDA5 interactions with long dsRNA and poly I:C. These studies suggest that the CARD domains in RIG-I and MDA5 may be arranged differently in the context of the full-length protein, suggesting that their activation mechanisms will likely be different as well (Berke & Modis, 2012; Peisley et al, 2011). Electron microscopic (EM) analysis of MDA5 suggest that it tends to form long filamentous structures upon addition of long dsRNA, and the formation of such structures is mediated by cooperative binding of dsRNA (Berke & Modis, 2012; Peisley et al, 2011). However, the exact nature of the physiological RNA ligands and the structural basis for the differences in ligand recognition and its role in activation of RIG-I and MDA5 is still unclear.

Although the activation mechanisms of RIG-I and MDA5 may be different they share a common downstream signal transduction pathway. Upon activation, the CARD domains of

RIG-I and MDA5 interact with the CARD domain of the downstream adapter protein IPS-1 (Figure 1-8). IPS-1 contains a proline-rich region and a transmembrane domain, which keeps it anchored to the outer mitochondrial membrane (Broquet et al, 2011; Seth et al, 2005). Although it has been shown that IPS-1 anchoring to the mitochondrial membrane is absolutely essential for type I IFN signaling, the functional importance for this is still not understood. The proline-rich region is involved in recruiting a number of signaling molecules such as TRIF, TRAM, MyD88 and RIP1. Hence the signals transmitted through the TLRs and RLRs converge at this point and through conserved signaling mechanisms activate the transcription factors such as NF-κβ, IRF-3 and IRF-7 resulting in the production of inflammatory chemokines and cytokines (Crozat et al, 2009; Gack et al, 2007; Hausmann et al, 2008; Leung & Amarasinghe, 2012; Loo & Gale, 2011; Ramos & Gale, 2011) (Figure 1-8).

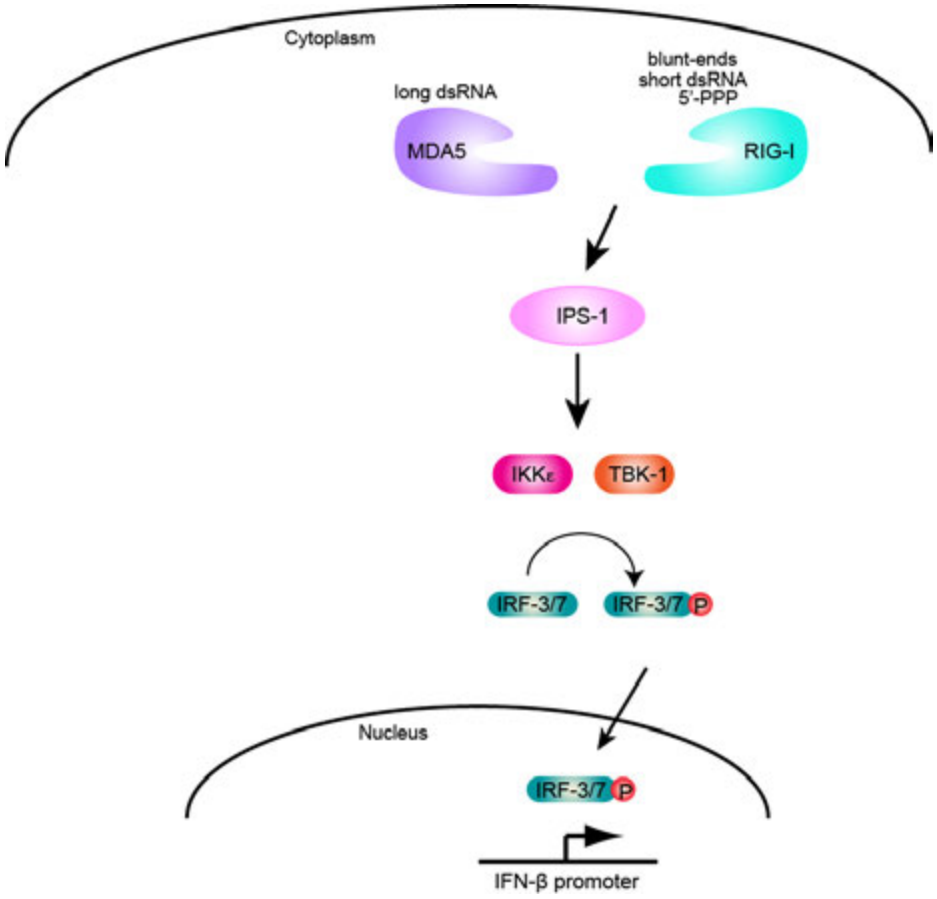

Figure 1-8. RLR mediated signaling.

RLRs are activated by short and long viral dsRNA ligands. Ligand induced conformational change of RLRs trigger signaling via the mitochondrial adapter protein IPS-1. IPS-1 activates the IFN kinases, which lead to activation of the IRF-3/7 transcription factors and production of type I IFN.

1.7 Type I IFN signaling pathway

Interferons are ubiquitously expressed cytokines that play a critical role in mediating innate immune responses, especially against viral infections. There are two major types of interferons, type I (includes IFN-α and β among others) and type II (IFN-γ). All type I IFNs bind to the cell surface receptor called type I IFN receptor, which consists of two subunits called IFNAR1 and 2. IFN-γ binds to the type II IFN receptor, which is also made of two subunits called IFNGR1 and 2 (de Weerd & Nguyen, 2012; Uze et al, 2007). These receptors are associated to intracellular non-receptor tyrosine kinases, which belong to the Janus kinase (JAK) family (Figure 1-9). IFNAR1 interacts with TYK2 and IFNAR2 interacts with JAK1 (Bonjardim et al, 2009; Onomoto et al, 2010). Upon ligand binding induced dimerization of the IFNAR receptor, the JAK1 and TYK2 kinases are activated through autophosphorylation. This triggers the canonical JAK-STAT pathway, in which the JAK1 and TYK2 phosphorylate and activate transcription factors called signal transducer and activation of transcription (STATs) (Monie et al, 2009; Zuniga et al, 2007). The STATs activated by type I IFNs include STAT1, 2, 3 and 5. Upon phosphorylation and activation, the STAT proteins form homodimers and different heterodimers and translocate to the nucleus. These STAT complexes then associate with another transcription factor called interferon regulatory factor 9 (IRF9), to form the mature ISGF3 complex, which binds to the specific promoter sequences called IFN-stimulated response elements (ISRE) and triggers the production of IFN stimulate genes (ISGs) (Figure 1-9) (Bonjardim et al, 2009).

The IFNGR1 and 2 are associated with JAK1 and JAK2 kinases respectively, and upon IFN-γ binding, these kinases trigger the phosphorylation and activation of predominantly STAT1 proteins, which form homodimers. The STAT1-STAT1 homodimer, then relocates to the nucleus where it binds to another specific promoter sequence called IFN-γ activated site (GAS) (van Boxel-Dezaire & Stark, 2007). While type I IFNs can also stimulate the induction of both ISRE and GAS regulated genes, IFN-γ is specific to the GAS element. Together the type I and II IFNs induce the production of a number of antiviral genes, that are important for mediating not only the innate immune response, but also upregulate many proteins that are necessary components of the adaptive immune response. Similar to the signaling pathways mediated by the various PRRs, there is considerable crosstalk between the type I and II IFN signaling pathways, the implications of which are not completely understood (Bonjardim et al, 2009; Crozat et al, 2009; Zuniga et al, 2007).

1.8 Viral inhibitors of innate immune responses

Viruses encode proteins that antagonize and attenuate the host innate immune responses by a variety of different mechanisms. RNA viruses in particular encode for proteins that target TLR3, RIG-I and MDA5 and their downstream signaling components, since these are the host receptors that recognizes viral RNA PAMPs. These viral proteins can be broadly classified into two types – inhibitors of type I IFN production and inhibitors of type I IFN responses. Inhibition of type I IFN production is a common mechanism adopted

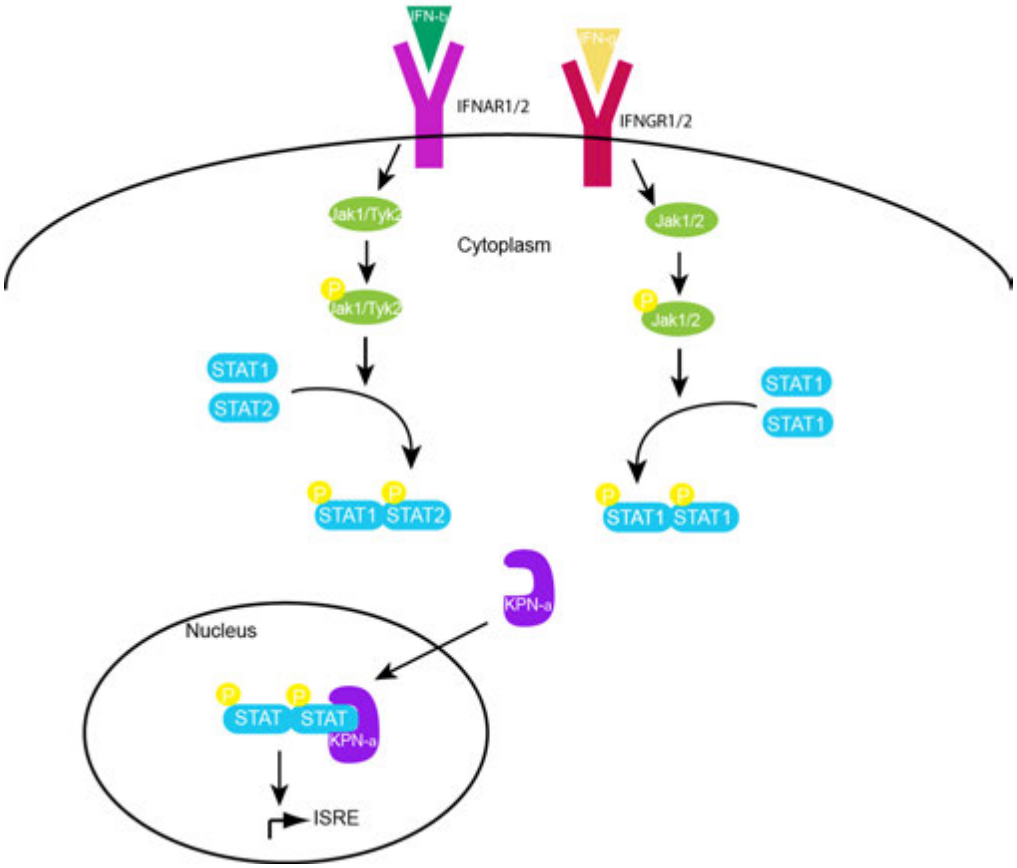

Figure 1-9. IFN mediated signaling.

Type I and II IFNs are recognized by cell surface receptors called IFNAR1/2 and IFNGR1/2 respectively, which activate the JAK-STAT pathways mediated by the Jak1/2 and Tyk2 kinases. This results in phosphorylation of the STAT transcription factors which turn on the transcription of ISGs.

by many different families of viruses. In the case of picornaviruses, type I IFN production is inhibited by the targeted proteolysis of MDA5 (Barral et al, 2007). The cleavage of MDA5 is not carried out by virus-encoded proteases such as 2Apro or 3Cpro, instead viral infection targets MDA5 to be degraded by caspases and the proteasomal pathway (Barral et al, 2007). RIG-I is also degraded in cells infected with poliovirus, rhinoviruses, echovirus, and encephalomyocarditis virus. In contrast to MDA-5, cleavage of RIG-I is not accomplished by cellular caspases or the proteasome. Rather, the viral proteinase 3C(pro) cleaves RIG-I, both in vitro and in cells (Barral et al, 2009). It has also been shown that in the case of paramyxoviruses such as measles, mumps, simian virus 5, Newcastle disease virus, Sendai virus, and human parainfluenza viruses, the highly conserved cysteine-rich C-terminal domain of the V proteins is involved in directly binding to MDA5 (Andrejeva et al, 2004). Using reporter gene assays, it has been shown that MDA5 overexpression stimulates both IRF-3 and NF-κβ transcription factors and that paramyxovirus V protein can block the MDA5 mediated activation of both these transcription factors (Andrejeva et al, 2004). In the case of human respiratory syncytial virus (RSV), NS2 directly binds to the N-terminal CARD domains of RIG-I, thus preventing the downstream effectors such as IPS-1 from interacting with the RIG-I CARDs (Ling et al, 2009). As a result, NS1 or NS2 deleted RSVs induce more IFN production than wild-type RSV in infected cells (Bossert et al, 2003; Jin et al, 2000). NS2 expression inhibits IFN transcription induced by both the RIG-I and TLR3 pathways (Ling et al, 2009). NS2 is thus able to antagonize both type I IFN production by direct inhibition of RIG-I and and type I IFN signaling by targeting STAT1 for degradation. The arenavirus Z protein directly interacts with RIG-I and prevents its association with the mitochondria-associated IPS-1 adapter protein (Fan et al, 2010). The expression of

arenavirus Z proteins also attenuates the activation of transcription factors NF-κβ and IRF-3 in infected cells (Fan et al, 2010). TRIM25 is a host protein with ubiquitin ligase activity, which mediates Lysine 63 linked ubiquitination of the N-terminal CARD domains of the RIG-I like receptor proteins (Gack et al, 2007). This ubiquitination activity is necessary for RIG-I mediated signal transduction and downstream IFN production. The NS1 protein from influenza virus inhibits the TRIM25 mediated ubiquitination of RIG-I, thus antagonizing IFN production (Gack et al, 2009). The aspartate residues 96 and 97 in NS1 interact with the coiled-coiled motif in the TRIM25 protein and prevent its oligomerization (Donelan et al, 2003). This is an example of an indirect mechanism by which viruses are able to inhibit RIG-I mediated signaling and IFN production. Another example is the Hepatitis C virus, which evades the innate immune responses by encoding for a protease NS3/4A, which cleaves the mitochondrial associated adapter proteins IPS-1. This cleavage of IPS-1 happens at residue 508, which is a cysteine, resulting in the removal of the N-terminal fragment of IPS-1 from the outer mitochondrial membrane (Li et al, 2005). NS3/4A binds to and co-localizes with MAVS in the mitochondrial membrane, and has been shown to cleave IPS-1 using *in vitro* experiments. This results in loss signaling through both the TLR3 and RIG-I like receptors both of which signal through the adapter protein IPS-1. Recent studies have suggested that filoviruses such as the Zaire *ebolavirus* (ZEBOV) can inhibit IFN production through its VP35 protein using multiple mechanisms which inhibit RIG-I recognition of viral RNA PAMPs and IRF-3/7 phosphorylation by the IFN kinases IKK-ε and TBK-1 (Basler et al, 2003; Basler et al, 2000; Hartman et al, 2004; Leung et al, 2009; Leung et al, 2010; Prins et al, 2009). Since the activation of NF-κβ is an important step in the innate immune response many viruses encode for proteins, which consist of ankyrin repeats in order to inhibit NF-κβ,

by targeting the regulatory protein NEMO (Wyler et al, 2007). Microplitis demolitor bracovirus encodes for protein, which is a molecular mimic of Iκβ and perform a similar functional role by binding to NF-κβ, preventing its phosphorylation and activation and retains it in the cytoplasm (Bitra et al, 2012). A238L protein from African swine fever virus also directly interacts with NF-κβ and prevents its nuclear transport (Silk et al, 2007). The Vaccinia virus N1 protein inhibits NF-κβ by inhibiting the IκB degradation, thus keeping NF-κβ in an inactive state (Maluquer de Motes et al, 2011).

The second class of viral proteins targets the components of the JAK-STAT pathway, which is activated upon binding of the secreted type I and type II IFNs to their respective cell-surface receptors, and phosphorylation of the receptor associated Janus family kinases. The STAT transcription factors are common factors, which result in establishment of antiviral state induced by both type I and II interferons. Many viruses encode proteins that inhibit IFN mediated signaling by interfering with STAT proteins. For example, both NS1 and NS2 proteins from respiratory syncytial virus have been shown to block IFN signaling by causing the proteasomal degradation of STAT2 (Lo et al, 2005). The simian virus V protein inhibits interferon signaling by targeting STAT1 for proteasomal degradation (Didcock et al, 1999). The Nipah virus V protein directly binds to STAT1 and STAT2 proteins to form high molecular-weight complexes that retain STAT proteins in the cytoplasm and prevents its translocation to the nucleus (Rodriguez et al, 2002). Vaccinia virus encodes for the CH1 protein, which has phosphatase activity, and this proteins binds to STAT proteins, dephosphorylates it and reverses its activation by the Janus kinases, thus inhibiting IFN mediated signaling in infected cells (Najarro et al, 2001). Recent studies have demonstrated

that filoviral proteins ZEBOV VP24 and MARV VP40 inhibit JAK-STAT signaling through distinct mechanisms. ZEBOV VP24 prevents the nuclear transport of phosphorylated STAT proteins by interacting with the karyopherin-α family of proteins, which are involved in shuttling cargo proteins across the nuclear-pore complex (Mateo et al, 2010; Reid et al, 2006; Reid et al, 2007). MARV VP40 on the other hand inhibits STAT phosphorylation by interacting with the upstream Janus kinases such as JAK1 (Valmas & Basler, 2011; Valmas et al, 2010).

1.9 Conclusions

Given the importance of interferons in triggering host innate and adaptive immunity, viruses encode proteins that interfere with both with IFN production and IFN mediated signaling through multiple mechanisms, both during early and late stages of infection. Some of these mechanisms involve hiding viral PAMPs from being recognized by host PRRs, interfering with components of the PRR mediated signaling cascade that mediate IFN production, and antagonizing IFN-mediated signaling by interfering with the JAK-STAT pathway. Filoviruses, which are the focus of my thesis also encode for proteins such as VP35 and VP24 from ZEBOV and VP40 from MARV, which antagonize the type I IFN pathway. Given that there are currently no approved treatments for filoviral infections, understanding the molecular details of the interactions between host and viral proteins that modulate the IFN responses, is key for identification of target proteins against which antivirals and therapeutics can be targeted.

1.10 References

Akira S, Takeda K (2004) Toll-like receptor signalling. *Nat Rev Immunol* **4:** 499-511

Akira S, Uematsu S, Takeuchi O (2006) Pathogen recognition and innate immunity. *Cell* **124:** 783-801

Andrejeva J, Childs KS, Young DF, Carlos TS, Stock N, Goodbourn S, Randall RE (2004) The V proteins of paramyxoviruses bind the IFN-inducible RNA helicase, mda-5, and inhibit its activation of the IFN-beta promoter. *Proc Natl Acad Sci U S A* **101:** 17264-17269

Barral PM, Morrison JM, Drahos J, Gupta P, Sarkar D, Fisher PB, Racaniello VR (2007) MDA-5 is cleaved in poliovirus-infected cells. *J Virol* **81:** 3677-3684

Barral PM, Sarkar D, Fisher PB, Racaniello VR (2009) RIG-I is cleaved during picornavirus infection. *Virology* **391:** 171-176

Barton GM, Medzhitov R (2003) Toll-like receptor signaling pathways. *Science* **300:** 1524-1525

Basler CF, Mikulasova A, Martinez-Sobrido L, Paragas J, Muhlberger E, Bray M, Klenk HD, Palese P, Garcia-Sastre A (2003) The Ebola virus VP35 protein inhibits activation of interferon regulatory factor 3. *J Virol* **77:** 7945-7956

Basler CF, Wang X, Muhlberger E, Volchkov V, Paragas J, Klenk HD, Garcia-Sastre A, Palese P (2000) The Ebola virus VP35 protein functions as a type I IFN antagonist. *Proc Natl Acad Sci U S A* **97:** 12289-12294

Bell JK, Askins J, Hall PR, Davies DR, Segal DM (2006) The dsRNA binding site of human Toll-like receptor 3. *Proc Natl Acad Sci U S A* **103:** 8792-8797

Bell JK, Botos I, Hall PR, Askins J, Shiloach J, Segal DM, Davies DR (2005) The molecular structure of the Toll-like receptor 3 ligand-binding domain. *Proc Natl Acad Sci U S A* **102:** 10976-10980

Berke IC, Modis Y (2012) MDA5 cooperatively forms dimers and ATP-sensitive filaments upon binding double-stranded RNA. *The EMBO journal* **31:** 1714-1726

Bikard D, Marraffini LA (2012) Innate and adaptive immunity in bacteria: mechanisms of programmed genetic variation to fight bacteriophages. *Curr Opin Immunol* **24:** 15-20

Binder M, Eberle F, Seitz S, Mucke N, Huber CM, Kiani N, Kaderali L, Lohmann V, Dalpke A, Bartenschlager R (2011) Molecular mechanism of signal perception and integration by the innate immune sensor retinoic acid-inducible gene-I (RIG-I). *J Biol Chem* **286:** 27278-27287

Bitra K, Suderman RJ, Strand MR (2012) Polydnavirus Ank proteins bind NF-kappaB homodimers and inhibit processing of Relish. *PLoS Pathog* **8:** e1002722

Bonilla FA, Oettgen HC (2010) Adaptive immunity. *The Journal of allergy and clinical immunology* **125:** S33-40

Bonjardim CA, Ferreira PC, Kroon EG (2009) Interferons: signaling, antiviral and viral evasion. *Immunology letters* **122:** 1-11

Bossert B, Marozin S, Conzelmann KK (2003) Nonstructural proteins NS1 and NS2 of bovine respiratory syncytial virus block activation of interferon regulatory factor 3. *J Virol* **77:** 8661-8668

Botos I, Liu L, Wang Y, Segal DM, Davies DR (2009) The toll-like receptor 3:dsRNA signaling complex. *Biochim Biophys Acta* **1789:** 667-674

Botos I, Segal DM, Davies DR (2011) The structural biology of Toll-like receptors. *Structure* **19:** 447-459

Brasier AR (2006) The NF-kappaB regulatory network. *Cardiovascular toxicology* **6:** 111-130

Broquet AH, Hirata Y, McAllister CS, Kagnoff MF (2011) RIG-I/MDA5/MAVS are required to signal a protective IFN response in rotavirus-infected intestinal epithelium. *J Immunol* **186:** 1618-1626

Brown J, O'Callaghan CA, Marshall AS, Gilbert RJ, Siebold C, Gordon S, Brown GD, Jones EY (2007) Structure of the fungal beta-glucan-binding immune receptor dectin-1: implications for function. *Protein science : a publication of the Protein Society* **16:** 1042-1052

Crozat K, Vivier E, Dalod M (2009) Crosstalk between components of the innate immune system: promoting anti-microbial defenses and avoiding immunopathologies. *Immunol Rev* **227:** 129-149

Cui S, Eisenacher K, Kirchhofer A, Brzozka K, Lammens A, Lammens K, Fujita T, Conzelmann KK, Krug A, Hopfner KP (2008) The C-terminal regulatory domain is the RNA 5'-triphosphate sensor of RIG-I. *Mol Cell* **29:** 169-179

de Bouteiller O, Merck E, Hasan UA, Hubac S, Benguigui B, Trinchieri G, Bates EE, Caux C (2005) Recognition of double-stranded RNA by human toll-like receptor 3 and

downstream receptor signaling requires multimerization and an acidic pH. *J Biol Chem* **280:** 38133-38145

de Weerd NA, Nguyen T (2012) The interferons and their receptors--distribution and regulation. *Immunology and cell biology* **90:** 483-491

Didcock L, Young DF, Goodbourn S, Randall RE (1999) The V protein of simian virus 5 inhibits interferon signalling by targeting STAT1 for proteasome-mediated degradation. *J Virol* **73:** 9928-9933

Donelan NR, Basler CF, Garcia-Sastre A (2003) A recombinant influenza A virus expressing an RNA-binding-defective NS1 protein induces high levels of beta interferon and is attenuated in mice. *J Virol* **77:** 13257-13266

Fairman-Williams ME, Guenther UP, Jankowsky E (2010) SF1 and SF2 helicases: family matters. *Curr Opin Struct Biol* **20:** 313-324

Fan L, Briese T, Lipkin WI (2010) Z proteins of New World arenaviruses bind RIG-I and interfere with type I interferon induction. *J Virol* **84:** 1785-1791

Feinberg H, Mitchell DA, Drickamer K, Weis WI (2001) Structural basis for selective recognition of oligosaccharides by DC-SIGN and DC-SIGNR. *Science* **294:** 2163-2166

Feinberg H, Park-Snyder S, Kolatkar AR, Heise CT, Taylor ME, Weis WI (2000) Structure of a C-type carbohydrate recognition domain from the macrophage mannose receptor. *J Biol Chem* **275:** 21539-21548

Feinberg H, Tso CK, Taylor ME, Drickamer K, Weis WI (2009) Segmented helical structure of the neck region of the glycan-binding receptor DC-SIGNR. *Journal of molecular biology* **394:** 613-620

Figdor CG, van Kooyk Y, Adema GJ (2002) C-type lectin receptors on dendritic cells and Langerhans cells. *Nat Rev Immunol* **2:** 77-84

Franchi L, McDonald C, Kanneganti TD, Amer A, Nunez G (2006) Nucleotide-binding oligomerization domain-like receptors: intracellular pattern recognition molecules for pathogen detection and host defense. *J Immunol* **177:** 3507-3513

Gack MU, Albrecht RA, Urano T, Inn KS, Huang IC, Carnero E, Farzan M, Inoue S, Jung JU, Garcia-Sastre A (2009) Influenza A virus NS1 targets the ubiquitin ligase TRIM25 to evade recognition by the host viral RNA sensor RIG-I. *Cell host & microbe* **5:** 439-449

Gack MU, Shin YC, Joo CH, Urano T, Liang C, Sun L, Takeuchi O, Akira S, Chen Z, Inoue S, Jung JU (2007) TRIM25 RING-finger E3 ubiquitin ligase is essential for RIG-I-mediated antiviral activity. *Nature* **446:** 916-920

Gay NJ, Gangloff M (2007) Structure and function of Toll receptors and their ligands. *Annu Rev Biochem* **76:** 141-165

Geijtenbeek TB, Gringhuis SI (2009) Signalling through C-type lectin receptors: shaping immune responses. *Nat Rev Immunol* **9:** 465-479

Gilmore TD (1999) The Rel/NF-kappaB signal transduction pathway: introduction. *Oncogene* **18:** 6842-6844

Gringhuis SI, den Dunnen J, Litjens M, van der Vlist M, Wevers B, Bruijns SC, Geijtenbeek TB (2009) Dectin-1 directs T helper cell differentiation by controlling noncanonical NF-kappaB activation through Raf-1 and Syk. *Nat Immunol* **10:** 203-213

Gringhuis SI, den Dunnen J, Litjens M, van Het Hof B, van Kooyk Y, Geijtenbeek TB (2007) C-type lectin DC-SIGN modulates Toll-like receptor signaling via Raf-1 kinase-dependent acetylation of transcription factor NF-kappaB. *Immunity* **26:** 605-616

Hartman AL, Towner JS, Nichol ST (2004) A C-terminal basic amino acid motif of Zaire ebolavirus VP35 is essential for type I interferon antagonism and displays high identity with the RNA-binding domain of another interferon antagonist, the NS1 protein of influenza A virus. *Virology* **328:** 177-184

Hausmann S, Marq JB, Tapparel C, Kolakofsky D, Garcin D (2008) RIG-I and dsRNA-induced IFNbeta activation. *PLoS One* **3:** e3965

Hollmig ST, Ariizumi K, Cruz PD, Jr. (2009) Recognition of non-self-polysaccharides by C-type lectin receptors dectin-1 and dectin-2. *Glycobiology* **19:** 568-575

Hong M, Yoon SI, Wilson IA (2012) Structure and functional characterization of the RNA-binding element of the NLRX1 innate immune modulator. *Immunity* **36:** 337-347

Iwasaki A, Medzhitov R (2004) Toll-like receptor control of the adaptive immune responses. *Nat Immunol* **5:** 987-995

Iwasaki A, Medzhitov R (2010) Regulation of adaptive immunity by the innate immune system. *Science* **327:** 291-295

Jenkins KA, Mansell A TIR-containing adaptors in Toll-like receptor signalling. *Cytokine* **49:** 237-244

Jiang F, Ramanathan A, Miller MT, Tang GQ, Gale M, Jr., Patel SS, Marcotrigiano J (2011) Structural basis of RNA recognition and activation by innate immune receptor RIG-I. *Nature* **479:** 423-427

Jin H, Zhou H, Cheng X, Tang R, Munoz M, Nguyen N (2000) Recombinant respiratory syncytial viruses with deletions in the NS1, NS2, SH, and M2-2 genes are attenuated in vitro and in vivo. *Virology* **273:** 210-218

Kageyama M, Takahasi K, Narita R, Hirai R, Yoneyama M, Kato H, Fujita T (2011) 55 Amino acid linker between helicase and carboxyl terminal domains of RIG-I functions as a critical repression domain and determines inter-domain conformation. *Biochem Biophys Res Commun* **415:** 75-81

Kang JY, Lee JO (2011) Structual Biology of the Toll-like receptor family. *Annu Rev Biochem* **80**: 917-941

Karin M, Ben-Neriah Y (2000) Phosphorylation meets ubiquitination: the control of NF-[kappa]B activity. *Annual review of immunology* **18:** 621-663

Kato H, Takeuchi O, Sato S, Yoneyama M, Yamamoto M, Matsui K, Uematsu S, Jung A, Kawai T, Ishii KJ, Yamaguchi O, Otsu K, Tsujimura T, Koh CS, Reis e Sousa C, Matsuura Y, Fujita T, Akira S (2006) Differential roles of MDA5 and RIG-I helicases in the recognition of RNA viruses. *Nature* **441:** 101-105

Kawai T, Akira S (2007) Signaling to NF-kappaB by Toll-like receptors. *Trends Mol Med* **13:** 460-469

Kawai T, Akira S (2010) The role of pattern-recognition receptors in innate immunity: update on Toll-like receptors. *Nat Immunol* **11:** 373-384

Kerrigan AM, Brown GD Syk-coupled C-type lectin receptors that mediate cellular activation via single tyrosine based activation motifs. *Immunol Rev* **234:** 335-352

Khan JA, Brint EK, O'Neill LA, Tong L (2004) Crystal structure of the Toll/interleukin-1 receptor domain of human IL-1RAPL. *J Biol Chem* **279:** 31664-31670

Kingeter LM, Lin X C-type lectin receptor-induced NF-kappaB activation in innate immune and inflammatory responses. *Cell Mol Immunol* **9:** 105-112

Kowalinski E, Lunardi T, McCarthy AA, Louber J, Brunel J, Grigorov B, Gerlier D, Cusack S (2011) Structural basis for the activation of innate immune pattern-recognition receptor RIG-I by viral RNA. *Cell* **147:** 423-435

Kufer TA (2008) Signal transduction pathways used by NLR-type innate immune receptors. *Mol Biosyst* **4:** 380-386

Kumar H, Kawai T, Akira S (2011) Pathogen recognition by the innate immune system. *Int Rev Immunol* **30:** 16-34

Langefeld T, Mohamed W, Ghai R, Chakraborty T (2009) Toll-like receptors and NOD-like receptors: domain architecture and cellular signalling. *Adv Exp Med Biol* **653:** 48-57

Leonard JN, Ghirlando R, Askins J, Bell JK, Margulies DH, Davies DR, Segal DM (2008) The TLR3 signaling complex forms by cooperative receptor dimerization. *Proc Natl Acad Sci U S A* **105:** 258-263

Leung DW, Amarasinghe GK (2012) Structural insights into RNA recognition and activation of RIG-I-like receptors. *Current Opinion in Structural Biology* **22:** 297-303

Leung DW, Basler CF, Amarasinghe GK (2012) RIG-I like receptors. *Trends in Microbiology*

Leung DW, Ginder ND, Fulton DB, Nix J, Basler CF, Honzatko RB, Amarasinghe GK (2009) Structure of the Ebola VP35 interferon inhibitory domain. *Proc Natl Acad Sci U S A* **106:** 411-416

Leung DW, Prins KC, Borek DM, Farahbakhsh M, Tufariello JM, Ramanan P, Nix JC, Helgeson LA, Otwinowski Z, Honzatko RB, Basler CF, Amarasinghe GK (2010) Structural basis for dsRNA recognition and interferon antagonism by Ebola VP35. *Nature Structural & Molecular Biology* **17:** 165-172

Li X, Ranjith-Kumar CT, Brooks MT, Dharmaiah S, Herr AB, Kao C, Li P (2009) The RIG-I-like receptor LGP2 recognizes the termini of double-stranded RNA. *J Biol Chem* **284:** 13881-13891

Li XD, Sun L, Seth RB, Pineda G, Chen ZJ (2005) Hepatitis C virus protease NS3/4A cleaves mitochondrial antiviral signaling protein off the mitochondria to evade innate immunity. *Proc Natl Acad Sci U S A* **102:** 17717-17722

Ling Z, Tran KC, Teng MN (2009) Human respiratory syncytial virus nonstructural protein NS2 antagonizes the activation of beta interferon transcription by interacting with RIG-I. *J Virol* **83:** 3734-3742

Liu L, Botos I, Wang Y, Leonard JN, Shiloach J, Segal DM, Davies DR (2008) Structural basis of toll-like receptor 3 signaling with double-stranded RNA. *Science* **320:** 379-381

Lo MS, Brazas RM, Holtzman MJ (2005) Respiratory syncytial virus nonstructural proteins NS1 and NS2 mediate inhibition of Stat2 expression and alpha/beta interferon responsiveness. *J Virol* **79:** 9315-9319

Loo YM, Fornek J, Crochet N, Bajwa G, Perwitasari O, Martinez-Sobrido L, Akira S, Gill MA, Garcia-Sastre A, Katze MG, Gale M, Jr. (2008) Distinct RIG-I and MDA5 signaling by RNA viruses in innate immunity. *J Virol* **82:** 335-345

Loo YM, Gale M, Jr. (2011) Immune signaling by RIG-I-like receptors. *Immunity* **34:** 680-692

Lu C, Ranjith-Kumar CT, Hao L, Kao CC, Li P (2011) Crystal structure of RIG-I C-terminal domain bound to blunt-ended double-strand RNA without 5' triphosphate. *Nucleic Acids Res* **39:** 1565-1575

Lu C, Xu H, Ranjith-Kumar CT, Brooks MT, Hou TY, Hu F, Herr AB, Strong RK, Kao CC, Li P (2010) The structural basis of 5' triphosphate double-stranded RNA recognition by RIG-I C-terminal domain. *Structure* **18:** 1032-1043

Luo D, Ding SC, Vela A, Kohlway A, Lindenbach BD, Pyle AM (2011) Structural insights into RNA recognition by RIG-I. *Cell* **147:** 409-422

Maluquer de Motes C, Cooray S, Ren H, Almeida GM, McGourty K, Bahar MW, Stuart DI, Grimes JM, Graham SC, Smith GL (2011) Inhibition of apoptosis and NF-kappaB activation by vaccinia protein N1 occur via distinct binding surfaces and make different contributions to virulence. *PLoS Pathog* **7:** e1002430

Mateo M, Reid SP, Leung LW, Basler CF, Volchkov VE (2010) Ebolavirus VP24 binding to karyopherins is required for inhibition of interferon signaling. *J Virol* **84:** 1169-1175

McGreal EP, Miller JL, Gordon S (2005) Ligand recognition by antigen-presenting cell C-type lectin receptors. *Curr Opin Immunol* **17:** 18-24

Monie TP, Moncrieffe MC, Gay NJ (2009) Structure and regulation of cytoplasmic adapter proteins involved in innate immune signaling. *Immunol Rev* **227:** 161-175

Moore CB, Bergstralh DT, Duncan JA, Lei Y, Morrison TE, Zimmermann AG, Accavitti-Loper MA, Madden VJ, Sun L, Ye Z, Lich JD, Heise MT, Chen Z, Ting JP (2008) NLRX1 is a regulator of mitochondrial antiviral immunity. *Nature* **451:** 573-577

Najarro P, Traktman P, Lewis JA (2001) Vaccinia virus blocks gamma interferon signal transduction: viral VH1 phosphatase reverses Stat1 activation. *J Virol* **75:** 3185-3196

Newton K, Dixit VM (2012) Signaling in innate immunity and inflammation. *Cold Spring Harbor perspectives in biology* **4**

Olive C (2012) Pattern recognition receptors: sentinels in innate immunity and targets of new vaccine adjuvants. *Expert review of vaccines* **11:** 237-256

Onomoto K, Onoguchi K, Takahasi K, Fujita T (2010) Type I interferon production induced by RIG-I-like receptors. *Journal of interferon & cytokine research : the official journal of the International Society for Interferon and Cytokine Research* **30:** 875-881

Peisley A, Lin C, Wu B, Orme-Johnson M, Liu M, Walz T, Hur S (2011) Cooperative assembly and dynamic disassembly of MDA5 filaments for viral dsRNA recognition. *Proc Natl Acad Sci U S A* **108:** 21010-21015

Prins KC, Cardenas WB, Basler CF (2009) Ebola virus protein VP35 impairs the function of interferon regulatory factor-activating kinases IKKepsilon and TBK-1. *J Virol* **83:** 3069-3077

Proell M, Riedl SJ, Fritz JH, Rojas AM, Schwarzenbacher R (2008) The Nod-like receptor (NLR) family: a tale of similarities and differences. *PLoS One* **3:** e2119

Ramos HJ, Gale M, Jr. (2011) RIG-I Like Receptors and Their Signaling Crosstalk in the Regulation of Antiviral Immunity. *Curr Opin Virol* **1:** 167-176

Reid SP, Leung LW, Hartman AL, Martinez O, Shaw ML, Carbonnelle C, Volchkov VE, Nichol ST, Basler CF (2006) Ebola virus VP24 binds karyopherin alpha1 and blocks STAT1 nuclear accumulation. *J Virol* **80:** 5156-5167

Reid SP, Valmas C, Martinez O, Sanchez FM, Basler CF (2007) Ebola virus VP24 proteins inhibit the interaction of NPI-1 subfamily karyopherin alpha proteins with activated STAT1. *J Virol* **81:** 13469-13477

Rodriguez JJ, Parisien JP, Horvath CM (2002) Nipah virus V protein evades alpha and gamma interferons by preventing STAT1 and STAT2 activation and nuclear accumulation. *J Virol* **76:** 11476-11483

Rothenfusser S, Goutagny N, DiPerna G, Gong M, Monks BG, Schoenemeyer A, Yamamoto M, Akira S, Fitzgerald KA (2005) The RNA helicase Lgp2 inhibits TLR-independent sensing of viral replication by retinoic acid-inducible gene-I. *J Immunol* **175:** 5260-5268

Seth RB, Sun L, Ea CK, Chen ZJ (2005) Identification and characterization of MAVS, a mitochondrial antiviral signaling protein that activates NF-kappaB and IRF 3. *Cell* **122:** 669-682

Shaw PJ, Lamkanfi M, Kanneganti TD NOD-like receptor (NLR) signaling beyond the inflammasome. *Eur J Immunol* **40:** 624-627

Silk RN, Bowick GC, Abrams CC, Dixon LK (2007) African swine fever virus A238L inhibitor of NF-kappaB and of calcineurin phosphatase is imported actively into the nucleus and exported by a CRM1-mediated pathway. *The Journal of general virology* **88:** 411-419

Sirard JC, Vignal C, Dessein R, Chamaillard M (2007) Nod-like receptors: cytosolic watchdogs for immunity against pathogens. *PLoS Pathog* **3:** e152

Sorbara MT, Philpott DJ (2011) Peptidoglycan: a critical activator of the mammalian immune system during infection and homeostasis. *Immunol Rev* **243:** 40-60

Sun J, Duffy KE, Ranjith-Kumar CT, Xiong J, Lamb RJ, Santos J, Masarapu H, Cunningham M, Holzenburg A, Sarisky RT, Mbow ML, Kao C (2006) Structural and functional analyses of the human Toll-like receptor 3. Role of glycosylation. *J Biol Chem* **281:** 11144-11151

Takada E, Okahira S, Sasai M, Funami K, Seya T, Matsumoto M (2007) C-terminal LRRs of human Toll-like receptor 3 control receptor dimerization and signal transmission. *Mol Immunol* **44:** 3633-3640

Takeuchi O, Akira S (2010) Pattern recognition receptors and inflammation. *Cell* **140:** 805-820

Uze G, Schreiber G, Piehler J, Pellegrini S (2007) The receptor of the type I interferon family. *Current topics in microbiology and immunology* **316:** 71-95

Valmas C, Basler CF (2011) Marburg virus VP40 antagonizes interferon signaling in a species-specific manner. *Journal of Virology* **85:** 4309-4317

Valmas C, Grosch MN, Schumann M, Olejnik J, Martinez O, Best SM, Krahling V, Basler CF, Muhlberger E (2010) Marburg virus evades interferon responses by a mechanism distinct from ebola virus. *PLoS Pathog* **6:** e1000721

van Boxel-Dezaire AH, Stark GR (2007) Cell type-specific signaling in response to interferon-gamma. *Current topics in microbiology and immunology* **316:** 119-154

Verstak B, Nagpal K, Bottomley SP, Golenbock DT, Hertzog PJ, Mansell A (2009) MyD88 adapter-like (Mal)/TIRAP interaction with TRAF6 is critical for TLR2- and TLR4-mediated NF-kappaB proinflammatory responses. *J Biol Chem* **284:** 24192-24203

Weis WI, Taylor ME, Drickamer K (1998) The C-type lectin superfamily in the immune system. *Immunol Rev* **163:** 19-34

Williams A, Flavell RA, Eisenbarth SC The role of NOD-like Receptors in shaping adaptive immunity. *Curr Opin Immunol* **22:** 34-40

Wyler E, Kaminska M, Coic YM, Baleux F, Veron M, Agou F (2007) Inhibition of NF-kappaB activation with designed ankyrin-repeat proteins targeting the ubiquitin-binding/oligomerization domain of NEMO. *Protein science : a publication of the Protein Society* **16:** 2013-2022

Ye Z, Ting JP (2008) NLR, the nucleotide-binding domain leucine-rich repeat containing gene family. *Curr Opin Immunol* **20:** 3-9

Yoneyama M, Fujita T (2009) RNA recognition and signal transduction by RIG-I-like receptors. *Immunol Rev* **227:** 54-65

Yoneyama M, Kikuchi M, Matsumoto K, Imaizumi T, Miyagishi M, Taira K, Foy E, Loo YM, Gale M, Jr., Akira S, Yonehara S, Kato A, Fujita T (2005) Shared and unique functions of the DExD/H-box helicases RIG-I, MDA5, and LGP2 in antiviral innate immunity. *J Immunol* **175:** 2851-2858

Yoneyama M, Kikuchi M, Natsukawa T, Shinobu N, Imaizumi T, Miyagishi M, Taira K, Akira S, Fujita T (2004) The RNA helicase RIG-I has an essential function in double-stranded RNA-induced innate antiviral responses. *Nat Immunol* **5:** 730-737

Zuniga EI, Hahm B, Oldstone MB (2007) Type I interferon during viral infections: multiple triggers for a multifunctional mediator. *Current topics in microbiology and immunology* **316:** 337-357

CHAPTER 2. FILOVIRUSES OVERVIEW

2.1 Introduction

The *Filoviridae* family of viruses, which includes *ebolavirus* (EBOV) and *marburgvirus* (MARV), are some of the most deadly pathogens known to infect humans. Outbreaks of these viruses have been infrequent but highly lethal. So far five species of EBOV – Ebola, Reston, Sudan, Tai Forest, and Bundibugyo have been identified(Feldmann & Geisbert, 2011). The MARV genus has only one species - Lake Victoria. Named after the German city Marburg, MARV was the first filovirus to be identified in 1967, during a deadly outbreak, when animal handlers working in Germany and Yugoslavia came into contact with bodily fluids of Green monkeys imported from Africa(Bausch et al, 2006; Gear et al, 1975). *Ebolavirus* was isolated in Central Africa in 1976 when an outbreak occurred in the Democratic Republic of Congo(1978b). Both Zaire and Sudan *ebolavirus* have caused deadly outbreaks in Africa, while there has been only one non-fatal, reported case of the Tai Forest *ebolavirus(1978a; Georges et al, 1999; Heymann et al, 1980; Towner et al, 2008)*. During these isolated but severe outbreaks, case fatalities between 20%-90% have been reported for the various species of filoviruses. Reston *ebolavirus* (REBOV) was discovered following an outbreak in Reston, Virginia, USA when animal handlers contracted the virus from macaques imported from Phillipines(Jahrling et al, 1990). While it caused severe disease and near 100% lethality in the infected macaques, the animal handlers recovered from the outbreak without any apparent symptoms even though they had seroconverted, suggesting that this

species may not cause disease in humans. More recently, REBOV has been isolated from a swine population in the Philippines, suggesting the zoonotic potential of filoviruses(Barrette et al, 2009). However limited data are currently available on the natural host range of filoviruses, with some studies indicating that several species of fruit bats maybe the natural reservoir(Leroy et al, 2005; Towner et al, 2009). A recent study reported the isolation of a genetically distinct filovirus called Lloviu virus from insectivorous bats in Cueva del Lloviu, Spain lending further support to the notion that bats may serve as the natural reservoir for filoviruses(Negredo et al, 2011). Of the different filoviruses identified so far, the Zaire *ebolavirus* (ZEBOV) has been the most virulent, with the highest fatality rates (~90%) among all outbreaks reported(Bwaka et al, 1999; Heymann et al, 1980). The zoonotic nature, rapid and severe disease progression, and the lack of vaccines or therapeutics make filoviruses a public health hazard and a potential agent of bioterrorism, following reports that suggested that filoviruses may spread through aerosol route in addition to direct contact with bodily fluids of infected animals(Alves et al, 2010; Leffel & Reed, 2004). One of the reasons attributed to the severity of filoviral infections is effective shut down of innate and adaptive immune response by virus encoded immune antagonists. It is extremely important to understand the molecular mechanisms of how these viral proteins mediate immune evasion, in order to develop strategies for designing antivirals.

2.2 Filovirus pathogenesis

Severe filoviral infections are characterized by early non-specific symptoms that progress to sever hemorrhagic fever during the final stages of the disease. The incubation

period ranges anywhere between a few days to about 2 weeks after which the patients start to develop symptoms such as fever, severe arthralgia and myalgia, nausea, vomiting, diarrhea, abdominal pain and maculopapular rashes, especially in the torso, indicative of dysregulation of coagulation and blood clotting mechanisms(Feldmann & Geisbert, 2011; Georges et al, 1999; Heymann et al, 1980). Infections are characterized by complete lack of innate immune responses, especially interferons and subsequent dysregulation of the adaptive immune responses. Further symptoms that develop include severe liver and kidney failure, massive internal hemorrhage in multiple organs, delirium and coma resembling septic shock syndrome(Hartman et al, 2010; Kortepeter et al, 2011). Both EBOV and MARV have broad host tropism, and replicate to high levels in key immune cells such as monocytes, macrophages, dendritic cells and hepatocytes. This results in severe dysregulation of pro-inflammatory cytokine release late during infection, causing massive inflammation and cytokine storms, which result in tissue and organ damage(Takada, 2012). Thus the early shutdown of innate immunity and the resulting dysregulation of adaptive immunity result in unchecked viral replication.

2.3 Filovirus replication cycle

Filoviruses are named after their signature pleomorphic, filamentous appearance in electron micrographs, often forming circular or shepherd's hook shaped virions(Baskerville et al, 1985; Ellis et al, 1978) (Figure 2-1A). Filoviruses belong to the order *Mononegavirales*; they have a single-stranded negative sense RNA genome. The 19-kilobase genome encodes seven structural proteins, nucleoprotein (NP), viral protein 35 (VP35), VP40, glycoprotein (GP),

VP30, VP24 and Large protein (L) (Figure 2-1B). The genome organization is most similar to rhabdoviruses and paramyxoviruses(Elliott et al, 1985; Feldmann & Geisbert, 2011). Conserved polyadenylation sites at the 3' and 5' UTR regions of the filoviral genome act as transcriptional start and stop sites(Sanchez et al, 1993). In addition the secondary structure at the 5' UTR of the genome regulates transcriptional initiation, replication and nucleocapsid formation(Crary et al, 2003). The nucleocapsid in the virion is composed of the RNA genome bound to NP and VP30(Becker et al, 1998; Welsch et al, 2010). The major and minor matrix proteins, VP40 and VP24 make up virion which is enclosed in a host-derived lipid bilayer membrane, which is embedded with trimeric spikes formed by the envelope protein, GP. Four proteins - NP, VP30, VP35 and the RNA-dependent RNA polymerase L form the viral polymerase complex(Elliott et al, 1985; Ellis et al, 1978)

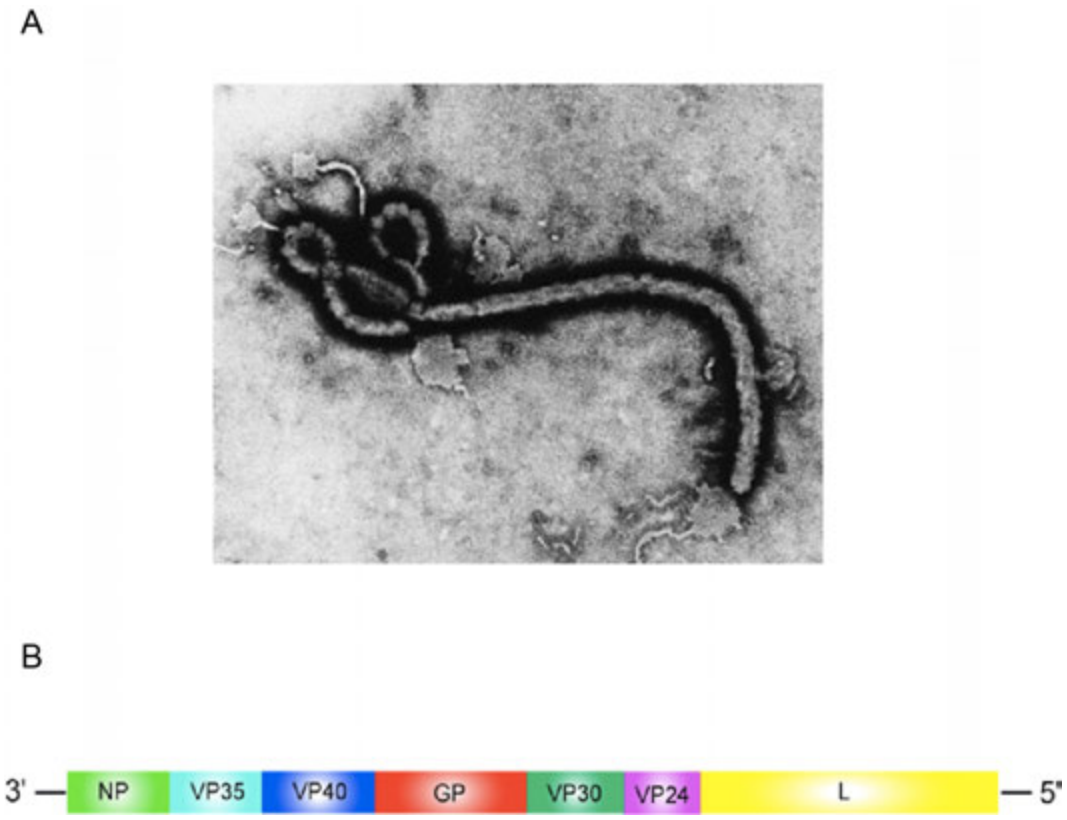

Figure 2-1. Filoviral genome organization.

(A) Filoviruses have a characteristic filamentous appearance as observed in this representative electron micrograph of the *ebolavirus* virion (Photo credit to Frederick Murphy). (http://www.cdc.gov/ncidod/dvrd/spb/mnpages/dispages/Fact_Sheets/Ebola_Fact_Booklet.pdf). (B) Filoviruses have a single stranded, anti-sense, non-segmented, genome of about 19 kilobases, encoding for seven structural proteins indicated.

Cell entry is the first step in the filovirus replication cycle. Filoviruses exhibit broad tissue tropism – they gain entry into the host through a wide variety of cell types including dendritic cells, monocytes, macrophages, epithelial cells, hepatocytes, and endothelial cells(Bosio et al, 2003; Feldmann & Geisbert, 2011). Hence it is likely that the viral envelope protein GP mediates interactions with a variety of cell surface receptors and host factors in order to gain entry into host cells. Although receptor specificity for filoviruses in different cell types is poorly understood, recent studies suggest that viral entry is mediated by GP interactions with the T-cell immunoglobulin mucin domain-1 (TIM-1) receptor in epithelial cells(Hunt et al, 2012; Kondratowicz et al, 2011). The C-type lectin receptors (CLRs), L-SIGN and DC-SIGN are also thought to be receptors involved in filoviral entry. It has been shown that the expression of these C-type lectin receptors enhances filvorial entry in some cell types(Marzi et al, 2007; Matsuno et al, 2010). The GP protein is cleaved by furin protease post-translationally into two subunits called GP1 and GP2, which are linked through disulfide bonds(Volchkov et al, 1998). The pre-fusion conformation of EBOV GP was structurally characterized by using a truncated form of GP bound to KZ52 antibody, which was previously isolated from a human survivor in the Democratic Republic of Congo(Lee et al, 2008; Maruyama et al, 1999) (Figure 2-2-A). The GP1 and GP2 subunits are involved in extensive protein-protein interactions to form the trimeric conformation. The EBOV GP has been proposed to undergo conformation changes to mediate viral and host membrane fusion by an unknown trigger which results in the GP2 subunit forming a six helix-bundle which represents the post-fusion conformation, and this conformation has also been structurally characterized(Malashkevich et al, 1999) (Figure 2-2B). This architecture of the GP2

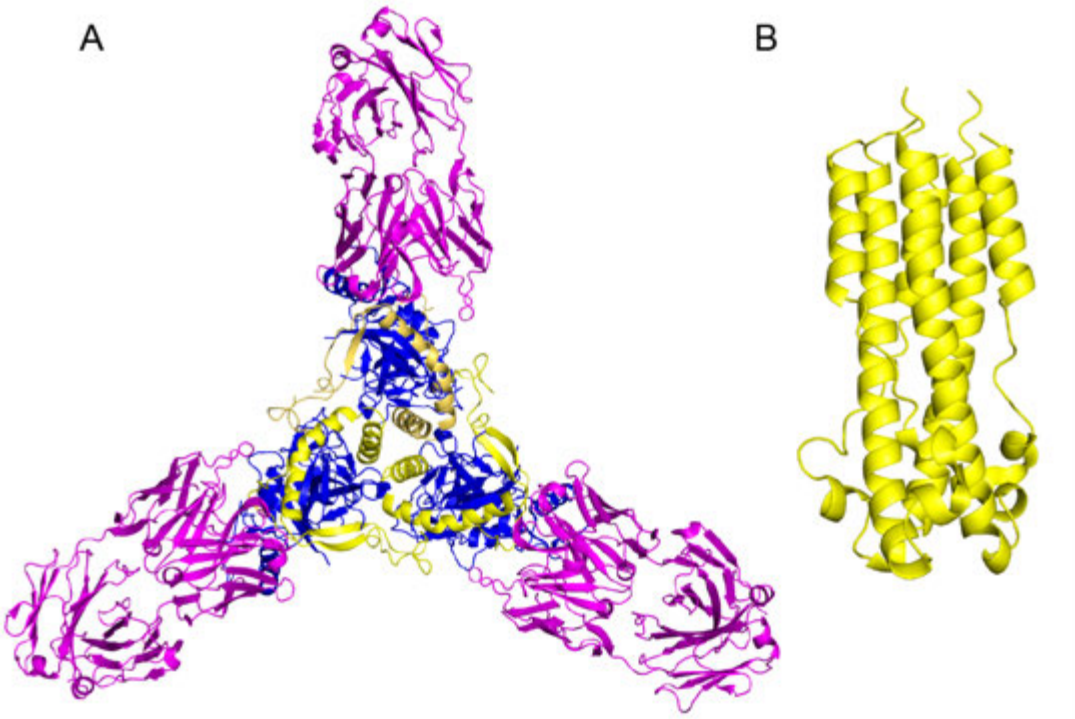

Figure 2-2. Structure of filoviral GP protein.

(A) Prefusion conformation of the EBOV GP trimer made of the GP1 (blue) and the GP2 (yellow) subunits which are disulfide linked and bound by the human antibody KZ52 (magenta) at the base of the trimeric region (PDB 3CSY)(Lee et al, 2008). (B) Fusion active conformation of the GP2 (yellow) subunit of EBOV shows a six-helix bundle similar in architecture to other viral membrane fusion proteins (PDB 2EBO)(Malashkevich et al, 1999).

subunit resembles that of other viral membrane fusion proteins such as the influenza virus and HIV. The GP protein of filoviruses is heavily glycosylated and the mucin-like domain and the glycan cap may mediate interactions with the CLRs(Lee et al, 2008; Lee & Saphire, 2009; Olal et al, 2012). However it is also likely that the mucin-like domain plays a role in enhancing adherence to host cells by interacting with cell-surface adhesion molecules, but may not play a direct role in the entry mechanism. Internalization of the virus particle into endosomes occurs predominantly through macropinocytosis, among other mechanisms, but both caveolin-dependent and clathrin-dependent endocytosis have been proposed as mechanisms of viral internalization(Aleksandrowicz et al, 2011; Hunt et al, 2012; Nanbo et al, 2010) (Figure 2-3). It has been shown that the tyrosine kinase receptor Axl, enhances EBOV uptake into cells, but other studies have shown that this is due to enhanced macropinocytosis in Axl expressing cells and not due to receptor mediated cell entry(Brindley et al, 2011; Hunt et al, 2011). It is currently unknown what the predominant mechanism of internalization is, and whether there is cell-type specificity associated with this process. It is also unknown whether multiple mechanisms may be at play in the same cell-type. More recently, multiple studies have reported that the host protein Niemann-Pick C1 (NPC1) protein may play an important role in the entry process(Carette et al, 2011; Cote et al, 2011). NPC1 is a host protein and primarily found on endosomal and lysosomal membranes, and plays a role in cholesterol homeostasis. This study showed that cells lacking NPC1 showed resistance to EBOV entry. This study was also able to show that it was NPC1 expression and not its function in lipid transport that led to this phenotype(Carette et al, 2011; Cote et al, 2011). However the exact mechanism by which NPC1 mediates EBOV entry is still unknown.

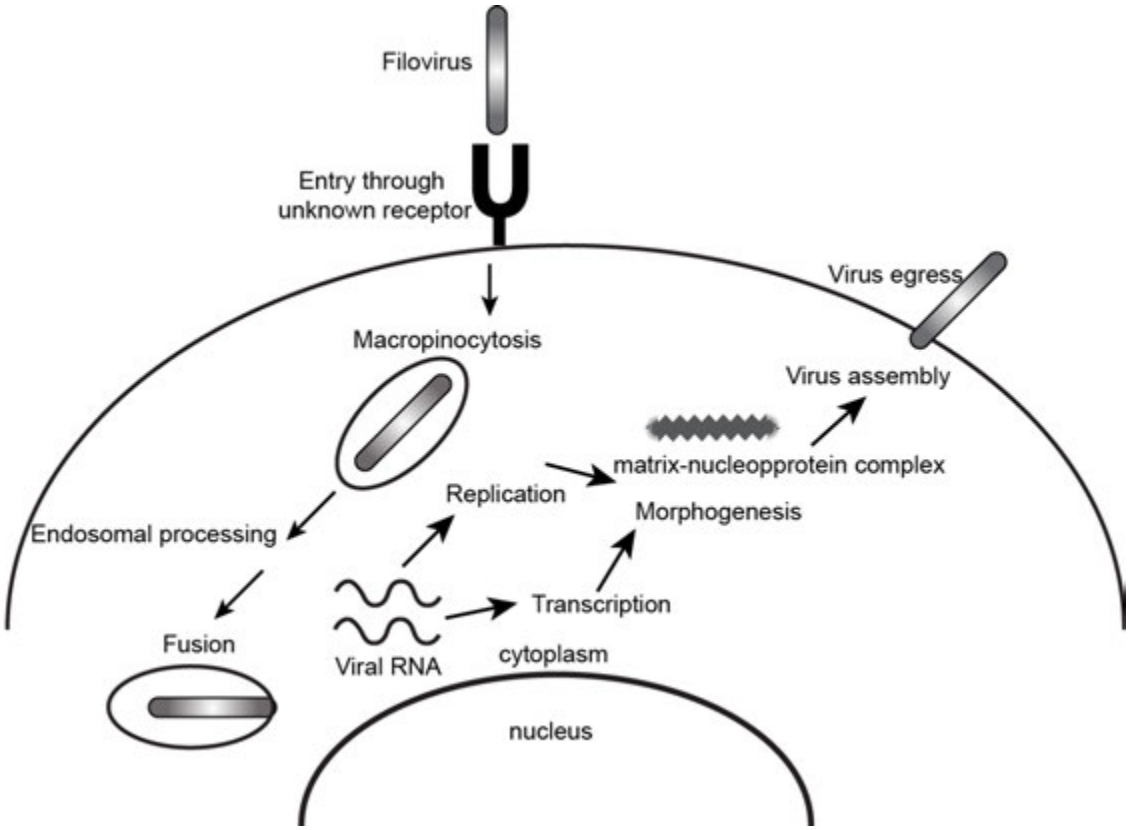

Figure 2-3. Filoviral replication cycle.

Filoviruses are enveloped viruses and gain entry into cells through multiple receptors whose identities and mechanisms are not clearly known. Filoviruses are thought to undergo macropinocytosis and endosomal processing upon entry. Once fusion occurs, the negative sense, single-stranded genome is released into the cytoplasm of the host cell, where it undergoes replication and transcription by the viral polymerase complex. The matrix and nucleoprotein complex first forms filamentous assemblies, into which the other viral proteins are recruited. These assemble at the plasma membrane through lipid rafts and viral budding is mediated by hijacking a number of host protein complexes (Figure adapted from Fields Virology).

Upon viral entry, the GP protein undergoes proteolytic processing by the cathepsin L and B enzymes, in the acidic environment of the endosome, resulting in membrane fusion and release of the RNA genome into the cytosol of the host cell(Bale et al; Brecher et al; Hunt et al, 2012). Cathepsin L cleaves off the mucin-like domain and the glycan cap of the filoviral GP, followed by further processing by Cathepsin B, which results in the fusion-ready state of GP. The exact nature or conformation of the functionally active GP is currently unknown. In addition to the full length GP protein that EBOV encodes, as a result of transcriptional frame shifting, it also encodes a truncated version of GP called soluble GP (sGP)(Mehedi et al, 2011). This soluble form of GP has been proposed to function as a decoy for the host immune responses during filoviral infections(Falzarano et al, 2006). Since filoviruses are negative sense single-stranded RNA viruses, the viral RNA-dependent RNA polymerase (RdRp) first transcribes the negative sense RNA genome into the positive sense messenger RNAs before viral protein synthesis can occur. In the filoviral genome, short regions of the stop site of the upstream gene overlap with regions of the start site of the downstream gene. The arrangement of genes from the 3' to the 5' end of the viral genome in addition to the cis-acting elements flanking each gene serves as a regulatory mechanism of gene expression(Crary et al, 2003; Sanchez et al, 1993). There is attenuated transcription of the genes that are farther from the 3' end of the genome, which means NP is the most highly expressed viral protein, whereas the viral polymerase L is the least expressed. The amount of NP transcribed regulates the switch from transcription to genome replication in infected cells. Genome replication involves synthesis of the full-length positive sense RNA strand, which can then act as a template to make the negative sense genomic RNA. The viral replication/transcription complex formed by NP, VP35, VP30 and L then synthesizes both

viral mRNA and positive sense template RNA for genome replication. The newly synthesized proteins, in particular NP, mediate the formation of new nucleocapsid. Filoviral NP has been reported to form helical assemblies with cellular RNA and form inclusion bodies when expressed in insect cells, similar to what is observed in filovirus infected cells, although VP30 and L are also recruited to the nucleocapsid. Additionally both matrix proteins VP40 and VP24 have been shown to play important roles in viral particle assembly mediated by interactions with a multitude of host proteins, the identities of which are not yet fully understood(Hartlieb et al, 2007; Huang et al, 2002).

VP40 is the major matrix protein and plays a very important structural role in maintaining the integrity of the virion. Like other matrix proteins, VP40 has been shown to interact with lipids and host cell membranes to mediate morphogenesis and budding of the virus, and also has been shown to important for the regulation of viral replication and transcription(Hoenen et al, 2010a; Hoenen et al, 2010b). Previous structural studies on EBOV VP40 have resulted in the crystal structures of both free (Figure 2-4A) and RNA-bound forms (Figure 2-4B) of VP40 in the monomeric and octameric state respectively(Dessen et al, 2000; Gomis-Ruth et al, 2003; Ruigrok et al, 2000). These structural studies collectively suggest that EBOV VP40 has a distinct fold when compared to previously characterized matrix proteins from viruses belonging to the *Mononegavirales* order. VP40 contains two structurally similar N- and the C-terminal domains, both consisting of beta sheets packed on the lateral surface by an alpha helix. The C-terminal domain consists of a highly hydrophobic surface, which may be involved in interactions with lipid membranes. The RNA-bound VP40 also assembles into an octamer by undergoing two major

conformational changes at both the N and the C-terminal domains stabilized by the RNA contacts made(Dessen et al, 2000; Gomis-Ruth et al, 2003; Ruigrok et al, 2000). These octameric assemblies of EBOV VP40 may recruit additional host proteins, such as Tsg101 at the plasma membrane of infected cells(Urata et al, 2007).

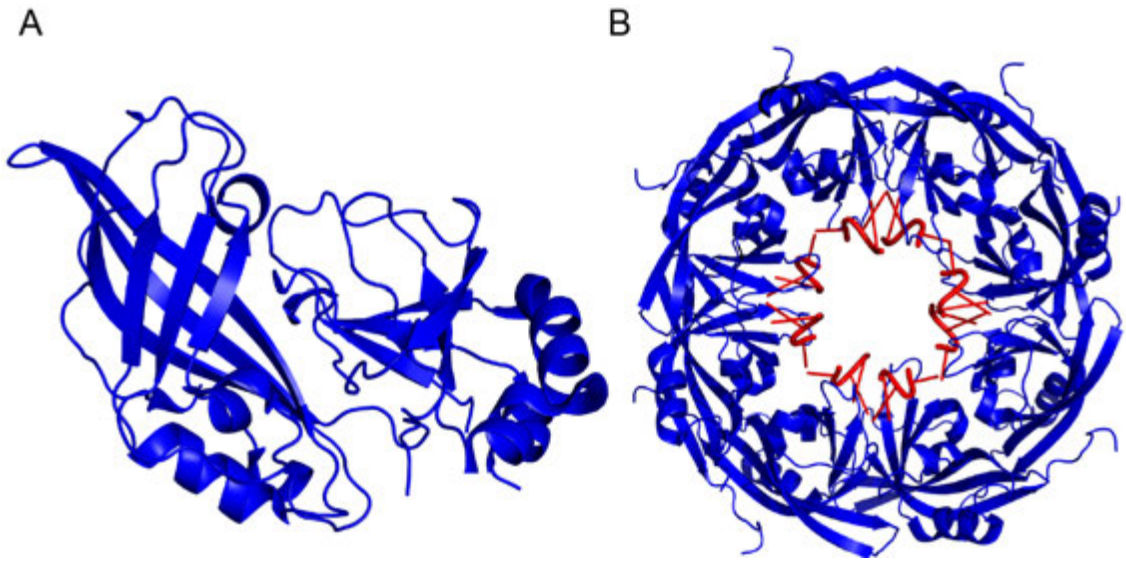

Figure 2-4. Crystal structures of EBOV VP40.

(A) ZEBOV VP40 (blue) consists of structurally similar N and C-terminal domains of beta-sheets packed against an alpha-helix. (B) VP40 (blue) oligomerizes into ring-shaped octamers upon RNA (orange) binding (PDB 1H2C)(Gomis-Ruth et al, 2003).

VP24 is the minor matrix protein, which in addition to being a structural protein in the virion serves to regulate nucleocapsid formation, viral replication and transcription and also plays an important role in viral morphogenesis and budding(Noda et al, 2007; Watanabe et al, 2007). In addition to all these functions recent studies have uncovered a novel mechanism by which VP24 inhibits type I IFN mediated signaling and thus serves as an immune antagonist. These studies support a model in which VP24 interacts with the karyopherin-alpha family of host proteins, which play an important role in trafficking activated transcription factors called STATs into the nucleus. VP24 is able to inhibit STAT accumulation in the nucleus by interacting with the karyopherin proteins(Mateo et al, 2010; Reid et al, 2006; Reid et al, 2007)(Figure 2-6). This was demonstrated by intracellular localization studies, which showed that in the presence of ZEBOV VP24, GFP-tagged, phosphorylated STAT1 accumulated in the cytoplasm of Vero cells. Recent structural studies on VP24 has resulted in crystal structures of REBOV and SEBOV VP24 proteins, which show that the VP24 protein has a novel triangular pyramid fold, made of both alpha helices and beta sheets (Figure 2-5A and B)(Zhang et al). Mapping of residues from REBOV and SEBOV onto the structure reveals that some surfaces of the pyramidal fold are conserved while others are not. The functional significance of these differences is still unknown. Taken together, these data support a novel mechanism, where VP24 inhibits IFN mediated signaling and antiviral gene production by interacting with karyopherin proteins to inhibit the nuclear translocation of activated STAT proteins.

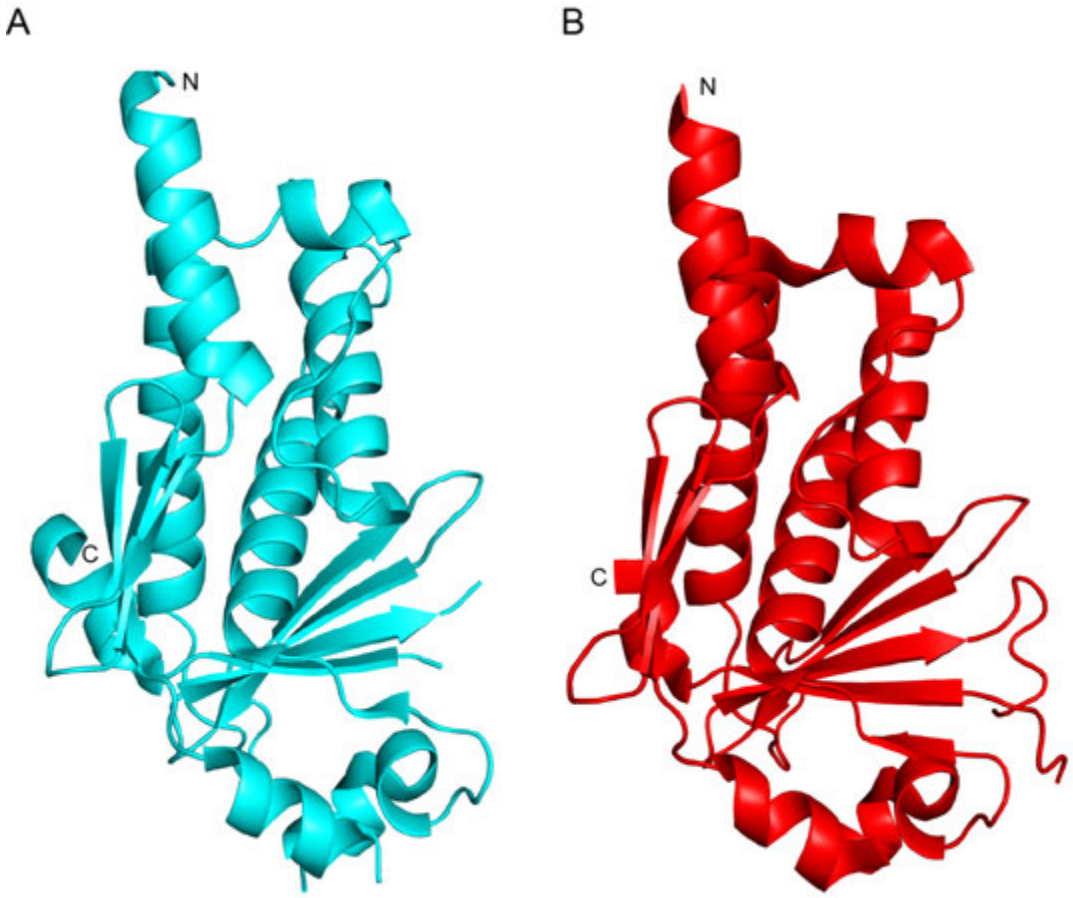

Figure 2-5. Crystal structures of EBOV VP24.

A novel pyramidal fold of VP24 protein from (A) Reston EBOV (cyan representation) and (B) Sudan EBOV (red representation) (PDBs 4D9O and 3VNE)(Zhang et al).

VP30 plays a very important role in capsid formation and regulates the transcriptional activity of the replication complex through interactions with specific RNA secondary structures in the transcriptional start sites of the viral genomic RNA(Weik et al, 2002). It has also been shown that phosphorylation state of VP30 modulates its activity in transcription, with hyper-phosphorylation leading to transcriptional inhibition. A cluster of serine residues in the N-terminus of VP30 have been shown to be functionally important phosphorylation sites, as mutation of these residues to phosphomimetic aspartate residues downregulated the transcriptional activity of VP30 in a minigenome assay(Modrof et al, 2002). Recent structural studies on VP30 have resulted in crystal structure of the C-terminal domain of VP30, which is a dimer in solution (Figure 2-6). In addition, full length VP30 has also been shown to form hexamers both *in vitro* and *in vivo*. These studies showed that EBOV VP30 plays an essential role in transcriptional activation, likely through stabilization of the viral mRNA(Hartlieb et al, 2007).

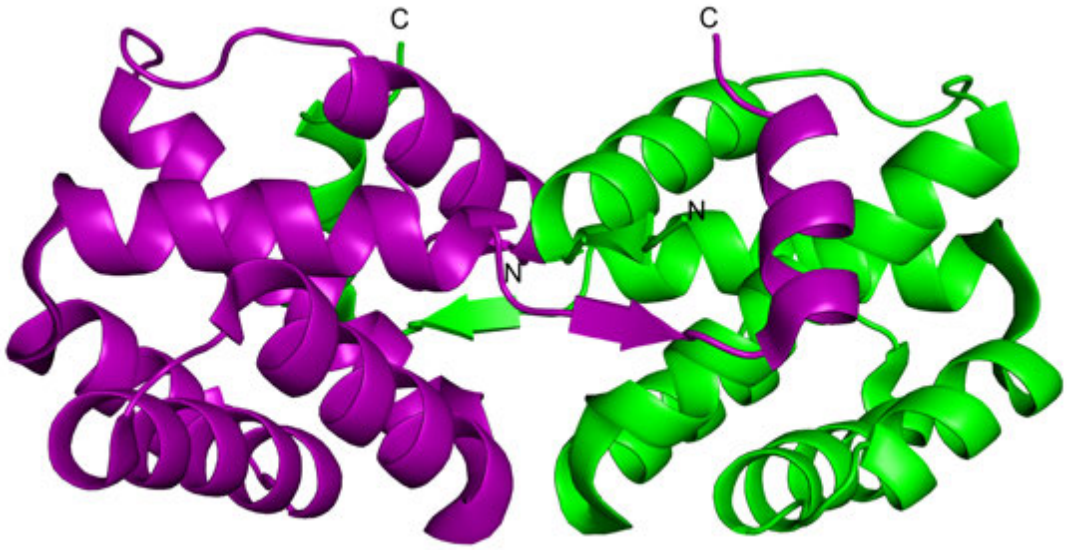

Figure 2-6. Crystal structure of EBOV VP30.

The C-terminal domain of EBOV VP30 shows a six-helix core with the seventh helix forming the dimeric interface for the head to head packing of the two monomers (depicted as magenta and green cartoon representation) (PDB 2I8B)(Hartlieb et al, 2007).

VP35 plays multiple critical roles by functioning as a co-factor in the viral replication complex and in mediating immune evasion. EBOV VP35 was identified as a type I IFN antagonist using a recombinant influenza virus in which the NS1 gene was deleted and replaced by each filoviral gene in growth complementation assays. Among the filoviral genes, only VP35 had the ability to rescue the growth of the NS1-deleted virus in 293T cells(Basler et al, 2000). VP35 able to was suppress the activation of IFN-beta promoter and IFN-beta production in 293T cells by Sendai virus infection or poly I:C transfection suggesting a potential role for it in immune evasion, similar to influenza NS1(Basler et al, 2000). VP35 was also proposed to be an RNA binding protein, based on sequence alignments with influenza NS1 which suggested that a short stretch of residues in ZEBOV VP35, which includes R305, K309, and R312 in the C-terminal domain, were conserved in NS1(Hartman et al, 2004). These residues were are important for RNA binding in NS1 protein, and mutation of these residues to alanine also resulted in diminished RNA binding and IFN inhibition in VP35, suggesting that they may have a potential role in IFN antagonist function of VP35 through which it can potentially inhibit RIG-I like receptor mediated IFN-beta promoter activation(Cardenas et al, 2006; Hartman et al, 2004). Using C-terminal truncation mutants of ZEBOV VP35, subsequent studies showed that the deletion of last 40 residues of VP35 was enough to disrupt its IFN antagonist functions, suggesting that the IFN inhibitory function was localized to the C-terminus of the protein(Hartman et al, 2004). We recently solved the crystal structure of the C-terminal IFN inhibitory domain (IID) of Zaire (PDB 3FKE) (Figure 2-7B) and Reston VP35 IID (PDB 3L2A) (Figure 2-7C) in the free form and Zaire VP35 IID in the

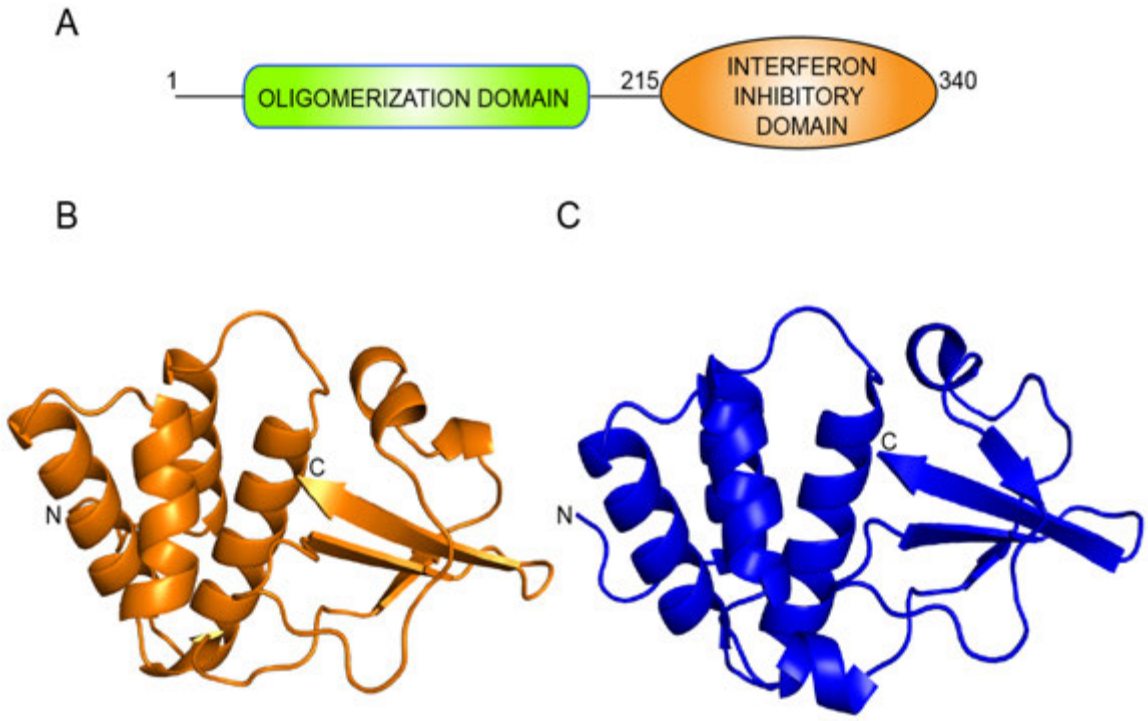

Figure 2-7. Crystal structures of EBOV VP35 IID.

(A) ZEBOV VP35 is a two domain proteins with the coiled-coil oligomerization motif (blue) at the N-terminus and the interferon inhibitory domain at the C-terminus (orange). Residue numbering is for ZEBOV VP35. (B) Cartoon representation of structure of ZEBOV VP35 IID in orange (PDB 3FKE) revealed a novel dsRNA binding protein fold with an alpha helical and a beta sheet subdomain(Leung et al, 2009). (C) Cartoon representation of structure of REBOV VP35 IID in blue (PDB 3L2A) shows that the overall fold of IID is highly conserved between the two proteins(Leung et al, 2010b).

dsRNA-bound form (PDB 3L25 and 3L26)(Leung et al, 2009; Leung et al, 2010a; Leung et al, 2010b). Subsequently the REBOV VP35 IID-dsRNA structure was solved by others (PDB 3KS8)(Kimberlin et al, 2010). Both ZEBOV and REBOV VP35 IID form a novel dsRNA-binding fold consisting of an alpha helical subdomain and a beta sheet subdomain. This is structurally distinct from the canonical dsRNA binding domains which consists of a αββββα fold(Masliah et al, 2012). The ZEBOV and REBOV VP35 IID structures had near identical structures(Leung et al, 2010b). EBOV VP35 IID contains two patches of basic residues, the first basic patch (FBP), including residues K222, R225, K248, and K251 is located on the a-helical subdomain of IID (Figure 2-8B) whereas the central basic patch (CBP), consisting of residues R305, K309, R312, K319, R322 and K339, is located on the beta-sheet subdomain of IID (Figure 2-8A)(Leung et al, 2009). In Reston VP35 IID the corresponding CBP residues consist of R301, K308, R311 and K328, which are equivalent to the R312, K319, R322 and K339 residues in ZEBOV VP35. Through biochemical characterization and mutational analysis we found that the residues in the FBP were critical for ZEBOV VP35-NP interactions, and alanine substitutions of the FBP residues resulted in loss of NP binding as assessed by *in vitro* pull-down assays(Prins et al, 2010). This loss of NP binding was correlated to defective replication complex, since alanine substitutions of FBP residues of VP35 resulted in loss of viral replication activity as assessed by a minigenome assay(Prins et al, 2010). This suggests a critical role for ZEBOV VP35-NP interactions in viral replication complex formation. The ZEBOV VP35-dsRNA bound structure showed that the CBP residues are involved in direct interactions with the phosphodiester backbone of the dsRNA through direct and water-mediated hydrogen bonds. Lack of base-specific contacts suggested that

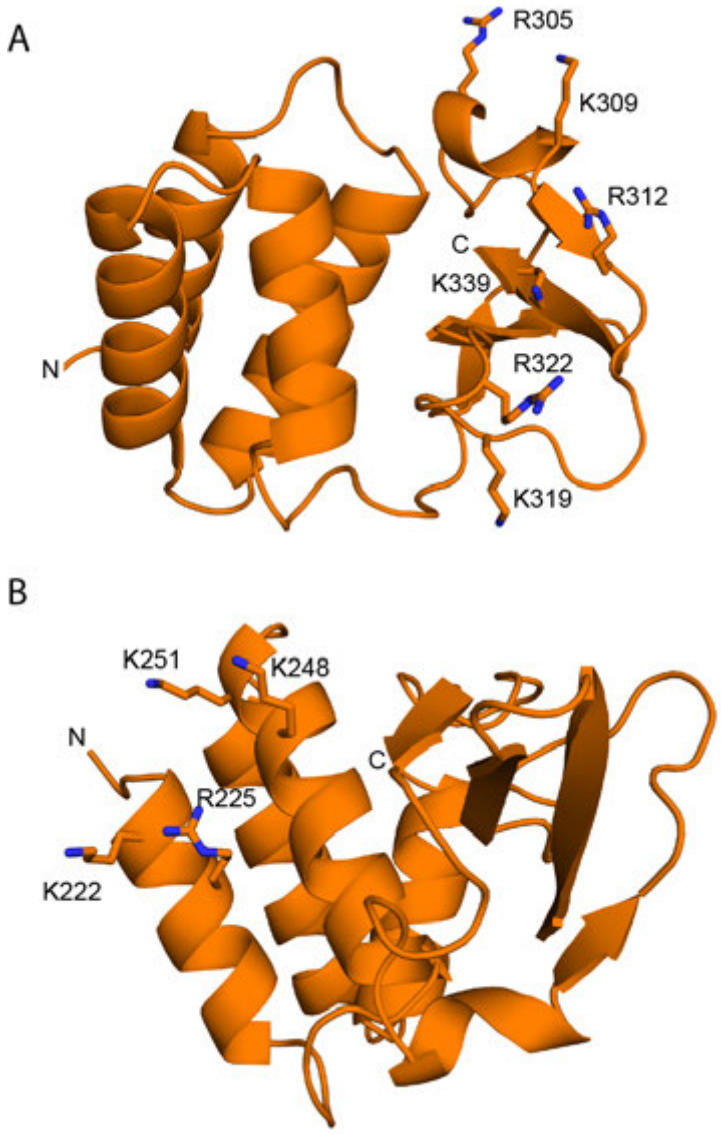

Figure 2-8. Functionally important residues in ZEBOV VP35 IID.

(A) Central basic patch residues in the beta sheet subdomain R305, K309, R312, K319, R322 and K339 are highlighted as sticks. (B) First basic patch residues (FBP) in the alpha helical subdomain K222, R225, K248 and K251 are highlighted as sticks (PDB 3FKE)(Leung et al, 2009).

VP35 binds dsRNA in a sequence independent manner. In addition to the backbone contacts, ZEBOV VP35 can also interact with the blunt-ends through conserved hydrophobic residues such as F239 and I340. Together, this data suggests that the central basic patch (CBP) residues and surrounding basic residues contribute to dsRNA binding and play an important role in VP35 mediated IFN antagonism.

Once the host immune system has been successfully evaded to facilitate viral protein production and viral genomic replication, new nucleocapsids are assembled with the viral genomic RNA and these viral components are transported through the host golgi and trans-golgi pathway to the cell surface, in preparation for viral egress. The host protein complex called endosomal sorting complex required for transport (ESCRT)-1 has been implicated in forming multivesicular bodies carrying viral proteins, that are involved in budding and egress. The viral GP undergoes glycosylation and processing by getting transported through the host golgi apparatus and is expressed on the cell surface(Dolnik et al, 2010; Silvestri et al, 2007). New virions are assembled near the host cell membrane, mediated by the transport and localization of viral proteins embedded in lipid raft-like structures, and these virions then undergo cell egress, acquiring the GP-decorated host membrane in the process (Figure 2-2).

2.4 Differences between ebolavirus and marburgvirus

In order to develop panfiloviral therapeutics or vaccines, it is important to gain insights into the differences and similarities between ZEBOV and MARV. Despite the overall similarities in genome size and organization, virion structure and disease

characteristics, EBOV and MARV have important and interesting differences not only in host tropism, mechanisms of viral entry, viral replication and transcription strategies, but also in mechanisms of immune evasion(Basler & Amarasinghe, 2009; Enterlein et al, 2009; Feldmann et al, 1999; Hartman et al, 2008; Mehedi et al, 2011; Mittler et al, 2011; Muhlberger et al, 1998; Muhlberger et al, 1999; Valmas & Basler, 2011; Valmas et al, 2010). At the level of genome organization, several differences have been observed between ZEBOV and MARV. For example, the filoviral genome has short specific sequences at the untranslated regions (UTRs) of both the 5' and 3' ends(Enterlein et al, 2009). These short stretches of RNA regulate transcriptional initiation, termination, replication and genome encapsidation. Previous work has shown that a single stem-loop secondary structure at the 3' UTR of NP in the ZEBOV genome regulates VP30 mediated transcriptional initiation(Weik et al, 2002). Similar studies of the MARV genome have shown that the RNA secondary structure at the 3' UTR of NP is substantially different, consisting of two stem-loop regions. While the first stem-loop structure is also found in the ZEBOV 3' UTR, the second stem-loop is MARV genome specific and is responsible for transcription initiation that occurs independent of VP30 protein in MARV. This is consistent with recent studies that were aimed at developing an artificial minigenome model to study filoviral transcription and replication, which revealed that EBOV and MARV had distinct nucleocapsid requirements. While only NP, VP35 and L were required and sufficient to carry out both genome replication and transcription in the case of MARV, EBOV required four nucleocapsid proteins – NP, VP35, L and VP30 to carry out transcription(Muhlberger et al, 1998; Muhlberger et al, 1999). Moreover, if one of the three proteins NP, VP35 or L was exchanged with the heterologous protein, genome replication or transcription did not occur,

suggesting significant differences in nucleocapsid formation. Transcriptional profiling and bioinformatics analysis of human hepatocytes infected with EBOV and MARV suggest that the viruses are similar in their ability to regulate TLR, Type I IFN, and PKR mediated signaling pathways. Notably, both EBOV and MARV were able to regulate antiviral ISGs and inflammatory cytokine production in hepatocytes(Kash et al, 2006). However, when these cells were analyzed for the phosphorylation states of STAT1 and STAT2, MARV infected cells, but not EBOV infected cells, showed significant reduction of STAT phosphorylation. Given that both EBOV and MARV were able to inhibit the production of ISGs, these data suggest that there may be distinct underlying immune evasion mechanisms. Unlike EBOV VP24, MARV VP24 does not participate in inhibiting type I IFN signaling. Instead recent studies have shown that MARV VP40 can inhibit the JAK-STAT pathway by direct inhibition of phosphorylation of STAT proteins by interacting with the JAK1 and TYK2 kinases(Valmas & Basler, 2011; Valmas et al, 2010). Thus MARV VP40, in addition to its role in the virion as a matrix protein, is able to inhibit not only type I IFN signaling but also type II IFN signaling, because both these IFNs use common Janus kinases to activate the downstream transcription factors STAT and IRF-9. MARV VP40, by inhibiting this signal transduction cascade upstream of phosphorylation of STATs and IRF-9, can inhibit the transcription of both ISGs and genes under the GAS promoter.

2.5 Conclusions

Key differences in genome organization, transcription, replication, host entry, viral tropism, and immune evasion mechanisms of the viral proteins suggests that MARV and EBOV are distinct viruses, even though they retain some overall similarities. These

observations motivate our undertaking studies that aim to understand differences in structural, functional and mechanistic aspects of filoviral proteins, especially VP35, in order to characterize unique aspects of these two viruses. Most of the mechanistic studies addressing immune evasion by filoviruses have been done in EBOV, particularly in ZEBOV, highlighting the lack of understanding of how the corresponding proteins in MARV function. This underscores the need for studying MARV proteins in order to develop strategies to target common mechanisms that these two deadly filoviruses may use for immune evasion.

2.6 References

(1978a) Ebola haemorrhagic fever in Sudan, 1976. Report of a WHO/International Study Team. *Bulletin of the World Health Organization* **56:** 247-270

(1978b) Ebola haemorrhagic fever in Zaire, 1976. *Bulletin of the World Health Organization* **56:** 271-293

Aleksandrowicz P, Marzi A, Biedenkopf N, Beimforde N, Becker S, Hoenen T, Feldmann H, Schnittler HJ (2011) Ebola virus enters host cells by macropinocytosis and clathrin-mediated endocytosis. *J Infect Dis* **204 Suppl 3:** S957-967

Alves DA, Glynn AR, Steele KE, Lackemeyer MG, Garza NL, Buck JG, Mech C, Reed DS (2010) Aerosol exposure to the angola strain of marburg virus causes lethal viral hemorrhagic Fever in cynomolgus macaques. *Veterinary pathology* **47:** 831-851

Bale S, Liu T, Li S, Wang Y, Abelson D, Fusco M, Woods VL, Jr., Saphire EO Ebola virus glycoprotein needs an additional trigger, beyond proteolytic priming for membrane fusion. *PLoS Negl Trop Dis* **5:** e1395

Barrette RW, Metwally SA, Rowland JM, Xu L, Zaki SR, Nichol ST, Rollin PE, Towner JS, Shieh WJ, Batten B, Sealy TK, Carrillo C, Moran KE, Bracht AJ, Mayr GA, Sirios-Cruz M, Catbagan DP, Lautner EA, Ksiazek TG, White WR, McIntosh MT (2009) Discovery of swine as a host for the Reston ebolavirus. *Science* **325:** 204-206

Baskerville A, Fisher-Hoch SP, Neild GH, Dowsett AB (1985) Ultrastructural pathology of experimental Ebola haemorrhagic fever virus infection. *The Journal of pathology* **147:** 199-209

Basler CF, Amarasinghe GK (2009) Evasion of interferon responses by Ebola and Marburg viruses. *Journal of Interferon and Cytokine Research* **29:** 511-520

Basler CF, Wang X, Muhlberger E, Volchkov V, Paragas J, Klenk HD, Garcia-Sastre A, Palese P (2000) The Ebola virus VP35 protein functions as a type I IFN antagonist. *Proc Natl Acad Sci U S A* **97:** 12289-12294

Bausch DG, Nichol ST, Muyembe-Tamfum JJ, Borchert M, Rollin PE, Sleurs H, Campbell P, Tshioko FK, Roth C, Colebunders R, Pirard P, Mardel S, Olinda LA, Zeller H, Tshomba A, Kulidri A, Libande ML, Mulangu S, Formenty P, Grein T, Leirs H, Braack L, Ksiazek T, Zaki S, Bowen MD, Smit SB, Leman PA, Burt FJ, Kemp A, Swanepoel R (2006) Marburg hemorrhagic fever associated with multiple genetic lineages of virus. *New England Journal of Medicine* **355:** 909-919

Becker S, Rinne C, Hofsass U, Klenk HD, Muhlberger E (1998) Interactions of Marburg virus nucleocapsid proteins. *Virology* **249:** 406-417

Bosio CM, Aman MJ, Grogan C, Hogan R, Ruthel G, Negley D, Mohamadzadeh M, Bavari S, Schmaljohn A (2003) Ebola and Marburg viruses replicate in monocyte-derived dendritic cells without inducing the production of cytokines and full maturation. *Journal of Infectious Diseases* **188:** 1630-1638

Brecher M, Schornberg KL, Delos SE, Fusco ML, Saphire EO, White JM Cathepsin cleavage potentiates the Ebola virus glycoprotein to undergo a subsequent fusion-relevant conformational change. *J Virol* **86:** 364-372

Brindley MA, Hunt CL, Kondratowicz AS, Bowman J, Sinn PL, McCray PB, Jr., Quinn K, Weller ML, Chiorini JA, Maury W (2011) Tyrosine kinase receptor Axl enhances entry of Zaire ebolavirus without direct interactions with the viral glycoprotein. *Virology* **415:** 83-94

Bwaka MA, Bonnet MJ, Calain P, Colebunders R, De Roo A, Guimard Y, Katwiki KR, Kibadi K, Kipasa MA, Kuvula KJ, Mapanda BB, Massamba M, Mupapa KD, Muyembe-Tamfum JJ, Ndaberey E, Peters CJ, Rollin PE, Van den Enden E (1999) Ebola hemorrhagic fever in Kikwit, Democratic Republic of the Congo: clinical observations in 103 patients. *Journal of Infectious Diseases* **179 Suppl 1:** S1-7

Cardenas WB, Loo YM, Gale M, Jr., Hartman AL, Kimberlin CR, Martinez-Sobrido L, Saphire EO, Basler CF (2006) Ebola virus VP35 protein binds double-stranded RNA and inhibits alpha/beta interferon production induced by RIG-I signaling. *J Virol* **80:** 5168-5178

Carette JE, Raaben M, Wong AC, Herbert AS, Obernosterer G, Mulherkar N, Kuehne AI, Kranzusch PJ, Griffin AM, Ruthel G, Dal Cin P, Dye JM, Whelan SP, Chandran K, Brummelkamp TR (2011) Ebola virus entry requires the cholesterol transporter Niemann-Pick C1. *Nature* **477:** 340-343

Cote M, Misasi J, Ren T, Bruchez A, Lee K, Filone CM, Hensley L, Li Q, Ory D, Chandran K, Cunningham J (2011) Small molecule inhibitors reveal Niemann-Pick C1 is essential for Ebola virus infection. *Nature* **477:** 344-348

Crary SM, Towner JS, Honig JE, Shoemaker TR, Nichol ST (2003) Analysis of the role of predicted RNA secondary structures in Ebola virus replication. *Virology* **306:** 210-218

Dessen A, Volchkov V, Dolnik O, Klenk HD, Weissenhorn W (2000) Crystal structure of the matrix protein VP40 from Ebola virus. *EMBO J* **19:** 4228-4236

Dolnik O, Kolesnikova L, Stevermann L, Becker S (2010) Tsg101 is recruited by a late domain of the nucleocapsid protein to support budding of Marburg virus-like particles. *J Virol* **84:** 7847-7856

Elliott LH, Kiley MP, McCormick JB (1985) Descriptive analysis of Ebola virus proteins. *Virology* **147:** 169-176

Ellis DS, Simpson IH, Francis DP, Knobloch J, Bowen ET, Lolik P, Deng IM (1978) Ultrastructure of Ebola virus particles in human liver. *Journal of clinical pathology* **31:** 201-208

Enterlein S, Schmidt KM, Schumann M, Conrad D, Krahling V, Olejnik J, Muhlberger E (2009) The marburg virus 3' noncoding region structurally and functionally differs from that of ebola virus. *J Virol* **83:** 4508-4519

Falzarano D, Krokhin O, Wahl-Jensen V, Seebach J, Wolf K, Schnittler HJ, Feldmann H (2006) Structure-function analysis of the soluble glycoprotein, sGP, of Ebola virus. *Chembiochem : a European journal of chemical biology* **7:** 1605-1611

Feldmann H, Geisbert TW (2011) Ebola haemorrhagic fever. *Lancet*

Feldmann H, Volchkov VE, Volchkova VA, Klenk HD (1999) The glycoproteins of Marburg and Ebola virus and their potential roles in pathogenesis. *Archives of virology Supplementum* **15:** 159-169

Gear JS, Cassel GA, Gear AJ, Trappler B, Clausen L, Meyers AM, Kew MC, Bothwell TH, Sher R, Miller GB, Schneider J, Koornhof HJ, Gomperts ED, Isaacson M, Gear JH (1975) Outbreake of Marburg virus disease in Johannesburg. *British Medical Journal* **4:** 489-493

Georges AJ, Leroy EM, Renaut AA, Benissan CT, Nabias RJ, Ngoc MT, Obiang PI, Lepage JP, Bertherat EJ, Benoni DD, Wickings EJ, Amblard JP, Lansoud-Soukate JM, Milleliri JM, Baize S, Georges-Courbot MC (1999) Ebola hemorrhagic fever outbreaks in Gabon, 1994-1997: epidemiologic and health control issues. *Journal of Infectious Diseases* **179 Suppl 1:** S65-75

Gomis-Ruth FX, Dessen A, Timmins J, Bracher A, Kolesnikowa L, Becker S, Klenk HD, Weissenhorn W (2003) The matrix protein VP40 from Ebola virus octamerizes into pore-like structures with specific RNA binding properties. *Structure* **11:** 423-433

Hartlieb B, Muziol T, Weissenhorn W, Becker S (2007) Crystal structure of the C-terminal domain of Ebola virus VP30 reveals a role in transcription and nucleocapsid association. *Proc Natl Acad Sci U S A* **104:** 624-629

Hartman AL, Ling L, Nichol ST, Hibberd ML (2008) Whole-genome expression profiling reveals that inhibition of host innate immune response pathways by Ebola virus can be reversed by a single amino acid change in the VP35 protein. *J Virol* **82:** 5348-5358

Hartman AL, Towner JS, Nichol ST (2004) A C-terminal basic amino acid motif of Zaire ebolavirus VP35 is essential for type I interferon antagonism and displays high identity with

the RNA-binding domain of another interferon antagonist, the NS1 protein of influenza A virus. *Virology* **328:** 177-184

Hartman AL, Towner JS, Nichol ST (2010) Ebola and marburg hemorrhagic fever. *Clinics in laboratory medicine* **30:** 161-177

Heymann DL, Weisfeld JS, Webb PA, Johnson KM, Cairns T, Berquist H (1980) Ebola hemorrhagic fever: Tandala, Zaire, 1977-1978. *Journal of Infectious Diseases* **142:** 372-376

Hoenen T, Biedenkopf N, Zielecki F, Jung S, Groseth A, Feldmann H, Becker S (2010a) Oligomerization of Ebola virus VP40 is essential for particle morphogenesis and regulation of viral transcription. *J Virol* **84:** 7053-7063

Hoenen T, Jung S, Herwig A, Groseth A, Becker S (2010b) Both matrix proteins of Ebola virus contribute to the regulation of viral genome replication and transcription. *Virology* **403:** 56-66

Huang Y, Xu L, Sun Y, Nabel GJ (2002) The assembly of Ebola virus nucleocapsid requires virion-associated proteins 35 and 24 and posttranslational modification of nucleoprotein. *Mol Cell* **10:** 307-316

Hunt CL, Kolokoltsov AA, Davey RA, Maury W (2011) The Tyro3 receptor kinase Axl enhances macropinocytosis of Zaire ebolavirus. *J Virol* **85:** 334-347

Hunt CL, Lennemann NJ, Maury W (2012) Filovirus entry: a novelty in the viral fusion world. *Viruses* **4:** 258-275

Jahrling PB, Geisbert TW, Dalgard DW, Johnson ED, Ksiazek TG, Hall WC, Peters CJ (1990) Preliminary report: isolation of Ebola virus from monkeys imported to USA. *Lancet* **335:** 502-505

Kash JC, Muhlberger E, Carter V, Grosch M, Perwitasari O, Proll SC, Thomas MJ, Weber F, Klenk HD, Katze MG (2006) Global suppression of the host antiviral response by Ebola- and Marburgviruses: increased antagonism of the type I interferon response is associated with enhanced virulence. *J Virol* **80:** 3009-3020

Kimberlin CR, Bornholdt ZA, Li S, Woods VL, Jr., MacRae IJ, Saphire EO (2010) Ebolavirus VP35 uses a bimodal strategy to bind dsRNA for innate immune suppression. *Proc Natl Acad Sci U S A* **107:** 314-319

Kondratowicz AS, Lennemann NJ, Sinn PL, Davey RA, Hunt CL, Moller-Tank S, Meyerholz DK, Rennert P, Mullins RF, Brindley M, Sandersfeld LM, Quinn K, Weller M, McCray PB, Jr., Chiorini J, Maury W (2011) T-cell immunoglobulin and mucin domain 1 (TIM-1) is a receptor for Zaire Ebolavirus and Lake Victoria Marburgvirus. *Proc Natl Acad Sci U S A* **108:** 8426-8431

Kortepeter MG, Bausch DG, Bray M (2011) Basic clinical and laboratory features of filoviral hemorrhagic fever. *J Infect Dis* **204 Suppl 3:** S810-816

Lee JE, Fusco ML, Hessell AJ, Oswald WB, Burton DR, Saphire EO (2008) Structure of the Ebola virus glycoprotein bound to an antibody from a human survivor. *Nature* **454:** 177-182

Lee JE, Saphire EO (2009) Ebolavirus glycoprotein structure and mechanism of entry. *Future Virol* **4:** 621-635

Leffel EK, Reed DS (2004) Marburg and Ebola viruses as aerosol threats. *Biosecurity and bioterrorism : biodefense strategy, practice, and science* **2:** 186-191

Leroy EM, Kumulungui B, Pourrut X, Rouquet P, Hassanin A, Yaba P, Delicat A, Paweska JT, Gonzalez JP, Swanepoel R (2005) Fruit bats as reservoirs of Ebola virus. *Nature* **438:** 575-576

Leung DW, Ginder ND, Fulton DB, Nix J, Basler CF, Honzatko RB, Amarasinghe GK (2009) Structure of the Ebola VP35 interferon inhibitory domain. *Proc Natl Acad Sci U S A* **106:** 411-416

Leung DW, Prins KC, Borek DM, Farahbakhsh M, Tufariello JM, Ramanan P, Nix JC, Helgeson LA, Otwinowski Z, Honzatko RB, Basler CF, Amarasinghe GK (2010a) Structural basis for dsRNA recognition and interferon antagonism by Ebola VP35. *Nature Structural & Molecular Biology* **17:** 165-172

Leung DW, Shabman RS, Farahbakhsh M, Prins KC, Borek DM, Wang T, Muhlberger E, Basler CF, Amarasinghe GK (2010b) Structural and Functional Characterization of Reston Ebola Virus VP35 Interferon Inhibitory Domain. *J Mol Biol*

Malashkevich VN, Schneider BJ, McNally ML, Milhollen MA, Pang JX, Kim PS (1999) Core structure of the envelope glycoprotein GP2 from Ebola virus at 1.9-A resolution. *Proc Natl Acad Sci U S A* **96:** 2662-2667

Maruyama T, Rodriguez LL, Jahrling PB, Sanchez A, Khan AS, Nichol ST, Peters CJ, Parren PW, Burton DR (1999) Ebola virus can be effectively neutralized by antibody produced in natural human infection. *J Virol* **73:** 6024-6030

Marzi A, Moller P, Hanna SL, Harrer T, Eisemann J, Steinkasserer A, Becker S, Baribaud F, Pohlmann S (2007) Analysis of the interaction of Ebola virus glycoprotein with DC-SIGN (dendritic cell-specific intercellular adhesion molecule 3-grabbing nonintegrin) and its homologue DC-SIGNR. *J Infect Dis* **196 Suppl 2:** S237-246

Masliah G, Barraud P, Allain FH (2012) RNA recognition by double-stranded RNA binding domains: a matter of shape and sequence. *Cellular and molecular life sciences : CMLS*

Mateo M, Reid SP, Leung LW, Basler CF, Volchkov VE (2010) Ebolavirus VP24 binding to karyopherins is required for inhibition of interferon signaling. *J Virol* **84:** 1169-1175

Matsuno K, Kishida N, Usami K, Igarashi M, Yoshida R, Nakayama E, Shimojima M, Feldmann H, Irimura T, Kawaoka Y, Takada A (2010) Different potential of C-type lectin-mediated entry between Marburg virus strains. *J Virol* **84:** 5140-5147

Mehedi M, Falzarano D, Seebach J, Hu X, Carpenter MS, Schnittler HJ, Feldmann H (2011) A new Ebola virus nonstructural glycoprotein expressed through RNA editing. *J Virol* **85:** 5406-5414

Mittler E, Kolesnikova L, Hartlieb B, Davey R, Becker S (2011) The cytoplasmic domain of Marburg virus GP modulates early steps of viral infection. *J Virol* **85:** 8188-8196

Modrof J, Muhlberger E, Klenk HD, Becker S (2002) Phosphorylation of VP30 impairs ebola virus transcription. *J Biol Chem* **277:** 33099-33104

Muhlberger E, Lotfering B, Klenk HD, Becker S (1998) Three of the four nucleocapsid proteins of Marburg virus, NP, VP35, and L, are sufficient to mediate replication and transcription of Marburg virus-specific monocistronic minigenomes. *Journal of Virology* **72:** 8756-8764

Muhlberger E, Weik M, Volchkov VE, Klenk HD, Becker S (1999) Comparison of the transcription and replication strategies of marburg virus and Ebola virus by using artificial replication systems. *Journal of Virology* **73:** 2333-2342

Nanbo A, Imai M, Watanabe S, Noda T, Takahashi K, Neumann G, Halfmann P, Kawaoka Y (2010) Ebolavirus is internalized into host cells via macropinocytosis in a viral glycoprotein-dependent manner. *PLoS Pathog* **6:** e1001121

Negredo A, Palacios G, Vazquez-Moron S, Gonzalez F, Dopazo H, Molero F, Juste J, Quetglas J, Savji N, de la Cruz Martinez M, Herrera JE, Pizarro M, Hutchison SK, Echevarria JE, Lipkin WI, Tenorio A (2011) Discovery of an ebolavirus-like filovirus in europe. *PLoS Pathog* **7:** e1002304

Noda T, Halfmann P, Sagara H, Kawaoka Y (2007) Regions in Ebola virus VP24 that are important for nucleocapsid formation. *J Infect Dis* **196 Suppl 2:** S247-250

Olal D, Kuehne AI, Bale S, Halfmann P, Hashiguchi T, Fusco ML, Lee JE, King LB, Kawaoka Y, Dye JM, Jr., Saphire EO (2012) Structure of an antibody in complex with its mucin domain linear epitope that is protective against Ebola virus. *J Virol* **86:** 2809-2816

Prins KC, Binning JM, Shabman RS, Leung DW, Amarasinghe GK, Basler CF (2010) Basic residues within the ebolavirus VP35 protein are required for its viral polymerase cofactor function. *J Virol* **84:** 10581-10591

Reid SP, Leung LW, Hartman AL, Martinez O, Shaw ML, Carbonnelle C, Volchkov VE, Nichol ST, Basler CF (2006) Ebola virus VP24 binds karyopherin alpha1 and blocks STAT1 nuclear accumulation. *J Virol* **80:** 5156-5167

Reid SP, Valmas C, Martinez O, Sanchez FM, Basler CF (2007) Ebola virus VP24 proteins inhibit the interaction of NPI-1 subfamily karyopherin alpha proteins with activated STAT1. *J Virol* **81:** 13469-13477

Ruigrok RW, Schoehn G, Dessen A, Forest E, Volchkov V, Dolnik O, Klenk HD, Weissenhorn W (2000) Structural characterization and membrane binding properties of the matrix protein VP40 of Ebola virus. *J Mol Biol* **300:** 103-112

Sanchez A, Kiley MP, Holloway BP, Auperin DD (1993) Sequence analysis of the Ebola virus genome: organization, genetic elements, and comparison with the genome of Marburg virus. *Virus Res* **29:** 215-240

Silvestri LS, Ruthel G, Kallstrom G, Warfield KL, Swenson DL, Nelle T, Iversen PL, Bavari S, Aman MJ (2007) Involvement of vacuolar protein sorting pathway in Ebola virus release independent of TSG101 interaction. *J Infect Dis* **196 Suppl 2:** S264-270

Takada A (2012) Filovirus tropism: cellular molecules for viral entry. *Frontiers in microbiology* **3:** 34

Towner JS, Amman BR, Sealy TK, Carroll SA, Comer JA, Kemp A, Swanepoel R, Paddock CD, Balinandi S, Khristova ML, Formenty PB, Albarino CG, Miller DM, Reed ZD, Kayiwa JT, Mills JN, Cannon DL, Greer PW, Byaruhanga E, Farnon EC, Atimnedi P, Okware S, Katongole-Mbidde E, Downing R, Tappero JW, Zaki SR, Ksiazek TG, Nichol ST, Rollin PE (2009) Isolation of genetically diverse Marburg viruses from Egyptian fruit bats. *PLoS Pathog* **5:** e1000536

Towner JS, Sealy TK, Khristova ML, Albarino CG, Conlan S, Reeder SA, Quan PL, Lipkin WI, Downing R, Tappero JW, Okware S, Lutwama J, Bakamutumaho B, Kayiwa J, Comer JA, Rollin PE, Ksiazek TG, Nichol ST (2008) Newly discovered ebola virus associated with hemorrhagic fever outbreak in Uganda. *PLoS Pathogens* **4:** e1000212

Urata S, Noda T, Kawaoka Y, Morikawa S, Yokosawa H, Yasuda J (2007) Interaction of Tsg101 with Marburg virus VP40 depends on the PPPY motif, but not the PT/SAP motif as in the case of Ebola virus, and Tsg101 plays a critical role in the budding of Marburg virus-like particles induced by VP40, NP, and GP. *J Virol* **81:** 4895-4899

Valmas C, Basler CF (2011) Marburg virus VP40 antagonizes interferon signaling in a species-specific manner. *Journal of Virology* **85:** 4309-4317

Valmas C, Grosch MN, Schumann M, Olejnik J, Martinez O, Best SM, Krahling V, Basler CF, Muhlberger E (2010) Marburg virus evades interferon responses by a mechanism distinct from ebola virus. *PLoS Pathog* **6:** e1000721

Volchkov VE, Feldmann H, Volchkova VA, Klenk HD (1998) Processing of the Ebola virus glycoprotein by the proprotein convertase furin. *Proc Natl Acad Sci U S A* **95:** 5762-5767

Watanabe S, Noda T, Halfmann P, Jasenosky L, Kawaoka Y (2007) Ebola virus (EBOV) VP24 inhibits transcription and replication of the EBOV genome. *J Infect Dis* **196 Suppl 2:** S284-290

Weik M, Modrof J, Klenk HD, Becker S, Muhlberger E (2002) Ebola virus VP30-mediated transcription is regulated by RNA secondary structure formation. *Journal of Virology* **76:** 8532-8539

Welsch S, Kolesnikova L, Krahling V, Riches JD, Becker S, Briggs JA (2010) Electron tomography reveals the steps in filovirus budding. *PLoS Pathog* **6:** e1000875

Zhang AP, Bornholdt ZA, Liu T, Abelson DM, Lee DE, Li S, Woods VL, Jr., Saphire EO The ebola virus interferon antagonist VP24 directly binds STAT1 and has a novel, pyramidal fold. *PLoS Pathog* **8:** e1002550

CHAPTER 3. STRUCTURAL BASIS FOR IMMUNE EVASION BY EBOLA VP35

Leung DW, Prins KC, Borek DM, Farahbakhsh M, Tufariello JM, Ramanan P, Nix JC, Helgeson LA, Otwinowski Z, Honzatko RB, Basler CF, and Amarasinghe GK. **Structural basis for dsRNA recognition and interferon antagonism by Ebola VP35.** Nat Stuct Mol Biol. 2010 Feb;17(2):165-172.

Prins KC, Selpeut S, Leung DW, Reynard O, Volchkova VA, Reid SP, Ramanan P, Cardenas WB, Amarasinghe GK, Volchkov VE, and Basler CF. **Mutations abrogating VP35 interaction with dsRNA render Ebola virus avirulent in guinea pigs.** J Virol. 2010 Mar;84(6);3004-15.

Structural and biochemical experiments were designed and implemented by Dr. Daisy Leung and Dr. Gaya Amarasinghe. Cloning, expression, purification, crystallization, data collection and processing for ZEBOV VP35 IID-dsRNA complex was performed by Dr. Daisy Leung and Dr. Gaya Amarasinghe. I was involved in the expression, purification of ^{15}N-labeled RIG-I protein and performed NMR experiments. I was also involved in identification and optimization of crystallization conditions for the K319A/R322A mutant of ZEBOV VP35 IID. Mina Farahbakhsh and Luke Helgeson optimized crystallization conditions for the R312A and K339A mutants of ZEBOV VP35 IID respectively. Dr.

Dominika Borek, Dr. Zbysek Otwinowski, Dr. Jay Nix and Dr. Richard Honzatko provided help and insight in data collection, processing and structure determination. Dr. Christopher Basler and colleagues designed and performed the cell-based assays. Dr. Victor Volchkov and colleagues designed and performed the experiments with recombinant ebolavirus.

3.1 Introduction

VP35 is a critical protein and plays multiple roles in the viral replication cycle(Basler & Amarasinghe, 2009). It functions as a structural protein in the virion, mediates transcription and replication as an integral part of the viral replication complex, and functions as an immune antagonist through multiple mechanisms. VP35 has an N-terminal oligomerization domain and a C-terminal interferon inhibitory domain (IID). Structural and biochemical work from our lab identified VP35 IID as a novel RNA binding fold that specifically recognizes dsRNA in a sequence independent fashion. These studies also identified a number of key basic residues that mediate both the dsRNA binding and NP-binding/replication functions of VP35. In order to further understand the mechanisms by which VP35 mediates immune evasion and to understand the structural basis for dsRNA binding, we conducted structural studies on VP35 IID-dsRNA complex.

3.2 Materials and methods

Cloning, protein expression and purification. The coding region of ZEBOV (Mayinga strain), REBOV VP35 IID, full length RIG-I (residues 1-925) and RIG-I C-terminal domain (residues 792-925) was subcloned using Nde1 and BamH1 restriction enzyme sites into a modified pET15b expression vector, downstream of a MBP fusion tag and a TEV cleavage site. Using primers containing the desired mutations, mutant ZEBOV VP35 IID constructs were generated by overlap PCR, digested with restriction enzymes Nde1 and BamH1 and ligated into the same pET vector described above. PCR and DNA sequencing subsequently confirmed the presence of mutations. All the constructs mentioned above were expressed as MBP-fusion proteins by culturing transformed BL21(DE3) cells in LB media at 37°C until an OD_{600} of 0.7. Cells were then chilled in ice and induced with 0.5mM IPTG and cultured overnight at 18°C. Cells were harvested by centrifugation at 10,000 g at 4°C for 10 minutes. Harvested cells were resuspended in lysis buffer containing 25mM sodium phosphate (pH 7.0), 1M NaCl, 5mM β-mercaptoethanol and a protease inhibitor cocktail, flash frozen using liquid nitrogen, and stored at -80°C. Cells were thawed and lysed using an Emulsiflex-C5 homogenizer (Avestin) and clarified by centrifugation at 30,000 g for 30 minutes. The supernatant was then purified using a combination of affinity, cation exchange and size exclusion chromatographic columns (GE Healthcare). The MBP fusion tag was cleaved prior to final purification by using tobacco etch virus (TEV) protease. Protein purity was assessed by SDS-PAGE followed by Coomassie blue staining.

Crystallization, data collection and processing. Initial crystallization trials with purified Zaire VP35 IID K319A/R322A were performed using standard Hampton sparse-matrix screens using hanging-drop vapor diffusion methods and subsequent optimization of hits was done with in-house prepared chemicals. Single, plate shaped crystals of VP35 IID K319A/R322A was obtained in well solution containing 0.1M Bis-Tris pH 6.75, 0.2M ammonium sulfate, and 28% PEG 3350 at protein concentration of 7 mg/mL. Crystals were soaked in well solution containing 10% and 25% glycerol before plunge-freezing in liquid nitrogen. Diffraction data was collected at the Advanced Light Source (ALS), beamline 4.2.2 and Advanced Photon Source (APS), beamline 19 ID. 180 frames were collected at a crystal to detector distance of 125 mm using an oscillation range of 1°.

Diffraction data were indexed, scaled and merged using HKL-3000 (Otwinowski & Minor, 1997). Intensities were converted to structure factors using CCP4 suite. Phases for ZEBOV VP35 IID K319A/R322A mutant and ZEBOV VP35 IID-dsRNA complex structures were determined using molecular replacement with chain B from wildtype ZEBOV VP35 IID crystal structure (3FKE) as search model. Molecular replacement was performed using MOLREP in the CCP4 suite, and the resulting model was refined using REFMAC5 (Murshudov et al, 1997). Water addition and manual model building was performed using Coot (Emsley & Cowtan, 2004). TLS parameters were refined using the TLMSD server (Painter & Merritt, 2006). Final validation was performed using MOLPROBITY server (Chen et al, 2010).

3.3 Structure of EBOV VP35 IID-dsRNA complex

We solved the crystal structure of ZEBOV VP35 IID in complex with 8bp dsRNA using both native (3L25) and selenomethionine (SeMet) labeled protein (3L26). Both structures were solved using molecular replacement with the ZEBOV VP35 IID structure (PDB 3FKE) as the search model. Since the SeMet dataset was the higher resolution dataset, we used this for further processing and analysis. For the SeMet dataset, we observed four molecules of VP35 IID and one molecule of 8bp dsRNA, with a two fold non-crystallographic symmetry, where two of the VP35 IID molecules (chains A and B) are symmetry related to the other two VP35 IID molecules (chains C and D) (Figure 3-1). The overall structure of VP35 IID is very similar compared to the free structure, suggesting that the molecule does not undergo a conformational change during dsRNA binding. Additionally, majority of the contacts are with dsRNA backbone suggesting that VP35 IID recognizes the A form dsRNA helix in a sequence independent manner.

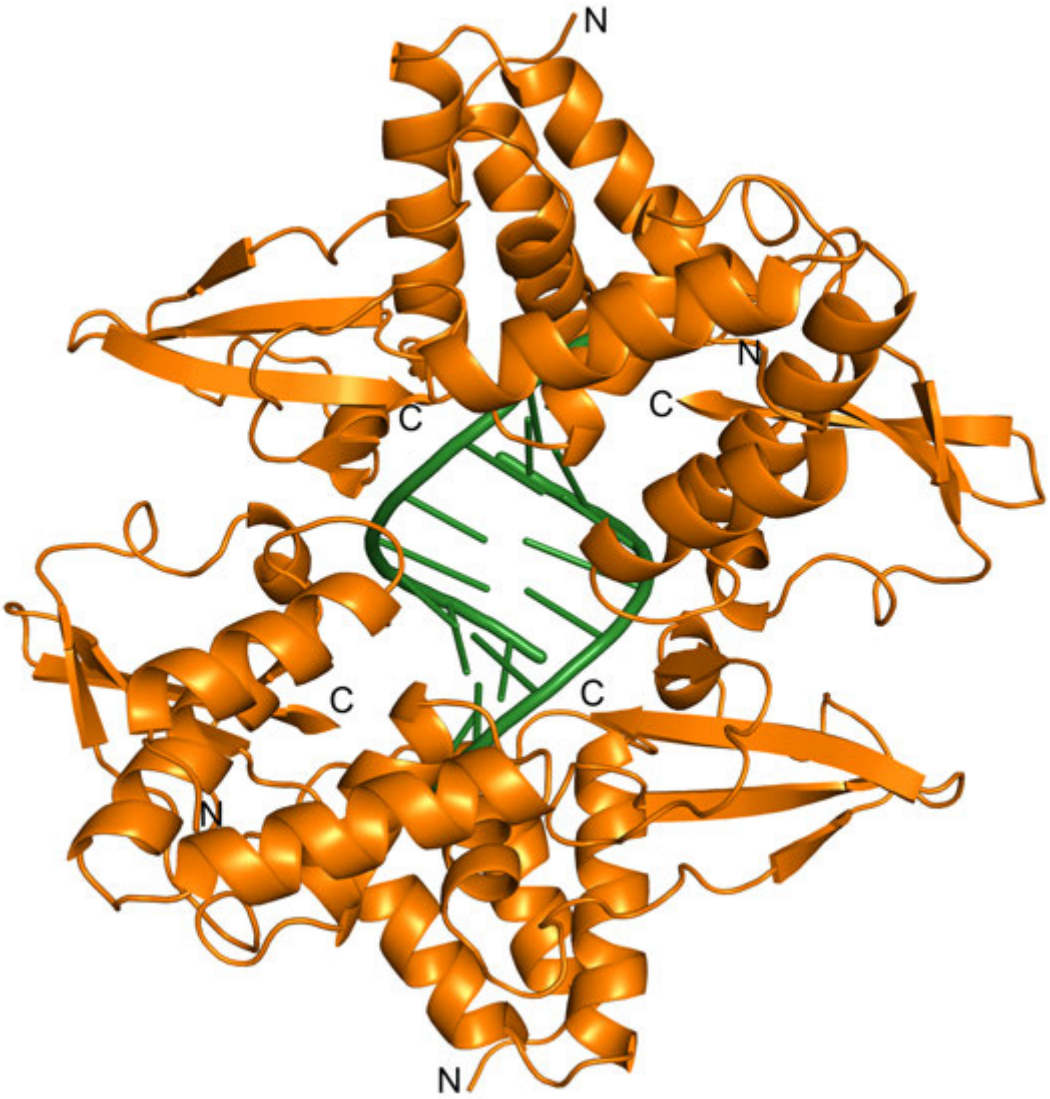

Figure 3-1. Structure of ZEBOV VP35 IID in complex with 8bp dsRNA.

Four molecules of **Z**EBOV VP35 IID (orange) binds to one molecule of 8bp dsRNA (green) backbone and blunt ends. Of the four molecules, which binds dsRNA, two are involved predominantly in VP35-VP35 interactions, while the other two are involved in VP35-dsRNA interactions (PDB 3L26)(Leung et al, 2010).

3.4 CBP residues are involved in VP35-VP35 and VP35-dsRNA interactions

The dsRNA-bound structure of ZEBOV VP35 IID (Figure 3-1) confirms the role of CBP residues in dsRNA binding, as these residues make direct contacts with the phosphate backbone of dsRNA (Figure 3-2A). For example, the side chain NH1 and NH2 atoms of R312 contact the dsRNA U5 O1P and O2P atoms through hydrogen bonds. Similarly the side chain NH2 atom of R322 hydrogen bonds with the C7 O2P and G6 O1P atoms of the dsRNA. Additional residues that mediate VP35-dsRNA interactions include T237, S272, Q274, K309, S310 and I340. In addition to these contacts with dsRNA, the CBP residues R312, R322 and K339 are also involved in salt bridges with the acidic residues such as E262, E269 and D271 of the neighboring VP35 molecule (Figure 3-2B). Hence the CBP residues are not only important for dsRNA binding but also are part of the protein-protein interaction interface. Consistent with the structure mutation of any of the CBP residues, especially R312, R322 and K339 results in complete loss of dsRNA binding as demonstrated by *in vitro* isothermal titration calorimetry experiments (Figure 3-2C). The VP35 IID molecule also interacts with the dsRNA blunt ends by hydrophobic stacking of residues such as F239, I340 and Q274 and thus covers the ends of dsRNA (Figure 3-3). This is very similar to the recognition mode of RIG-I. This structural data suggests that ZEBOV VP35 IID can mimic the RNA binding mode of RIG-I and thus compete with it for dsRNA binding. We also solved the crystal structures of the CBP mutants R312A, K339A and K319A/R322A (Figure 3-4) and were able to show that mutations of these residues do not cause overall changes in

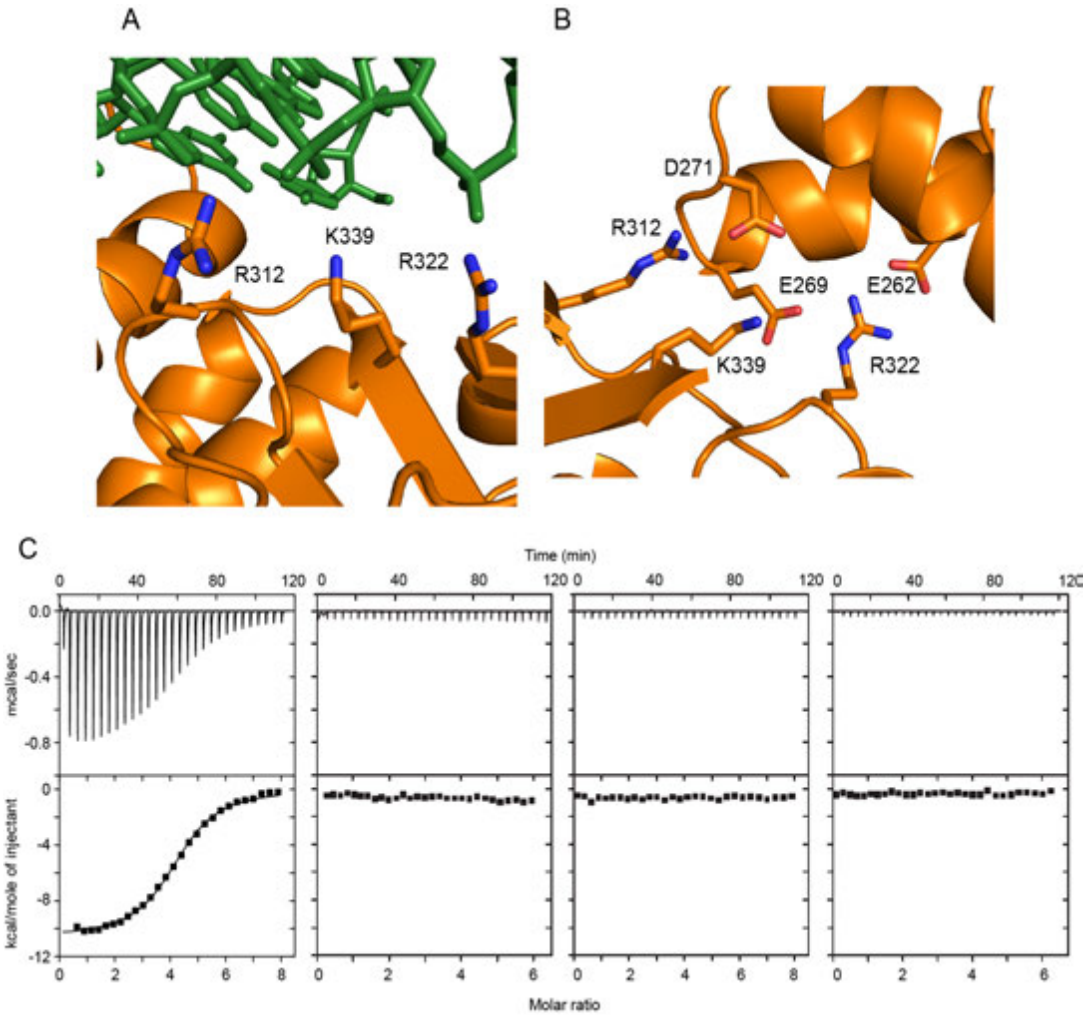

Figure 3-2. CBP residues are important for VP35-VP35 and VP35-dsRNA interactions.

(A) ZEBOV VP35 IID binds to dsRNA (green sticks) through the basic residues contain within the CBP such as R312, K339 and R322 (orange sticks). (B) The CBP residues are also involved in protein-protein interactions with acidic residues such as E262, E269 and D271 (PDB 3L26). (C) ITC data of ZEBOV VP35 IID WT, R312A, R322A and K339A (from left to right) shows that mutation of CBP residues to alanine, leads to loss of dsRNA binding *in vitro* (Leung et al, 2010).

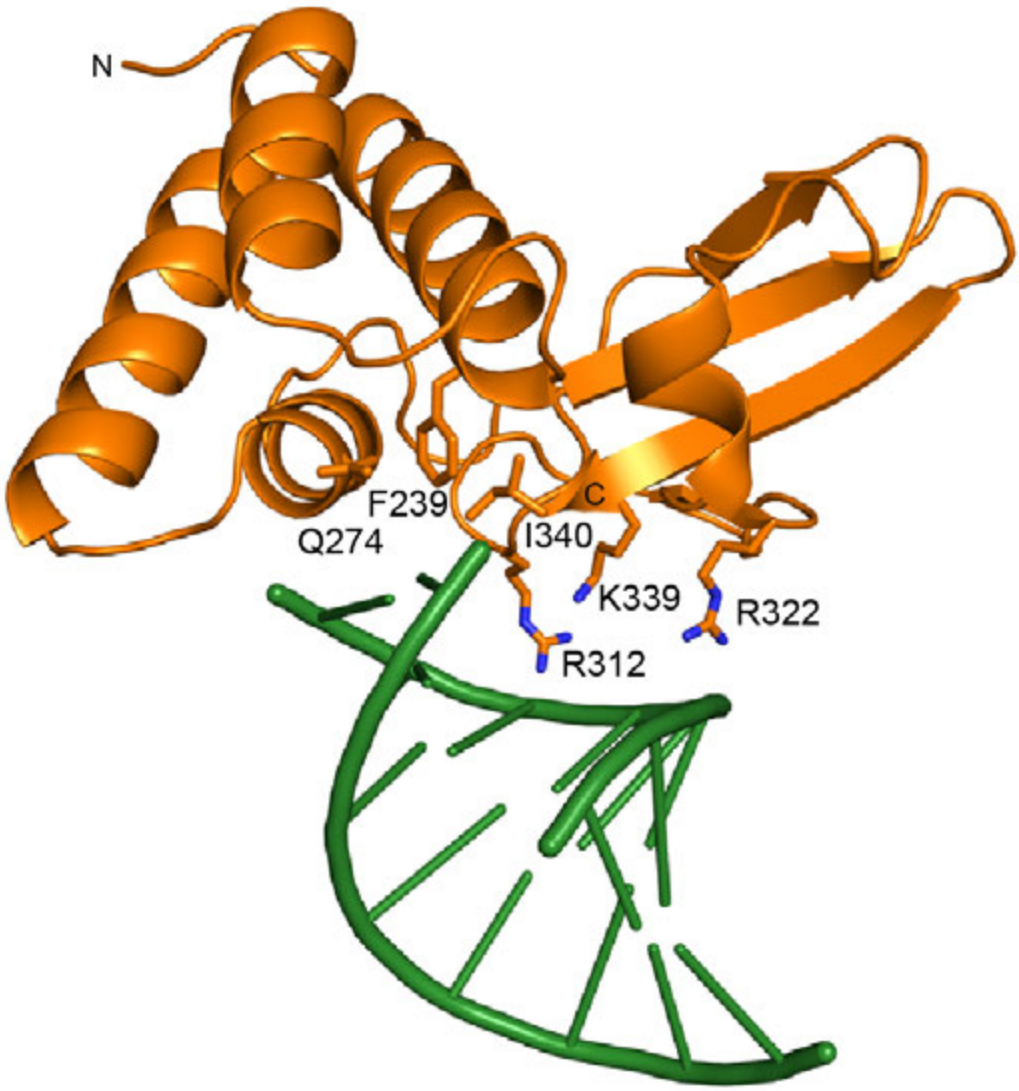

Figure 3-3. VP35 IID caps the blunt-ends of dsRNA.

ZEBOV VP35 IID in addition to binding the dsRNA backbone interacts with the blunt ends of dsRNA mediated by the side chain of residues F239, I340 and Q274 (PDB 3L25)(Leung et al, 2010).

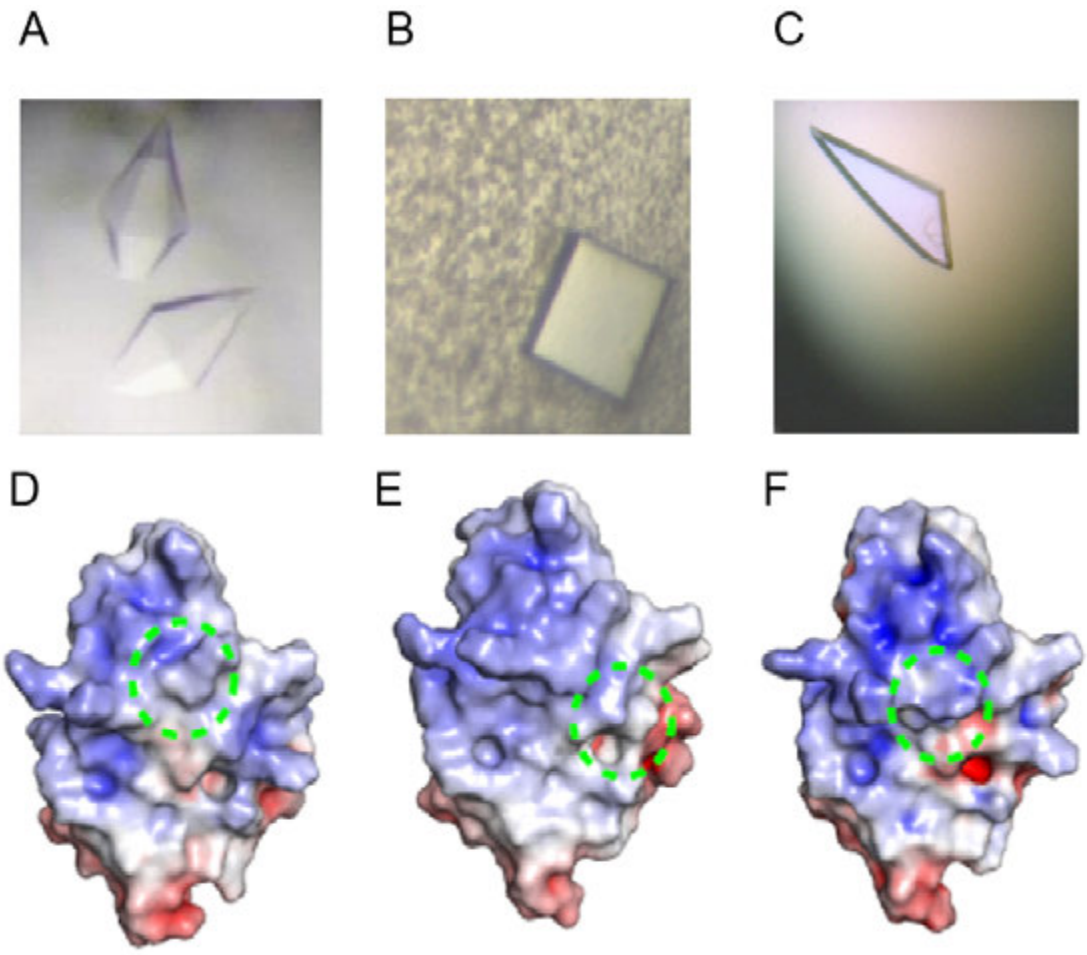

Figure 3-4. Structure of CBP mutants of ZEBOV VP35 IID.

Representative crystals of ZEBOV VP35 IID (A) R312A, (B) K339A and (C) K319A/R322A. The electrostatic surface (red, white and blue represent negative, neutral and positive electrostatic potentials respectively) representation of ZEBOV VP35 IID (range -10 to +10 kT), shows the loss of the positive charge on the surface of the molecule highlighted by dotted green circles for each of the three CBP mutants (D) R312A (PDB 3L27), (E) K339A(PDB 3L28) and (F) K319A/R322A(PDB 3L29)(Leung et al, 2010; Prins et al, 2010).

the structure, but results in changes in the surface electrostatics of the molecule, which affects dsRNA binding.

In order to assess the role of dsRNA binding and its contribution to IFN antagonism by preventing RIG-I like receptors from binding to viral RNA PAMPs, we used a specific nuclear magnetic resonance (NMR) experiment called heteronuclear single quantum coherence (HSQC) experiment to record the spectra of ^{1}H, ^{15}N labeled ZEBOV VP35 IID in the presence and absence of RIG-I and dsRNA. First the experiment was done with only ZEBOV VP35 IID (black spectrum in Figure 3-5A,B and C). Upon addition of in-vitro transcribed (IVT) 8bp dsRNA, the intensities of the individual chemical shifts drop relative to the ZEBOV VP35 IID only spectrum, as a result of increased molecular size and slower tumbling time of the ZEBOV VP35 IID-dsRNA complex in solution (Figure 3-5B). Upon addition of purified RIG-I C-terminal domain (residues 792-925), the intensities did not result in increase in peak intensities, suggesting that ZEBOV VP35 IID can compete with RIG-I for dsRNA binding in solution. This observation is not a result of direct interactions between ZEBOV VP35 IID and RIG-I as addition of RIG-I to ZEBOV VP35 IID in the absence of dsRNA did not cause any chemical shift perturbations and showed peak intensities that were similar relative to the ZEBOV VP35 IID only spectrum. Our collaborators then assessed the effect of ZEBOV VP35 on RIG-I and RNA induced IFN-β promoter activation using *in vivo* assays (Figure 3-5E). These studies were able to show IVT 8-bp dsRNA or hairpin RNA transfection into 293T cells along with a plasmid encoding RIG-I protein, resulted in the activation of the IFN-β promoter as assessed by the luciferase

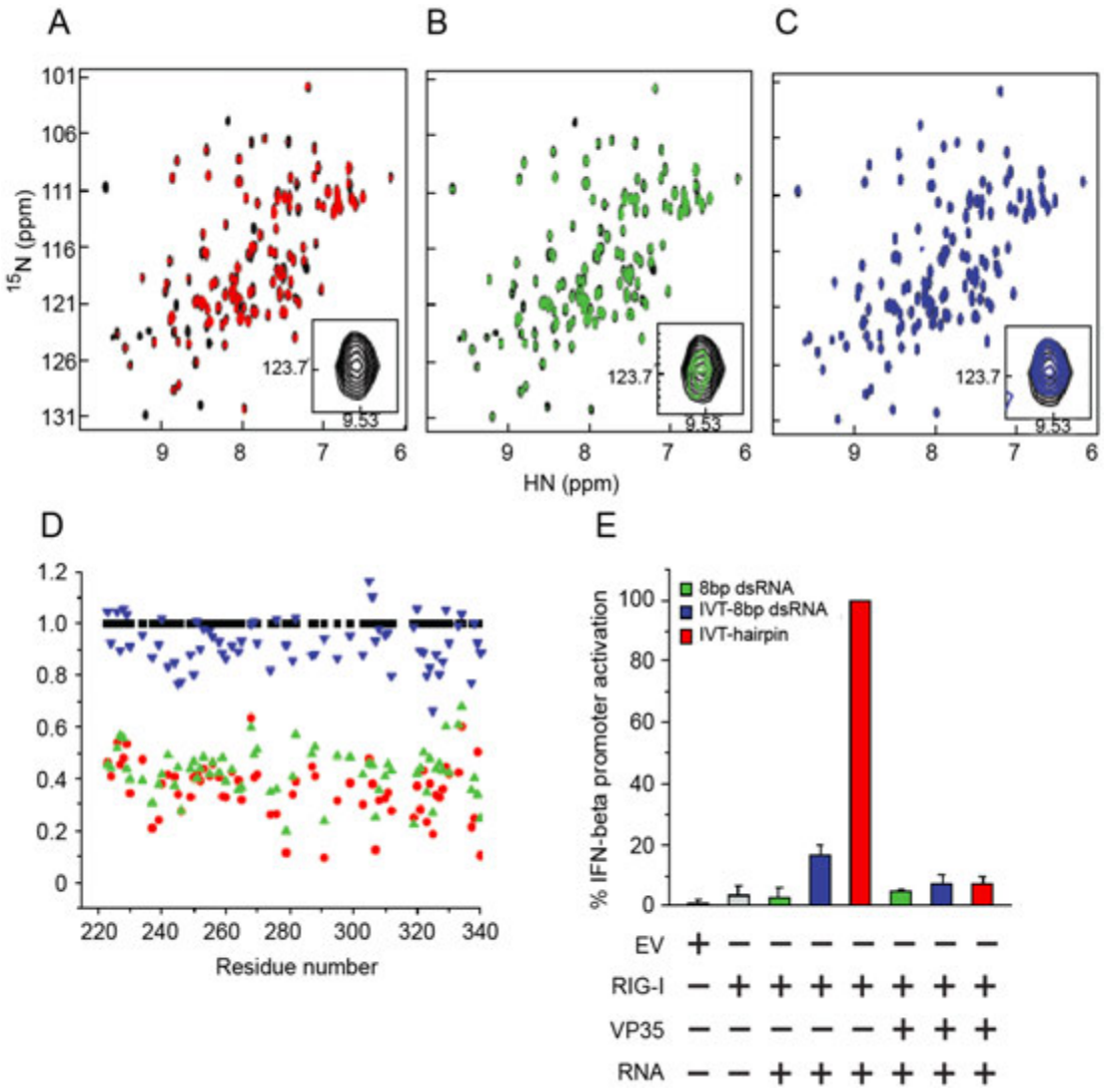

Figure 3-5. ZEBOV VP35 IID competes with RIG-I for dsRNA binding.

HSQC-NMR spectra of ZEBOV VP35 IID (black) after addition of (A) IVT-8bp dsRNA (red), (B) IVT-8bp dsRNA and RIG-I (green) and (C) RIG-I (blue). The peak for R312 residue is shown in the box for each of the three spectra. (D) The peak intensities of every residue from (A), (B) and (C) are plotted relative to the ZEBOV VP35 IID only spectra (black dotted line). (E) IFN-beta reporter activity assay induced by transfection of RIG-I and different RNA ligands in the presence and absence of ZEBOV VP35 (Leung et al, 2010).

reporter gene expression (Figure 3-5E). In contrast, when a plasmid encoding for ZEBOV VP35 was also transfected, the reporter gene expression was significantly less, suggesting that ZEBOV VP35 is able to inhibit IFN-β promoter activity induced as a result of RNA recognition by RIG-I (Figure 3-5E). Together these data support a model for filoviral immune evasion in which ZEBOV VP35 protein can potentially inhibit IFN production by sequestering viral RNA PAMPs from being recognized by RIG-I like receptors.

3.5 ZEBOV VP35 dsRNA binding is correlated with IFN inhibition *in vivo*

In order to assess the effect of these mutations on IFN inhibitory functions of VP35 *in vivo,* our collaborators used an IFN-β reporter assay, in which plasmids encoding either WT or mutant VP35 proteins were transfected into 293T cells, and monitored reporter activity induced by Sendai virus (SeV) infection (Figure 3-6). Our results suggest that the mutation of residues that abrogate RNA binding *in vitro* also diminish VP35's role as an IFN antagonist *in vivo*. In the case of ZEBOV VP35, mutations such as R312A, K339A, K319A/R322A were able to attenuate VP35's ability to inhibit SeV mediated IFN-β promoter activity, whereas mutation of residues in the FBP such as R222A, R225A, K248A and R251A do not have any effect on VP35 in this assay. This correlated well with IFN inhibition, as the same mutants that show diminished dsRNA binding also are impaired in inhbiting IFN-beta promoter activation in vivo. In addition to interacting the with dsRNA backbone, both ZEBOV and REBOV VP35 IIDs also interact with the blunt-ends of the dsRNA(Kimberlin et al, 2010; Leung et al, 2010). These are mediated through hydrophobic base-stacking

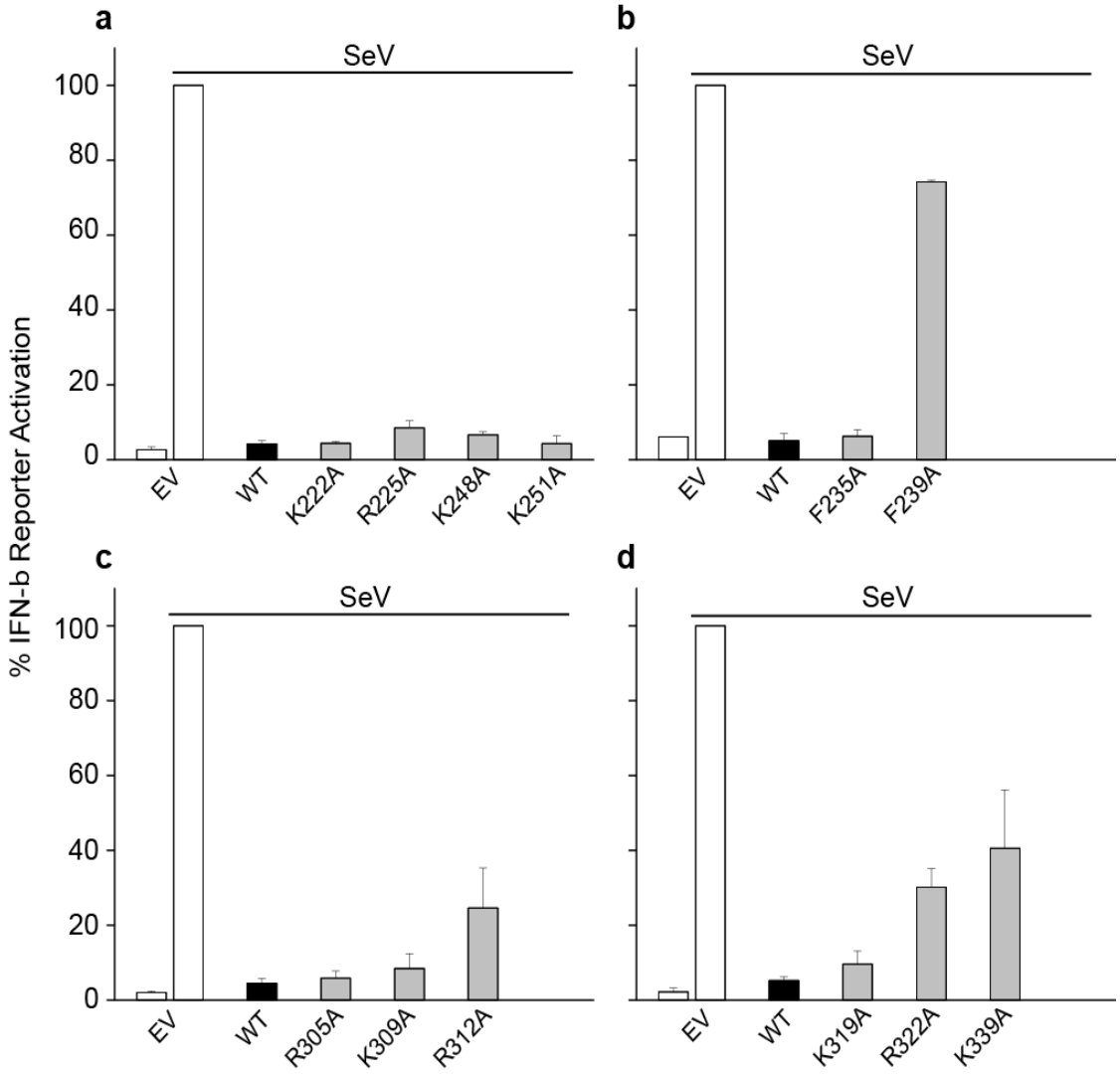

Figure 3-6. dsRNA binding and IFN inhibition are correlated.

(A) IFN-beta reporter activation assays showing that mutation of FBP residues does not have any effect on IFN inhibition by ZEBOV VP35 IID. Mutation of CBP residues (C and D), and end-cap residues such as F239A (last lane in B) result in attenuated dsRNA binding in vitro and corresponding loss of IFN inhibition in vivo (Leung et al, 2010).

contacts mediated by residues such as F239, I340 and Q274in ZEBOV and F228, I340 and Q263 in REBOV. Given the importance of the basic residues of this protein in both immune evasion and viral replication, it was previously shown that deletions or mutations of VP35 and its CBP residues resulted in attenuated growth of the virus in mice(Bray, 2001; Bray et al, 1999; Hartman et al, 2006).

3.6 Mutation of CBP residues renders recombinant ZEBOV avirulent in guinea pigs

Our collaborators extended our *in vitro* and cell-based assays by making recombinant ZEBOV virus carrying either the wildtype VP35 or the K319A/R322A mutation in VP35. In addition the GFP gene was engineered into the virus for monitoring the viral replication in cells. Using these viruses, our collaborators were able to show that both wildtype and the KRA virus were able to replicate efficiently in Vero cells, which lack IFN system (Figure 3-7). In contrast only the WT virus was able to replicate in 293T cells, which can mount an IFN response to counteract the viral infection. The KRA virus was attenuated in 293T cells, highlighting the importance of dsRNA binding and IFN inhibition in the early stages of viral infection (Figure 3-7). Dr. Basler and colleagues were also able to show that the viral protein expression of the KRA virus was severely attenuated in 293T cells, whereas there was robust expression of viral proteins in the case of wildtype virus infection. Subsequently, our collaborators were able to show, using a guinea pig adapted virus, that ZEBOV virus carrying mutations in the central basic patch residues (K319A/R322A) was attenuated and

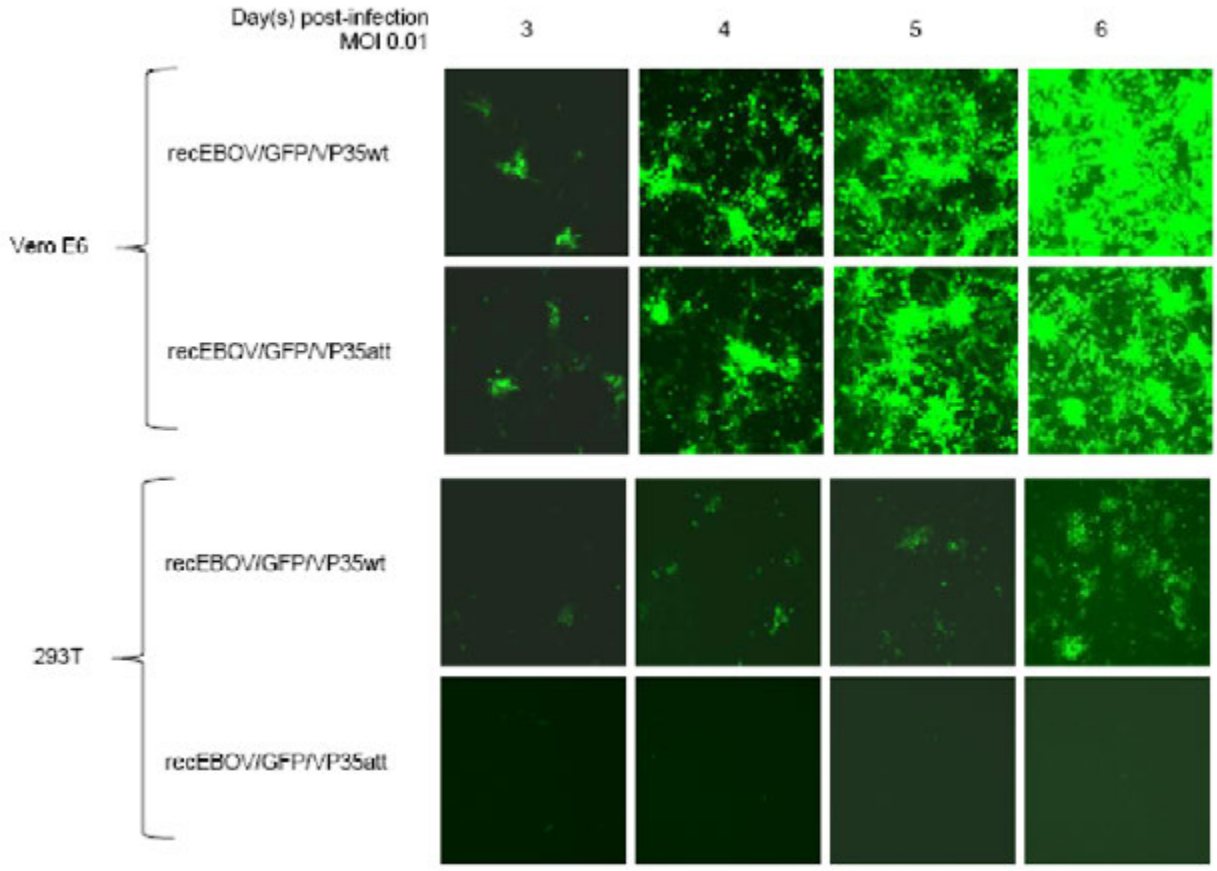

Figure 3-7. Replication of recombinant ZEBOV with CBP mutations is attenuated in 293T cells.

Recombinant ZEBOV virus containing wild type VP35 or VP35 containing K319A/R322A mutations were used to infect Vero cells (top two panels) or 293T cells (bottom two panels). Viral replication was visualized by monitoring expression of GFP which was engineered into the recombinant virus genomes (Prins et al, 2010).

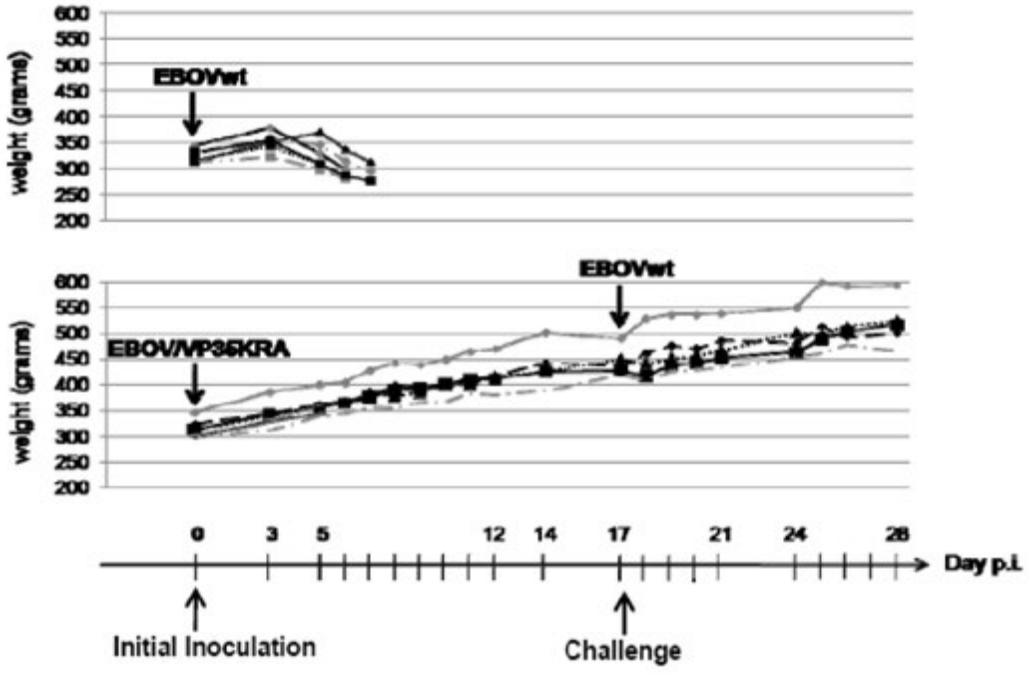

Figure 3-8. Recombinant ZEBOV VP35 IID with CBP mutations is avirulent in guinea pigs.

Recombinant ZEBOV with wild type (top) or K319A/R322A (bottom) containing VP35 were used to infect guinea pigs and the animals were monitored by measuring body weight over a period of time. Animals infected by wildtype VP35 containing viruses die in 1 week post infection, whereas the CBP mutation containing virus was attenuated and the animals were able to grow past 2 weeks without symptoms and was able to protect the animals from further infection by wildtype virus (Prins et al, 2010).

animals infected with this virus showed no external symptoms and survived past two weeks, whereas animals infected with recombinant wildtype virus succumbed to infection in one week (Figure 3-8)(Prins et al, 2010). Moreover, the animals that had been infected with the mutant virus were completely protected when re-challenged with the wildtype virus, highlighting the importance of the dsRNA binding function and its role in early inhibition of innate immune responses in the context of viral infection (Figure 3-8). This experiment suggests that disruption of the dsRNA binding function of VP35 could be a potential strategy to develop therapeutics against filoviruses.

3.7 Conclusions

.

Together this data supports a mechanism by which ZEBOV VP35 interferes with and prevents the recognition of viral RNA by RLRs and activation of the IFN-beta signaling pathway (Figure 3-9). The CBP residues, which make up the positively charged dsRNA binding surface of ZEBOV VP35 IID which includes R312, R322, and K339 play a critical role in IFN inhibition since alanine substitution of the CBP residues results in the loss of IFN inhibition in cell-based assays. In addition to the CBP, the coiled-coil region of VP35 (Figure 2-3A), which facilitates VP35 oligomerization, is also important for the IFN antagonist function of VP35. This suggests that the oligomerization motif on the amino-terminus facilitates the IFN antagonist activity on the carboxy-terminus. More recently the crystal structure of REBOV VP35 IID-dsRNA complex was also solved. The structure suggested a

binding mechanism similar to that of ZEBOV VP35 IID. REBOV VP35 IID also forms a ligand-induced dimer mediated by conserved residues of the central basic patch. Similar to involvement of F239, Q274 and I340 in end-capping of dsRNA in the ZEBOV structure, the corresponding residues in REBOV VP35 IID F228, Q263 and I329 participate in end-capping interactions with the blunt-ends of the dsRNA.

In addition to the dsRNA-dependent inhibition mechanisms, VP35 can inhibit IFN pathway independent of dsRNA. For example, recent studies have shown that VP35 transfection into 293T cells, affects the cellular localization of GFP-tagged IRF-3, causing it to be retained in the cytoplasm(Basler et al, 2003; Prins et al, 2009). These studies also show that VP35 can also inhibit IFN-beta production by preventing IKK-ε and TBK-1 from phosphorylating their downstream substrates – IRF-3 and 7. In vitro studies established that VP35 can act as a pseudosubstrate for the IFN kinases, thus suppressing IFN-beta production using an RNA-independent mechanism downstream of RIG-I like receptors. When IRF3-5D, a constitutively active mutant of IRF-3 with phosphomimetic aspartate mutations, is used to stimulate IFN-beta production in 293T cells, EBOV VP35 is impaired in its ability to inhibit IFN-beta production, suggesting that it inhibits only the pathway upstream of IRF-3 phosphorylation. In addition to the components of the IFN pathway, VP35 has also been reported to interact with a lot of other host proteins in order to evade host immune responses. For example, VP35 has been shown to inhibit the IFN induced gene PKR and prevent eIF2-alpha phosphorylation(Feng et al, 2007; Schumann et al, 2009). In addition, VP35 has also been reported to inhibit RNA silencing by sequestration of dsRNA and direct interactions with the components of the RNAi machinery such as PACT and TRBP(Fabozzi et al, 2011;

Haasnoot et al, 2007). VP35 has also been reported to hijack the host SUMOylation machinery and target host proteins for degradation(Basler & Amarasinghe, 2009; Chang et al, 2009). Hence in addition to its role in viral replication and transcription, VP35 mediates immune evasion through multiple mechanisms and is a good target for therapeutic development against filoviruses.

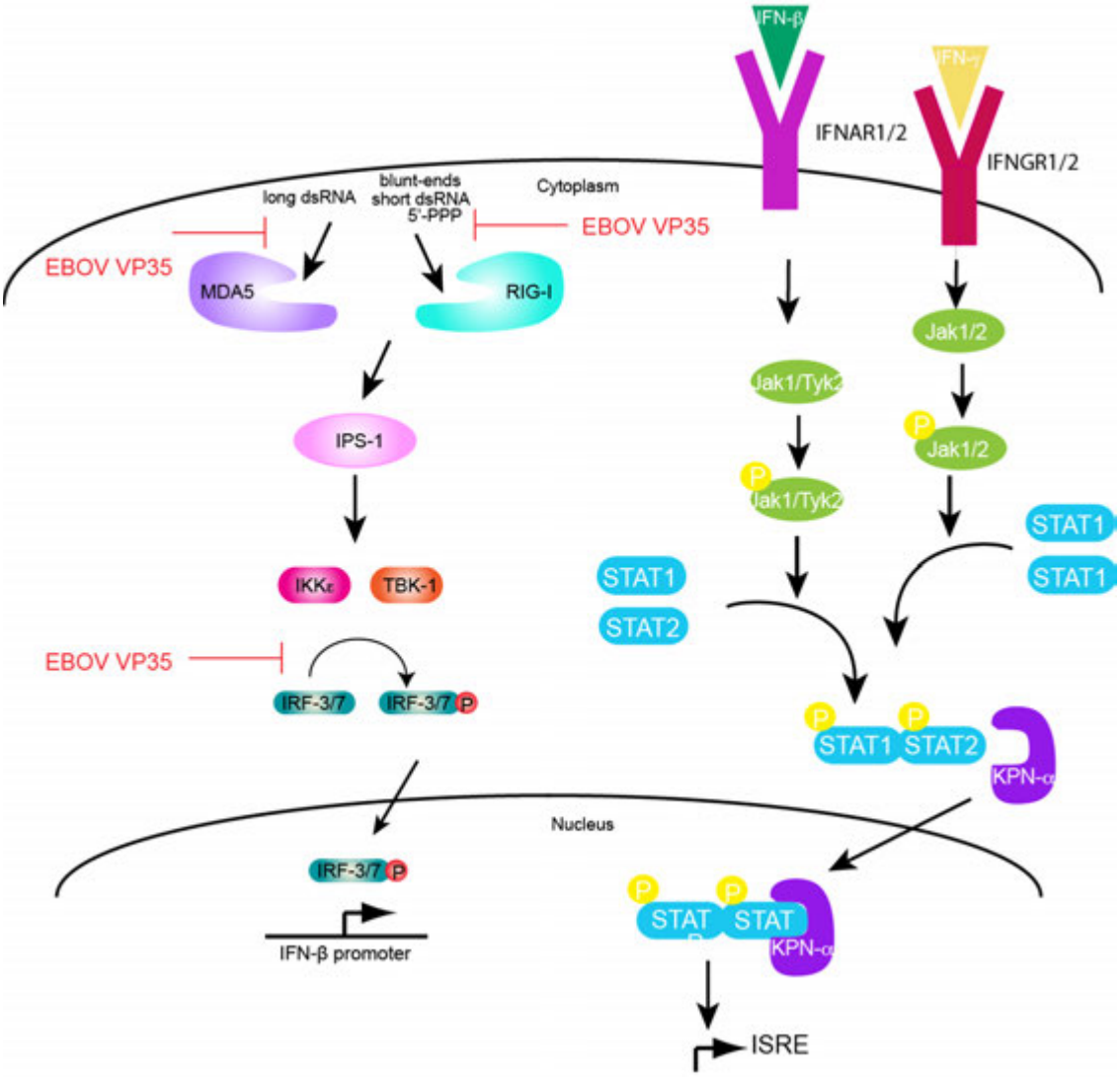

Figure 3-9. Mechanisms of EBOV proteins inhibition of host immune responses.

EBOV VP35 can bind to dsRNA and prevent activation of RIG-I like receptors. In addition VP35 can inhibit IRF-3 phosphorylation by acting as pseudo-substrate for the IFN kinases (Figure adapted from Ramanan et al, 2010).

3.8. References

Basler CF, Amarasinghe GK (2009) Evasion of interferon responses by Ebola and Marburg viruses. *Journal of Interferon and Cytokine Research* **29:** 511-520

Basler CF, Mikulasova A, Martinez-Sobrido L, Paragas J, Muhlberger E, Bray M, Klenk HD, Palese P, Garcia-Sastre A (2003) The Ebola virus VP35 protein inhibits activation of interferon regulatory factor 3. *J Virol* **77:** 7945-7956

Bray M (2001) The role of the Type I interferon response in the resistance of mice to filovirus infection. *J Gen Virol* **82:** 1365-1373

Bray M, Davis K, Geisbert T, Schmaljohn C, Huggins J (1999) A mouse model for evaluation of prophylaxis and therapy of Ebola hemorrhagic fever. *J Infect Dis* **179 Suppl 1:** S248-258

Chang TH, Kubota T, Matsuoka M, Jones S, Bradfute SB, Bray M, Ozato K (2009) Ebola Zaire virus blocks type I interferon production by exploiting the host SUMO modification machinery. *PLoS Pathog* **5:** e1000493

Chen VB, Arendall WB, Headd JJ, Keedy DA, Immormino RM, Kapral GJ, Murray LW, Richardson JS, Richardson DC (2010) MolProbity: all-atom structure validation for macromolecular crystallography. *Acta Crystallogr D Biol Crystallogr* **1**: 12-21

Emsley P, Cowtan K (2004) Coot: model-building tools for molecular graphics. *Acta Crystallogr D Biol Crystallogr* **12**: 2126-2132

Fabozzi G, Nabel CS, Dolan MA, Sullivan NJ (2011) Ebolavirus proteins suppress the effects of small interfering RNA by direct interaction with the mammalian RNA interference pathway. *J Virol* **85:** 2512-2523

Feng Z, Cerveny M, Yan Z, He B (2007) The VP35 protein of Ebola virus inhibits the antiviral effect mediated by double-stranded RNA-dependent protein kinase PKR. *J Virol* **81:** 182-192

Haasnoot J, de Vries W, Geutjes EJ, Prins M, de Haan P, Berkhout B (2007) The Ebola virus VP35 protein is a suppressor of RNA silencing. *PLoS Pathog* **3:** e86

Hartman AL, Dover JE, Towner JS, Nichol ST (2006) Reverse genetic generation of recombinant Zaire Ebola viruses containing disrupted IRF-3 inhibitory domains results in

attenuated virus growth in vitro and higher levels of IRF-3 activation without inhibiting viral transcription or replication. *J Virol* **80:** 6430-6440

Kimberlin CR, Bornholdt ZA, Li S, Woods VL, Jr., MacRae IJ, Saphire EO (2010) Ebolavirus VP35 uses a bimodal strategy to bind dsRNA for innate immune suppression. *Proc Natl Acad Sci U S A* **107:** 314-319

Leung DW, Prins KC, Borek DM, Farahbakhsh M, Tufariello JM, Ramanan P, Nix JC, Helgeson LA, Otwinowski Z, Honzatko RB, Basler CF, Amarasinghe GK (2010) Structural basis for dsRNA recognition and interferon antagonism by Ebola VP35. *Nature Structural & Molecular Biology* **17:** 165-172

Murshudov GN, Vagin AA, Dodson EJ (1997) Refinement of macromolecular structures by the maximum-likelihood method. *Acta Crystallogr D Biol Crystallogr* **3:** 240-255

Otwinowski Z, Minor W (1997) Processing of X-ray diffraction data collected in oscilation mode. *Methods Enzymol* **276:** 307-326

Painter J, Merritt EA (2006) Optimal description of a protein structure in terms of multiple groups undergoing TLS motion. *Acta Crystallogr D Biol Crystallogr* **4:** 439-450

Prins KC, Cardenas WB, Basler CF (2009) Ebola virus protein VP35 impairs the function of interferon regulatory factor-activating kinases IKKepsilon and TBK-1. *J Virol* **83:** 3069-3077

Prins KC, Delpeut S, Leung DW, Reynard O, Volchkova VA, Reid SP, Ramanan P, Cardenas WB, Amarasinghe GK, Volchkov VE, Basler CF (2010) Mutations abrogating VP35 interaction with double-stranded RNA render Ebola virus avirulent in guinea pigs. *J Virol* **84:** 3004-3015

Schumann M, Gantke T, Muhlberger E (2009) Ebola virus VP35 antagonizes PKR activity through its C-terminal interferon inhibitory domain. *J Virol* **83:** 8993-8997

CHAPTER 4. STRUCTURAL BASIS FOR MARBURG VIRUS VP35 MEDIATED IMMUNE EVASION MECHANISMS

Ramanan P, Edwards MR, Shabman RS, Leung DW, Endlich-Frazier AC, Borek DM, Otwinowski Z, Liu G, Huh J, Basler CF, and Amarasinghe GK. **Structural basis for Marburg virus VP35 mediated immune evasion mechanisms.** Manuscript accepted for publication in Proceedings of the National Academy of Sciences of the United States of America.

Structural and biochemical experiments were designed and implemented by me, with guidance from Dr. Gaya Amarasinghe and Dr. Daisy Leung. Initial identification of domain boundaries, cloning, expression, purification and identification of crystallization conditions for MARV VP35 IID, was performed by Dr. Daisy Leung. I subsequently optimized the construct space and identified new conditions to overcome diffraction related issues. In addition I identified conditions for crystallization of the MARV VP35 IID-dsRNA complex. I collected diffraction data at the Advanced Photon Source, beamline 19 ID with assistance from Dr. Gaya Amarasinghe, Dr. Daisy Leung and Dr. Dominika Borek. Dr. Zbysek Otwinowski, Dr. Dominika Borek, Dr. Daisy Leung and Dr. Gaya Amarasinghe provided insight and help in data processing, model building and refinement and validation of structure. I did the structural analysis and mutational studies based on structure, guided by Dr. Gaya Amarasinghe and Dr. Daisy Leung. Miss. Juyoung Huh cloned and expressed the RIG-I and MDA5 constructs used in the *in vitro* ATPase experiments. I performed

comparative RNA binding studies of MARV and ZEBOV VP35 with different RNA ligands. I performed ATPase assays with dsRNA and poly I:C to show inhibition of MDA5 and RIG-I by MARV and ZEBOV VP35. Dr. Gai Liu and I performed *in vitro* RNA binding and ATPase experiments with overhang containing dsRNA, characterizing selective inhibition of dsRNA PAMPs by MARV VP35 IID. Dr. Christopher Basler, Dr. Reed S. Shabman, Megan Edwards and Ariel Endlich-Frazier designed, performed and analyzed all the *in vivo* experiments, characterizing IFN inhibition by MARV VP35 IID. I wrote the initial draft of the manuscript, except for the cell biological assays, which was written by Dr. Christopher Basler and colleagues at Mount Sinai School of Medicine. The final draft of the paper was submitted after editorial approval of all the authors.

4.1 Introduction

MARV is one of the deadly filoviruses that cause hemorrhagic fever in humans(Gear et al, 1975; Towner et al, 2006). Many recent studies have shown that there are differences between MARV and EBOV not only at the genomic level but also at the level of viral protein structure and function(Enterlein et al, 2009; Muhlberger et al, 1998; Muhlberger et al, 1999; Sanchez et al, 1993; Valmas et al, 2010). Hence it is important to understand the similarities and differences between each of the viral proteins in EBOV and MARV in order to target common features for developing antivirals. In the case of EBOV, recent studies have shown that VP35 is a key protein involved in viral replication and immune antagonism and interacts with a range of different host proteins to mediate its immune antagonist function(Leung et al, 2010a; Leung et al, 2010b; Prins et al, 2010a; Prins et al, 2009; Prins et al, 2010b; Schumann

et al, 2009). The availability of high-resolution structural information on EBOV VP35 IID, makes it an attractive therapeutic target, since it is well conserved across the different filoviral family members(Leung et al, 2009; Leung et al, 2010c). However, there is no such information available on MARV VP35 protein. Here we discuss our structural, biochemical and cell-based studies conducted on MARV VP35 IID in order to understand the mechanisms of immune evasion by MARV VP35 and compare and contrast it to EBOV VP35.

4.2 Materials and methods

Cloning, protein expression and purification. The coding region of MARV (Musoke strain) VP35 IID, full length RIG-I (residues 1-925), RIG-I ΔCARDs (residues 230-925), full length MDA5 (residues 1-1025) and MDA5 ΔCARDs (residues 304-1025) was subcloned using Nde1 and BamH1 restriction enzyme sites into a modified pET15b expression vector, downstream of a MBP fusion tag and a TEV cleavage site. Using primers containing the desired mutations, mutant Zaire EBOV VP35 IID and MARV VP35 IID constructs were generated by overlap PCR, digested with restriction enzymes Nde1 and BamH1 and ligated into the same pET vector described above. PCR and DNA sequencing subsequently confirmed the presence of mutations. All the constructs mentioned above were expressed as MBP-fusion proteins by culturing transformed BL21(DE3) cells in LB media at 37°C until an OD_{600} of 0.7. Cells were then chilled in ice and induced with 0.5mM IPTG and cultured overnight at 18°C. Cells were harvested by centrifugation at 10,000 g at 4°C for 10 minutes. Harvested cells were resuspended in lysis buffer containing 25mM sodium

phosphate (pH 7.0), 1M NaCl, 5mM β-mercaptoethanol and a protease inhibitor cocktail, flash frozen using liquid nitrogen, and stored at -80°C. Cells were thawed and lysed using an Emulsiflex-C5 homogenizer (Avestin) and clarified by centrifugation at 30,000 g for 30 minutes. The supernatant was then purified using a combination of affinity, cation exchange and size exclusion chromatographic columns (GE Healthcare). The MBP fusion tag was cleaved prior to final purification by using tobacco etch virus (TEV) protease. Protein purity was assessed by SDS-PAGE followed by Coomassie blue staining.

Crystallization, data collection and processing. Crystallization trials were setup using purified MARV VP35 IID and 18bp dsRNA (Integrated DNA Technologies) mixed in 2:1 molar ratio using hanging-drop vapor diffusion method at room temperature in standard 24 well plates. Preliminary trials were performed using Hampton research kits and the resulting hits were optimized using in-house reagents. Single, three-dimensional rod-like crystals were obtained in well solution containing 0.1M ammonium citrate (pH 6.2), 0.1M ammonium citrate (pH 6.4), 0.25% ethylene glycol, 14% PEG 3350 and 0.23M ammonium sulfate. Crystals were cryoprotected by transferring them to well solutions containing 10% and 25% ethylene glycol for 10 seconds before plunge freezing in liquid nitrogen. Diffraction data was collected at the Advanced Photon Source (Beamline 19-ID). 440 frames of data were collected with a frame width of 0.5° and detector to crystal distance of 300 mm.

Diffraction data were indexed, scaled and merged using HKL-3000. Intensities were converted to structure factors using CCP4 suite. Phase determination for MARV VP35 IID-dsRNA complex was through molecular replacement by using chain B from wildtype

ZEBOV VP35 IID crystal structure (3FKE) as search model. Molecular replacement was performed using MOLREP in the CCP4 suite, and the resulting model was refined using REFMAC5. The resulting solution after molecular replacement provided a good model for the protein molecules in the structure. In order to model the dsRNA, an ideal A-form dsRNA helix was modeled and this model was manually built into the density for the dsRNA manually using Coot and merged with the protein model. Subsequent iterations of refinement and manual model building resulted in a satisfactory agreement between the model and experimental data for the structure as assessed by the final R_{work} and R_{free} values reported by REFMAC5 (Table 3-1). Water addition and manual model building was performed using Coot. TLS parameters were refined using the TLMSD server. Final validation was performed using MOLPROBITY server.

RNA binding studies. Isothermal titration calorimetry (ITC) assays to characterize protein-RNA interactions were performed using a VP-ITC (Microcal, North Hampton, MA). Protein samples for ITC studies were dialyzed overnight in a buffer containing 10mM HEPES pH 7.0, 150mM NaCl, 1mM $MgCl_2$ and 2mM Tris(2-carboxyethyl)phosphine (TCEP) and the dialyzed buffer was used to make the dsRNA. The raw data from VP-ITC was analyzed and processed using Origin software to obtain binding constants.

For the double-membrane dot-blot assays, 125 picomoles of dsRNA was labeled with g-^{32}P-ATP at 37°C for 1.5 hrs in a 50 µl reaction containing 1U/µl T4 polynucleotide kinase (New England Biolabs), 5µl 10X T4 PNK buffer and 50 µCi g-^{32}P-ATP (Perkin Elmer). After 1.5 hours, 5 µl of sodium acetate (pH 5.4) and 125µl of ethanol were added and the RNA was precipitated at -20°C for 2 hours. Precipitated RNA was pelleted by

centrifugation for 30 minutes at 4°C and resuspended in 8M urea. The labeled RNAs were separated on a 7M urea, 15% acrylamide gel to separate out free nucleotides from RNA. RNA was identified and excised from gel by UV-shadowing and eluted into water with 5mM EDTA. Eluted RNA was ethanol precipitated again as described above, dissolved in water, separated into aliquots and stored at -20°C. RNA binding assays were carried out using a dot-blot apparatus containing 96 wells. 50μL reactions, each containing varying protein concentrations in the range from 0 to 100μM and a constant 5nM g-^{32}P-labeled dsRNA concentration were setup in a 96 well plate. The protein-RNA complex was then applied to each of the 96 wells in the dot-blot apparatus. Using vacuum pressure, the sample was passed through two sets of membranes - a nitrocellulose membrane (0.2 μm pore size, Biorad) assembled on top of a Zetaprobe nylon membrane (0.2 μm pore size, Biorad). Prior to and after sample application, the wells are washed twice with 500 μL binding buffer containing 10mM HEPES (pH 7.0), 150mM NaCl, 2mM TCEP and 1mM MgCl2. The nylon and nitrocellulose membranes were air-dried and exposed to a phosphor screen (GE Healthcare) for 12-16 hours. Exposed screens were scanned using a Typhoon 9410 Variable Model Imager and quantified using ImageQuant software. Fractional binding was calculated as the ratio of the intensity of sample in nitrocellulose membrane to the sum of the intensities of nitrocellulose and nylon membranes. The resulting data were plotted using non-linear curve fitting function in Origin software to a one-site binding model to extract dissociation constants.

ATPase assays. The ATPase activities of RIG-I and MDA5 constructs were monitored using thin layer chromatography (TLC) assay. Briefly, 50μL reactions were set up in a buffer

containing 10mM HEPES pH 7.0, 150mM NaCl, 1mM $MgCl_2$ and 2mM TCEP, 100μM ATP, 5μCi g-^{32}P-ATP and RIG-I or MDA5. 30bp dsRNA (IDT) or poly I:C (InvivoGen, San Diego, CA) were used as activators for RIG-I and MDA5 respectively, and wildtype or mutant VP35 IID proteins were added at various concentrations. Reactions were quenched with 50mM EDTA at desired time points and spotted on a 20cm by 10cm polyethyleneimine (PEI)-cellulose resin coated TLC plate (Baker-Flex, Germany) and placed in a TLC chamber containing 0.6M potassium phosphate monobasic pH 3.4 buffer The solvent front was allowed to migrate until it reached 1 cm below the top of the TLC plate, air-dried, saran-wrapped and exposed to a phosphor screen (GE Healthcare) for 2-4 hours. Exposed screens were scanned using a Typhoon 9410 Variable Model Imager and quantified using ImageQuant software. ATPase activity for each lane was calculated by measuring the intensity of the inorganic phosphate. The resulting data were plotted using Origin software.

4.3 Biochemical comparison of ebolavirus and marburgvirus C-terminal domain

Filoviral VP35 protein is composed of an N-terminal oligomerization domain with putative coiled-coil regions(Moller et al, 2005; Reid et al, 2005), and a C-terminal interferon inhibitory domain (IID) (Leung et al, 2009). The C-terminal domain of VP35 is highly conserved among the different filoviruses, with about 90% similarity between the different species of EBOV and 57% similarity between ZEBOV and MARV (Figure 4-1). While some of the residues in the central basic patch such as R294, K298, R301 and K339 (corresponding

to residues R305, K309, R312 and K339 in ZEBOV VP35) are identical in both sequences, functionally important residues such as T308 and K311 (K319 and R322 in ZEBOV VP35) in the CBP and A214 and Y240 (R225 and K251 in ZEBOV VP35) in the FBP are not conserved. Guided by secondary structure analysis, sequence comparison with ZEBOV and REBOV VP35, we used an NMR-based domain mapping study to identifiy a C-terminal domain of MARV VP35, which would behave as an independently folded unit with solution properties that would make amenable for crystallography and biochemical characterization. We used heteronuclear single quantum correlation spectroscopy (HSQC) using uniformly ^{15}N-labeled protein. The HSQC experiment reports on the chemical shifts of the backbone amide group of each non-proline amino acid. These chemical shifts are exquisitely sensitive to the local chemical environment of the nuclei, which give rise to the NMR signal and hence report on the local secondary structure. While well folded proteins typically have unique well-dispersed chemical shifts with near uniform line widths and intensities, the amino acids present in disordered or unstructured regions of the protein give rise to chemical shifts that have markedly higher intensities and tend to show spectral crowding.

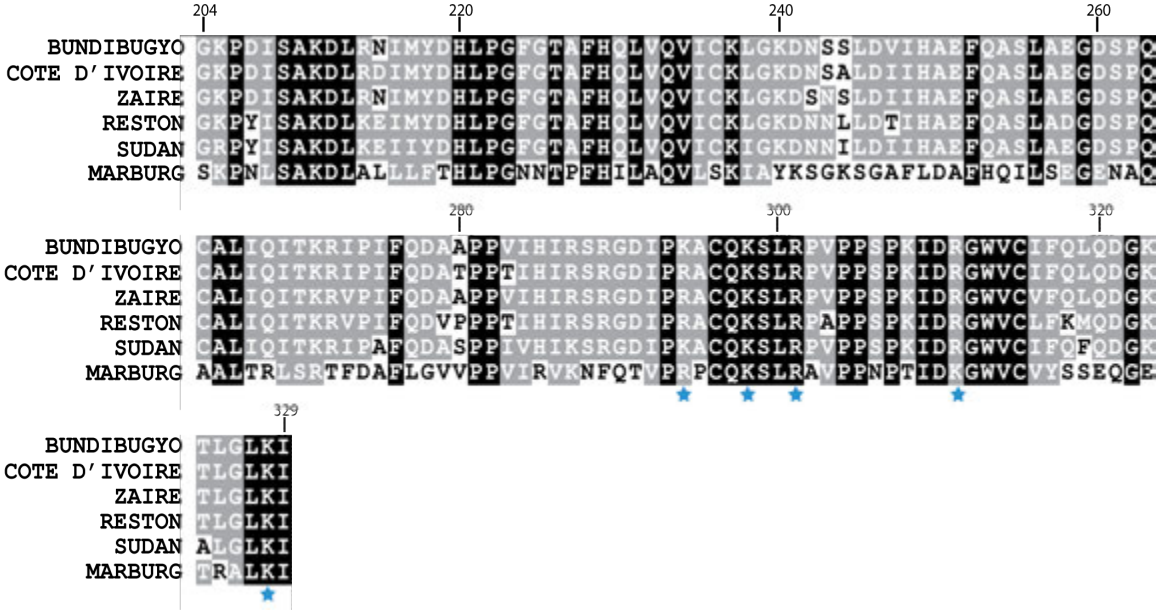

Figure 4-1. Multiple sequence alignment IID region of filoviral VP35 proteins.

Sequence alignment of VP35 IID region of the different EBOV species, Bundibugyo (accession number ACI28621.1), Tai Forest (accession number ACI28630.1), Zaire (accession number AAD14582.1), Reston (accession number BAB69004.1), Sudan (accession number ABY75322.1) with MARV (accession number CAA78115.1). Conserved and identical residues are highlighted in black boxes, similar residues in gray boxes and non-conserved residues in white boxes. The residue numbers indicated are for MARV VP35. The blue stars denote conserved basic residues belonging to the central basic patch.

Using this assay to guide our analysis, we were able to screen various N-terminal truncation constructs of MARV VP35 IID such as 166-329, 177-329, 182-329, 191-329 and 200-329. Extension of the N-terminus of the protein beyond residue 200 resulted in additional peaks at the center of the spectrum with markedly higher intensities relative to the rest of the spectrum (Figure 4-2), suggesting that these additional residues at the N-terminus are likely disordered in solution. Together, these data suggested that the construct comprising residues 200-329 would be suitable for further biochemical and structural characterization of the C-terminal domain of MARV VP35 (Figure 4-2). Subsequent expression, purification and size chromatography analysis of the proteins suggested that these proteins could be obtained at high purity and homogeneity using bacterial expression systems.

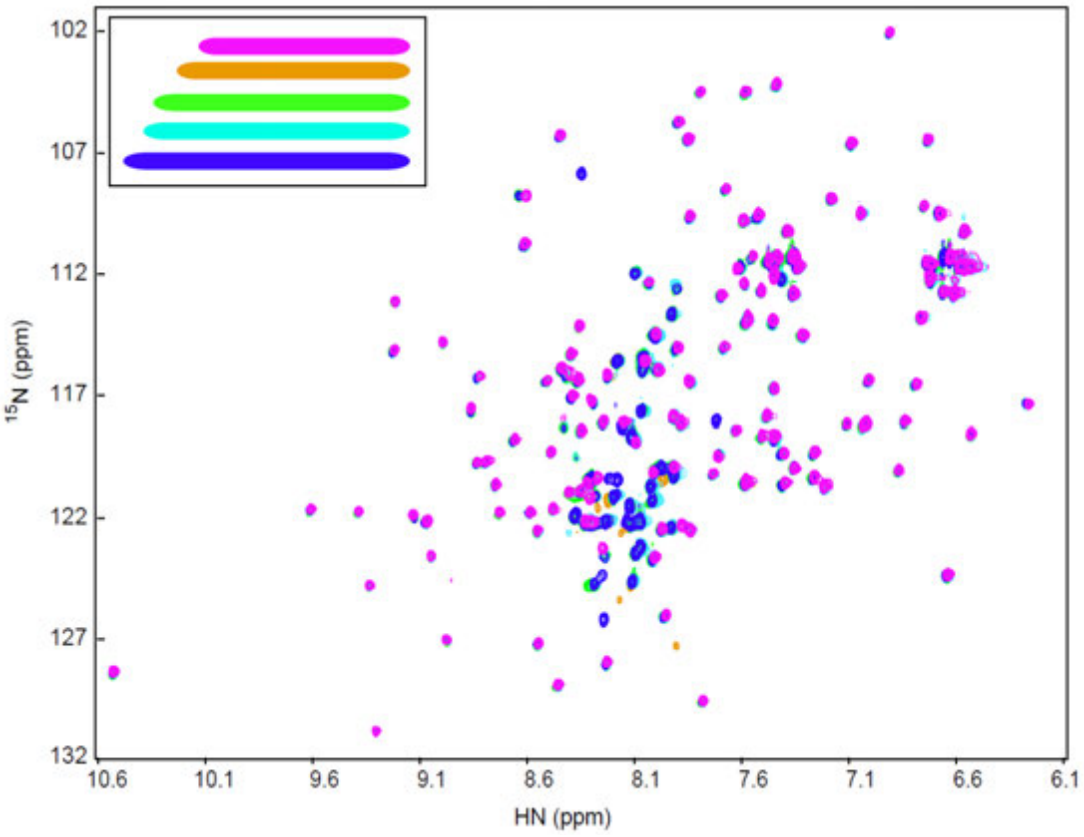

Figure 4-2. Identification of MARV VP35 IID domain boundary by NMR.

^{1}H- ^{15}N heteronuclear single quantum coherence (HSQC) spectral overlay of MARV VP35 IID constructs. Several N-terminal truncations of MARV VP35 IID (constructs indicated in blue, cyan, green, orange and pink) were tested for their solution properties.

We characterized the RNA binding characteristics of filoviral VP35 proteins using isothermal titration calorimetry and double-membrane filter binding assays. While ZEBOV VP35 is able to recognize and bind dsRNA ligands as small as 8 bp with a K_D of 0.54 ± 0.08 μM (Figure 4-3B), MARV VP35 preferentially binds longer dsRNA such as 18bp or 30bp (Figure 4-3C and D) with increasing affinity (K_D of 6.55 ± 0.6 μM for 18bp dsRNA and K_D of 1.31 ± 0.1 μM for 30bp dsRNA) and is completely incapable of binding 8 bp dsRNA (Figure 4-3A). In contrast ZEBOV VP35 IID binds to both 18bp and 30bp dsRNA with comparable affinities (K_D of 2.19 ± 0.1 μM for 18bp dsRNA and K_D of 2.24 ± 0.2 μM for 30bp dsRNA). Given the sequence similarity in the C-terminal domain of VP35 among filoviruses, it was not immediately evident why there are differences in the RNA binding characteristics of ZEBOV and MARV VP35. In order to understand this, we used X-ray crystallography to determine the three-dimensional structure of these proteins in both the free form and bound to dsRNA.

4.4 Structural studies of filoviral VP35 reveals distinct RNA binding modes

Since the goal of my thesis is to understand the structural and functional similarities and differences between ZEBOV and MARV VP35, we determined the crystal structure of the C-terminal domain of MARV VP35 (residues 204-329) in complex with a palindromic sequence of 18bp blunt-ended dsRNA. Crystallization was done using a 2:1 molar concentration of protein to dsRNA and drops were set up using hanging-drop vapor diffusion method to obtain single diffraction quality crystals with dimensions of approx. 150μm in length, 35μm in width and 25μm thickness (Figure 4-4A). The crystals diffracted to 2.0Å

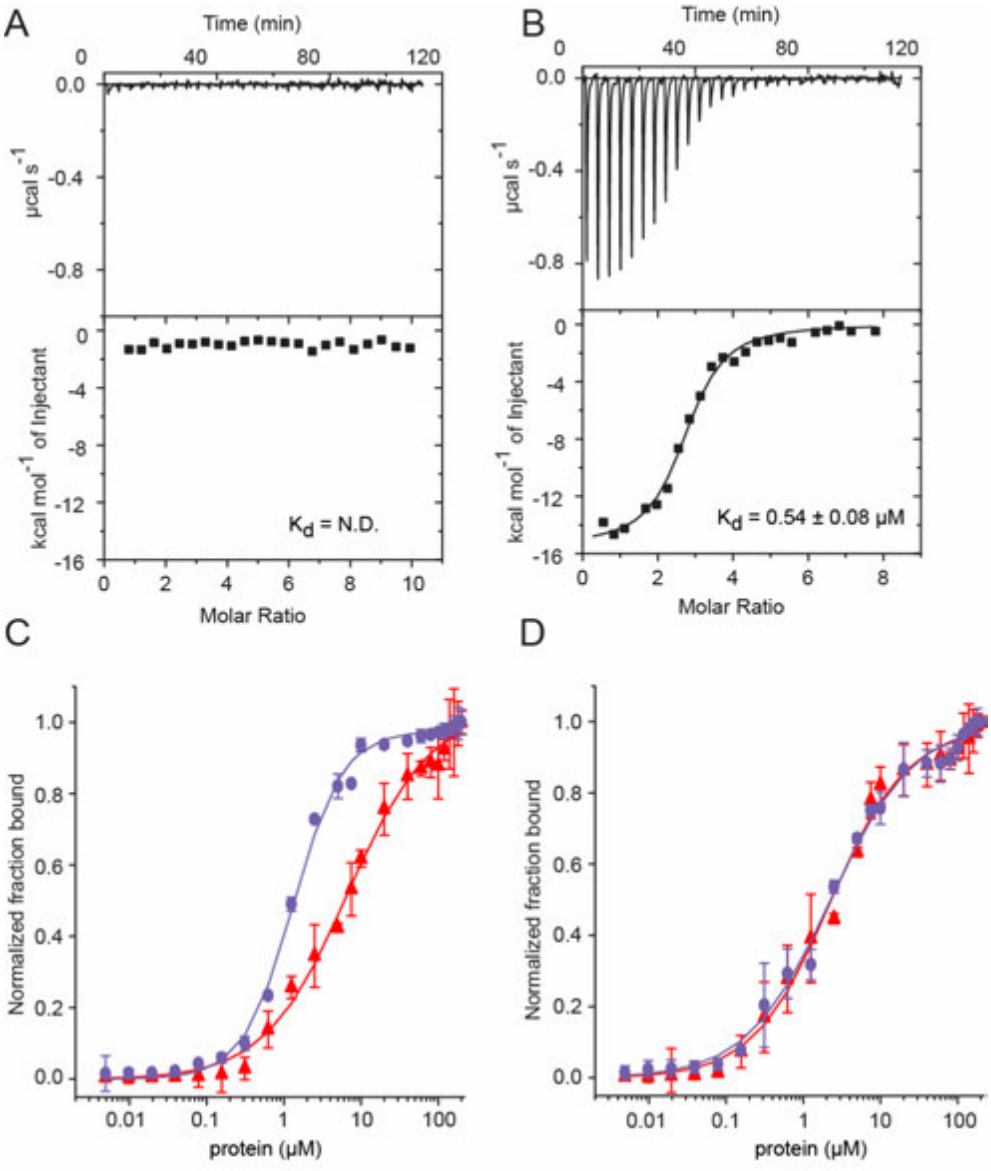

Figure 4-3. MARV VP35 IID binds to dsRNA in a length dependent manner.

Isothermal titration calorimetry of MARV VP35 IID (A) and ZEBOV VP35 IID (B) with 8bp dsRNA. Binding curves from double-membrane dot-blot assay for 18bp (purple circles) and 30bp (red triangles) dsRNA with MARV VP35 IID (C) and ZEBOV VP35 IID (D). Error bars represent s.d from two independent experiments.

resolution when exposed to a synchrotron radiation source (Figure 4-4B). We were able to obtain phases using one monomer of the ZEBOV VP35 IID structure (PDB: 3FKE) as the search model in molecular replacement (Figure 4-4C). We observed four molecules of MARV VP35 IID (chains A through D) and one 18bp dsRNA (chain E, F) in the crystallographic asymmetric unit (Figure 4-5A). Analysis of symmetry mates in the unit cell reveals an arrangement of molecules such that the dsRNA forms a pseudo-contiguous helix with a slight offset with the MARV VP35 IID molecules coating it along the backbone (Figure 4-5B). Notably, this is similar to the stoichiometry of 4 molecules of VP35 IID interacting with one molecule of dsRNA observed in the crystal structures of ZEBOV (PDB 3L25 and 3L26) and REBOV VP35 IID (PDB 3KS8) bound to dsRNA. The absence of base-specific contacts suggests that MARV interacts with dsRNA in a sequence independent fashion, similar to ZEBOV and REBOV VP35s. A number of conserved basic residues such as R294, K298, R301 and K328 form the positively charged protein surface that interacts through polar contacts with the negatively charged phosphodiester backbone of the RNA. The side chains of R294 and K298 interact with O1P of base U9, side chain of K328 and R301 interacts with the O2' of C13 (Figure 4-6B). These residues are identical in REBOV (R294, K298, R301 and K328) and ZEBOV (R305, K309, R312 and K339) and are also involved in critical contacts with RNA backbone. As expected, structural alignment of EBOV and MARV VP35 IID shows that the overall fold, with the alpha helical and the beta sheet subdomains are well conserved and all of the secondary structural elements almost identical to each other. The backbone RMSD for the overall alignment is 0.82 Å for ZEBOV and 0.72 Å for REBOV (Figure 4-9A and B). Despite these striking similarities, there are

some notable differences in the basic residues that constitute the RNA binding interface, between MARV and ZEBOV.

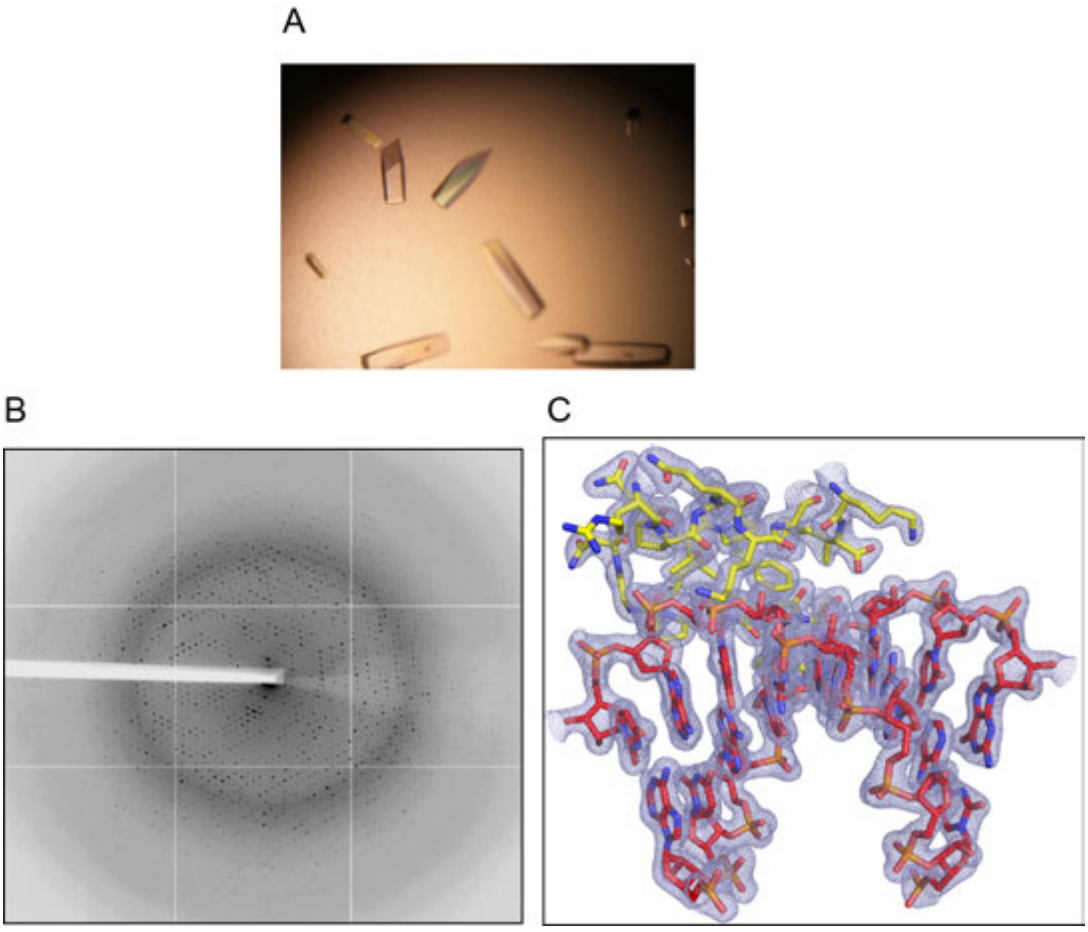

Figure 4-4. Crystallization of MARV VP35 IID-dsRNA complex.

(A) Representative crystals of MARV VP35 IID-18bp dsRNA complex obtained by hanging-drop vapor diffusion method. (B) Representative diffraction pattern of the crystals, which diffracted to 2.0Å resolution at the synchrotron. (C) 2Fo-Fc density map at 1σ showing electron density (blue mesh) for both the RNA (red sticks) and the protein (yellow sticks).

Table 4-1. Statistics for data collection and refinement for MARV VP35 IID-dsRNA complex.

	MARV VP35 IID-dsRNA complex
Data collection	
Space group	$P2_12_12_1$
Cell dimensions *a, b, c* (Å) *α, β, γ* (°)	 83.77, 93.38, 102.07 90, 90, 90
Resolution (Å)	50.00-2.01 (2.04-2.01)[a]
R_{sym} *or* R_{merge} (%)	9.4 (92.8)
$I/\sigma I$	22.9 (2.6)
Completeness (%)	100.0 (100.0)
Multiplicity of observation	8.7 (7.2)
Refinement	
Resolution (Å)	37.87-2.02 (2.07-2.02)
Number of reflections	45,910 (2577)
R_{work}/R_{free}	18.7/24.0
Completeness (%)	95.6 (48.6)
Number of non-hydrogen atoms	5048
B-factors Protein RNA Water	 15.6 (chain A) 16.2 (chain B) 21.4 (chain C) 15.3 (chain D) 17.5 (chain E) 19.5 (chain F) 32.5 (chain W)
R.m.s. deviations Bond lengths (Å) Bond angles (°)	 0.011 1.496
Ramachandran analysis Favored (%) Allowed (%) Disallowed (%)	 99.8 0.2 0.0

While residues T308 and K311 are completely solvent exposed and play no part in RNA binding in MARV VP35, the equivalent residues in REBOV (K308 and R311) and ZEBOV VP35 (K319 and R322) are part of a critical network of polar contacts with RNA. Other notable differences include contacts mediated by residues such as N261 and Q263 with O3' and O2' of base U11 respectively (Figure 4-6A). The corresponding residues in REBOV (S261 and Q263) are also involved in polar contacts with RNA, but not in the case of ZEBOV (S272 and Q274).

The most striking difference between dsRNA binding modes of MARV and EBOV VP35 IID is the absence of end-capping interactions (Figure 4-10A,B and C) Both the ZEBOV and REBOV VP35 IIDs interact with the blunt ends of dsRNA, through a series of hydrophobic contacts mediated through residues F239, I340 and Q274 in ZEBOV and F228, I329 and I267 in REBOV) (Figure 4-10D and E) (Kimberlin et al, 2010; Leung et al, 2010b). These end-capping interactions are facilitated through protein-protein interactions between VP35 IID molecules as observed in the crystal structures of both ZEBOV and REBOV VP35 IID. The interface between VP35 IID molecules is formed through a network of hydrogen-bonding interactions. The unique aspect of this interface is that the basic residues that are involved in RNA binding in one molecule of VP35 IID in the structure are involved in protein-protein interactions in the other molecule(Leung et al, 2010b). In the case of MARV VP35 IID, the conserved basic residues only interact with dsRNA and do not participate in

any intermolecular protein-protein interactions. In contrast, hydrogen-bonding interactions between side chain NH2 of R285 and backbone O atom of V280 and side chain OE1 of Q321

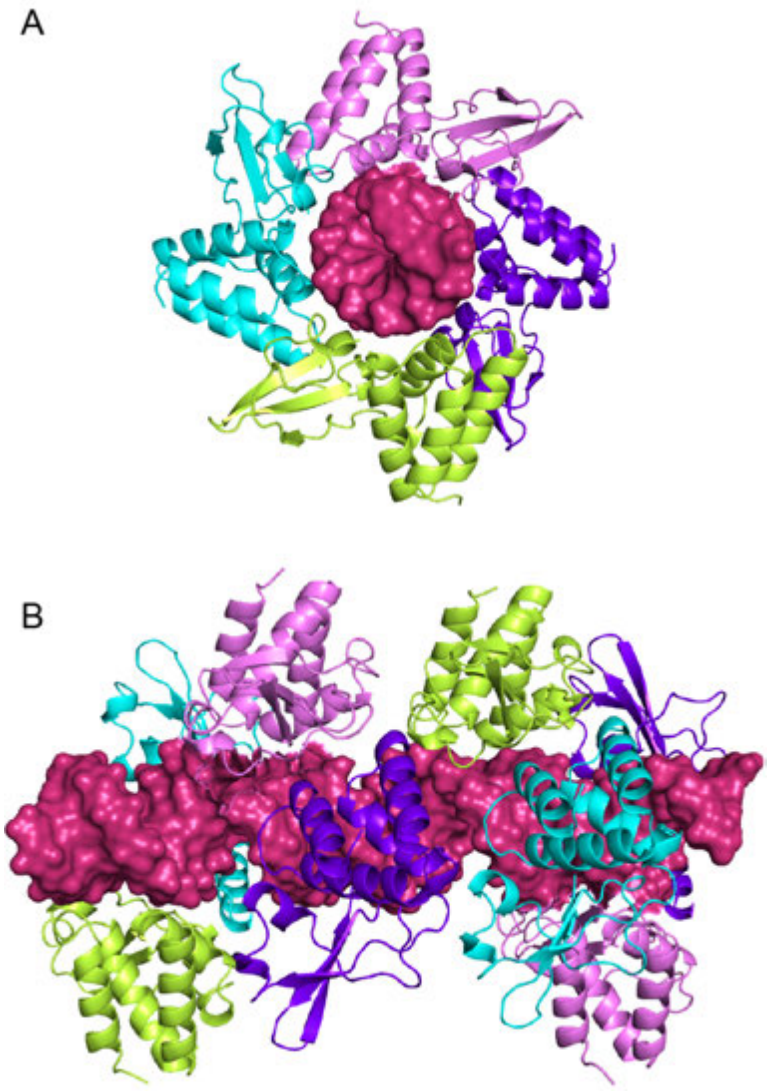

Figure 4-5. Crystal structure of MARV VP35 IID bound to 18bp dsRNA.

(A) Four molecules of MARV VP35 IID, chains A(cyan), B(purple), C(green) and D(pink) bind only to phosphodiester backbone of one 18bp dsRNA (depicted in red as surface representation). (B) Symmetry related molecules showing the coaxial, end-to-end

arrangement of two dsRNA molecules in the unit cell with MARV VP35 IID molecules coating along the backbone (PDB 4GHL).

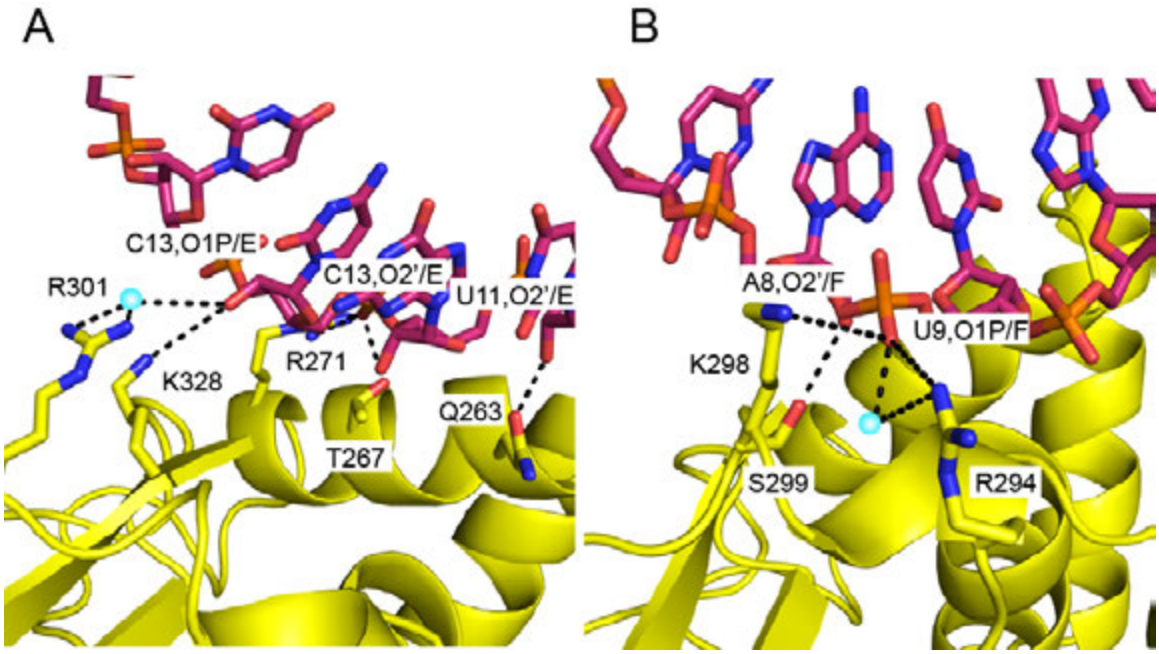

Figure 4-6. Residues involved in dsRNA binding in MARV VP35 IID.

(A) Side chains of residues R301, K328, R271, T267 and Q263 are engaged in hydrogen bonds with chain E of the dsRNA. (B) Residues such as K298, S299 and R294 form hydrogen bonds with chain F of dsRNA. Absence of base-specific contacts suggests a sequence independent binding mode to dsRNA.

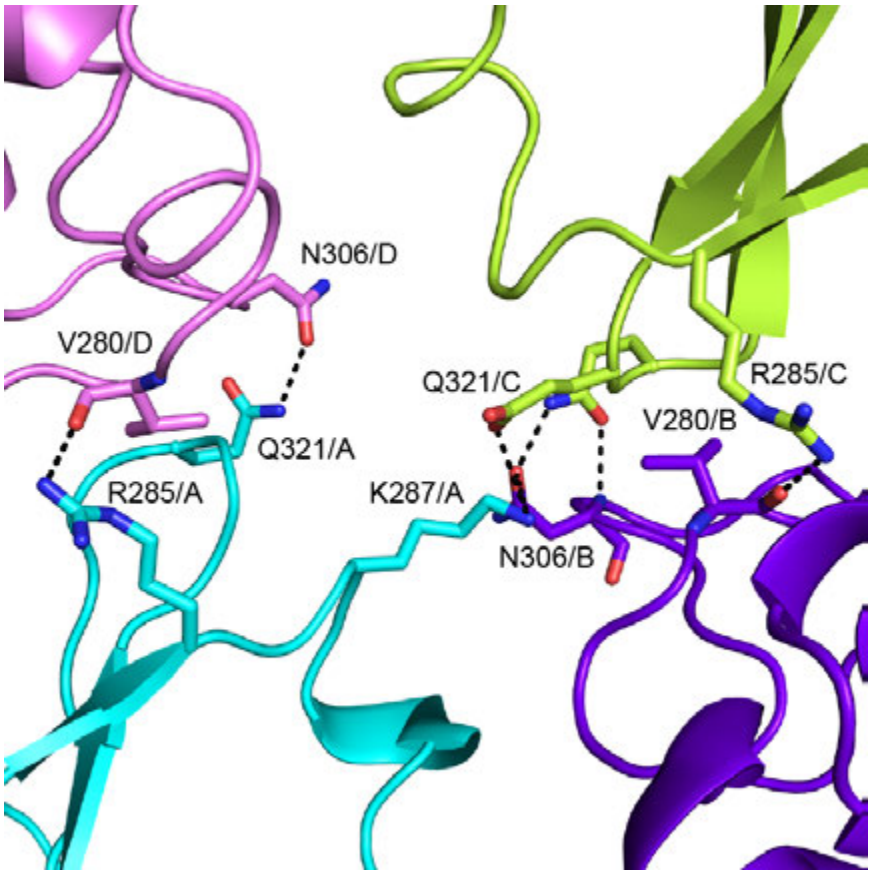

Figure 4-7. Residues involved in protein-protein interactions in MARV VP35 IID.

Side chains of residues R285, K287, N306 and Q321 are involved in hydrogen bond mediated protein-protein interactions with neighboring MARV VP35 IID monomers in the crystal structure.

and N and OD1 of N306 are observed between chains A and D and chains B and C in the asymmetric unit (Figure 4-7). These interactions are not as extensive as the protein-protein interactions observed in the case of Zaire and Reston EBOV(Kimberlin et al, 2010; Leung et al, 2010b) VP35 and may not be physiologically relevant in the case of MARV VP35 and may reflect crystal-packing contacts. In the case of MARV VP35, F228 (F239 in ZEBOV and F228 in REBOV) interacts with G12 base of dsRNA in contrast to its equivalent residues in ZEBOV and REBOV that pack against the blunt ends of the dsRNA (Figure 4-10F). In order to validate the importance of the residues that are observed in the crystal structure, we performed filter-binding assays of wildtype or mutant MARV VP35 IID constructs with 18bp and 30bp dsRNA (Figure 4-8). Consistent with the structure, mutation of residues involved in protein-dsRNA contacts resulted in diminished dsRNA binding, whereas mutation of residues involved in protein-protein interactions in the structure had no effect on dsRNA binding.

In order to test whether the absence of end-capping interactions was indeed physiologically relevant and not an artifact of crystallization, we assessed the ability of ZEBOV VP35 and MARV VP35 to bind 25bp dsRNA containing blunt ends, 5' overhang or 3' overhang using filter binding experiments. Our results show that while both ZEBOV and MARV VP35 are able to bind to blunt end dsRNA with similar affinities (K_D of 1.32μM for MARV VP35 IID and K_D of 2.14μM for ZEBOV VP35 IID), only MARV VP35 binds either 5' overhang or 3' overhang containing dsRNA with affinities similar to blunt end dsRNA (K_D of 1.69μM for 5' overhang dsRNA and K_D of 2.19μM for 3' overhang dsRNA) (Figure 4-11A). In contrast, EBOV VP35 binds to 5' overhang and 3' overhang containing dsRNA

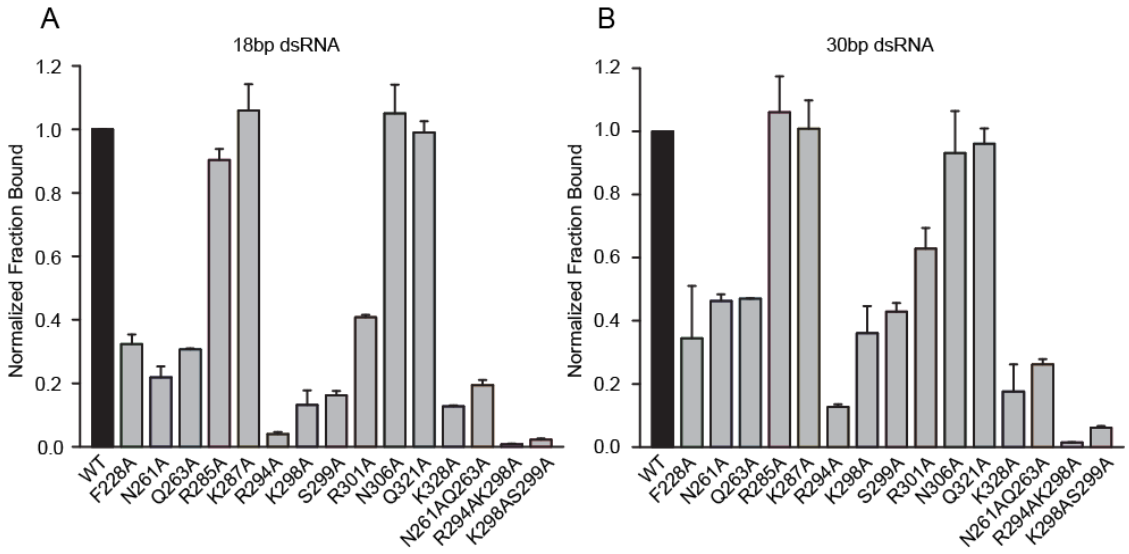

Figure 4-8. Mutation of residues involved in mediating dsRNA contacts in structure also diminish dsRNA binding *in vitro*.

Wildtype and mutant MARV VP35 IID proteins were assessed for their ability to bind 5'-end labeled (A) 18bp dsRNA and (B) 30bp dsRNA using double-membrane dot-blot experiments. Fractional binding of the mutants (gray bars) was normalized relative to wildtype protein (black bars). Error bars represent standard deviation from two independent experiments.

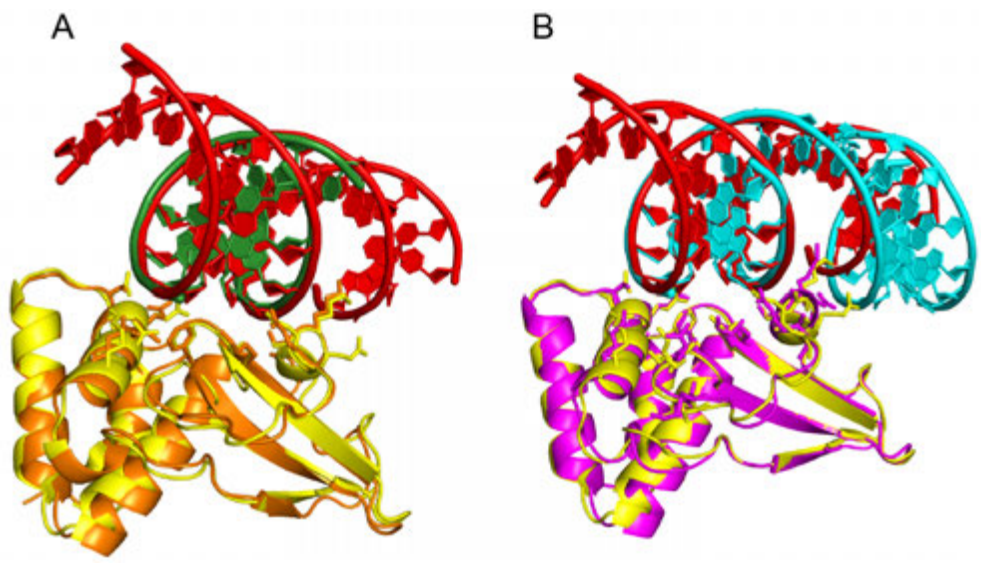

Figure 4-9. Overall fold of MARV VP35 IID is conserved and similar to EBOV.

Structural alignment of MARV VP35 IID (yellow) bound to 18bp dsRNA (red) with ZEBOV VP35 IID (orange) bound to 8bp dsRNA (green) and REBOV VP35 IID (magenta) bound to 18bp dsRNA (cyan) show that the overall fold containing the alpha helical and the beta sheet subdomains is conserved.

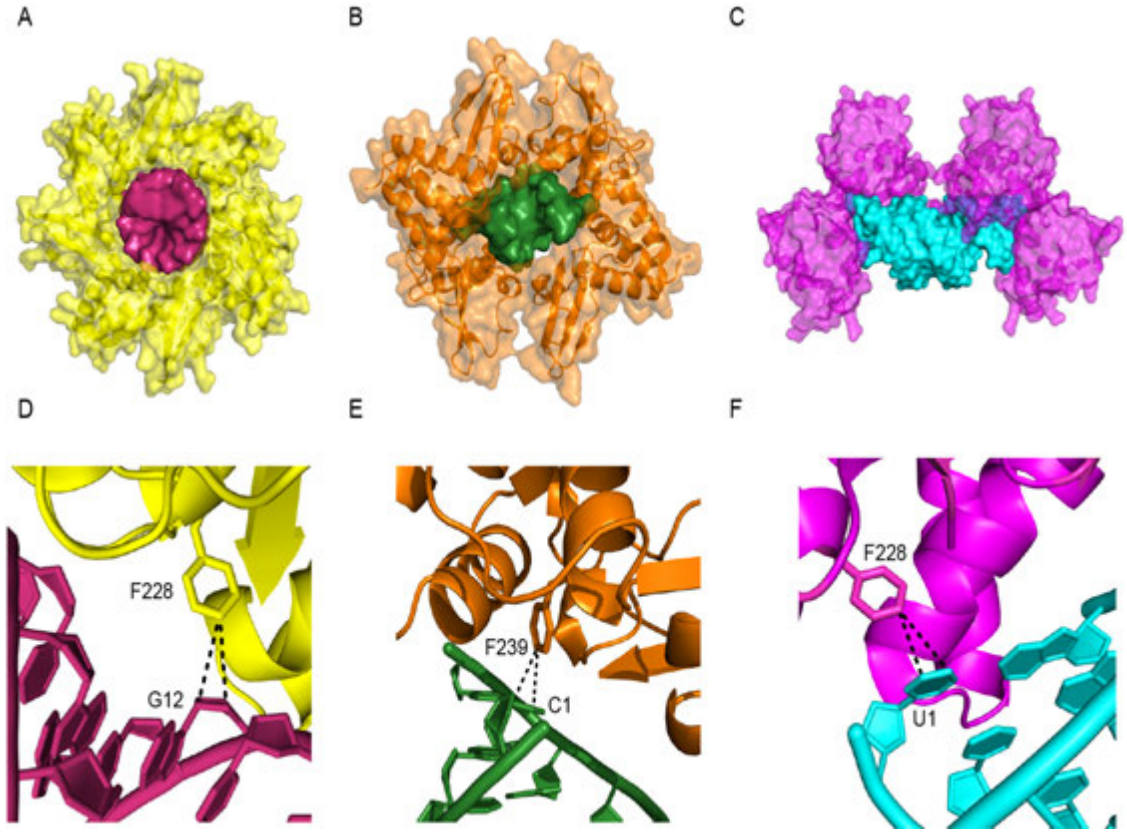

Figure 4-10. MARV VP35 IID does not bind dsRNA blunt ends unlike EBOV VP35 IID.

(A) MARV VP35 IID monomers (yellow) bind only to dsRNA backbone (yellow), whereas both (B) ZEBOV (orange) and (C) REBOV VP35 IID (magenta) bind to the respective dsRNAs (green and cyan respectively) as a dimer and contact both the blunt ends and the backbone. The F228 residue in (D) MARV VP35 IID contacts RNA base G12, which is in the middle of the dsRNA backbone, whereas the corresponding residues (E) F239 in ZEBOV VP35 IID and (F) F228 in REBOV VP35 IID end-cap the first base (C1 and U1 respectively) at the blunt-ends of the dsRNA.

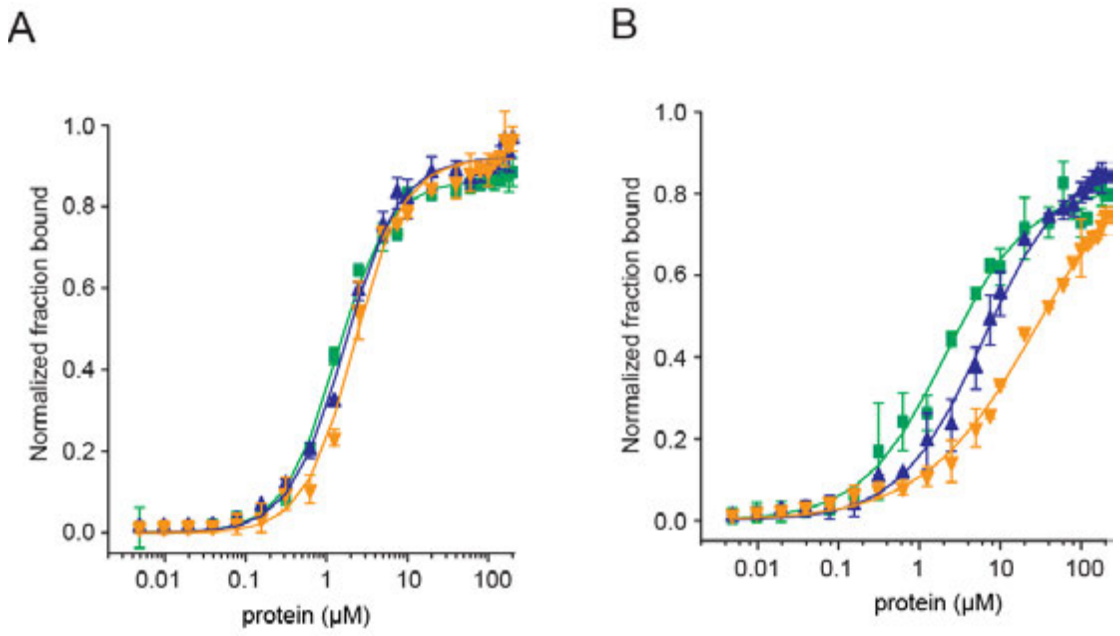

Figure 4-11. MARV VP35 IID is insensitive to overhangs in dsRNA, unlike EBOV.

Binding curves from dot blot assays for MARV VP35 IID (A) and ZEBOV VP35 IID (B) with 25bp blunt- end dsRNA (green squares), 25bp 5'overhang dsRNA (blue triangles) and 25bp 3' overhang dsRNA (orange inverted triangles). Error bars represent s.d. from two independent experiments.

with 3 and 15 fold lower affinity than blunt end dsRNA respectively (K_D of 6.16μM for 5' overhang dsRNA and K_D of 30.12μM for 3' overhang dsRNA) (Figure 4-11B). This data is consistent with our structures of ZEBOV VP35-dsRNA and MARV VP35-dsRNA complexes and suggests that MARV VP35, unlike ZEBOV VP35 does not recognize the dsRNA ends and binds only along the backbone. The dsRNA in the crystallographic unit cell is stacked coaxially in an end-to-end fashion forming a contiguous series of helices, coated by MARV VP35 IID molecules along its backbone, resembling beads on a string. This mode of RNA binding is unique and has not been observed with the EBOV VP35 proteins.

4.5 Filoviral VP35 differentially inhibits RIG-I and MDA5 ATPase activity

The absence of end-capping interactions and beads on a string model of RNA binding led us to hypothesize that our structure may have uncovered a novel mechanism MARV VP35 may employ as an immune evasion strategy, which is distinct from the mechanism we had proposed for ZEBOV VP35. This mode of binding may allow MARV VP35 to antagonize MDA5, the other key member of the RIG-I like receptor family of proteins involved in RNA sensing in the host cell. MDA5 has been long known to be activated by long dsRNA molecules including poly I:C and has been implicated in innate immune activation when host cells are infected by viruses with long RNA genomes(Kato et al, 2006). Recently, MDA5 has been shown to form filament-like structures by cooperative assembly on long dsRNA(Berke & Modis, 2012; Peisley et al, 2011).

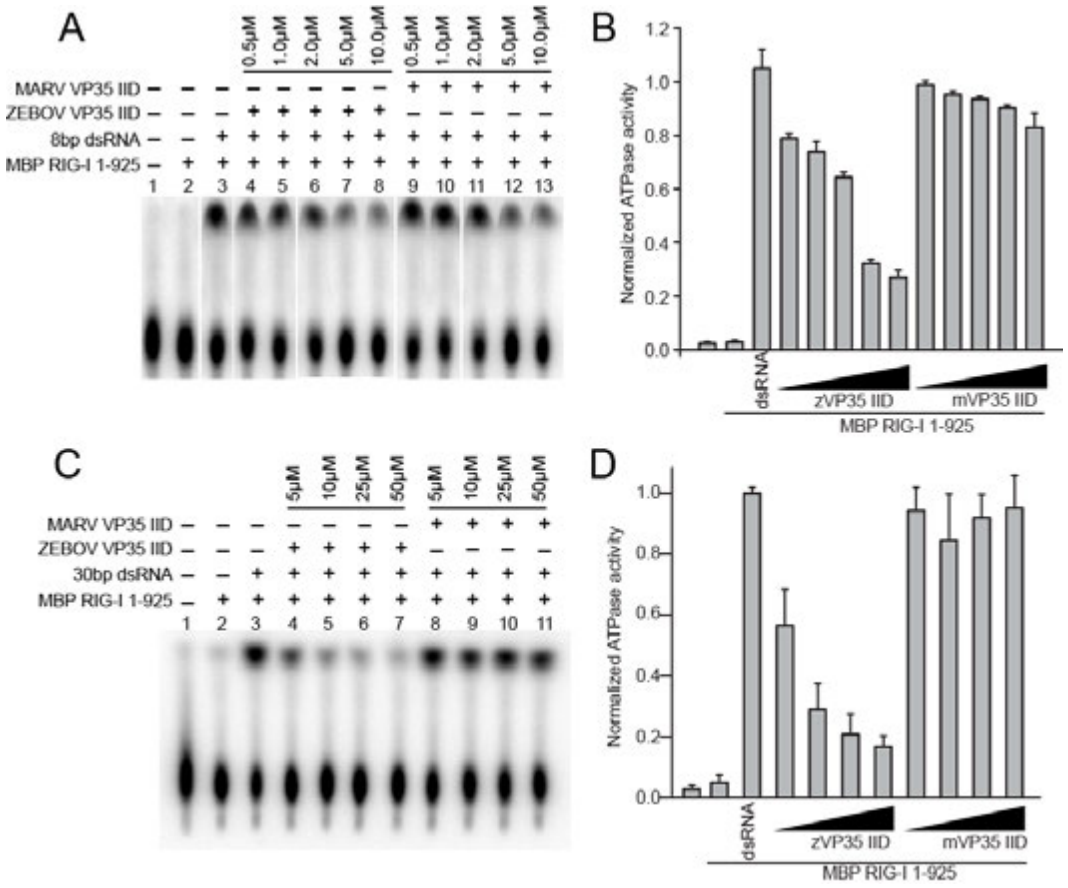

Figure 4-12. MARV VP35 IID cannot inhibit dsRNA activation of RIG-I.

The effect of 8 and 30 bp dsRNA and VP35 on ATPase activities of RIG-I and MDA5 were assessed by TLC. (A) 8 bp dsRNA and (C) 30bp dsRNA were used to activate RIG-I ATPase activity (lane 3). Zaire EBOV VP35 IID (lanes 4-7 in A and lanes 4-8 in C) and MARV VP35 IID (lanes 8-11 in A and lanes 9-13 in C) were tested for their abilities to inhibit RIG-I ATPase activity by these dsRNAs. The free inorganic phosphate in each lane (figure A and C) was quantified, normalized to lane 3 and plotted as normalized ATPase activity in figures B and D. Error bars represent standard deviation from two separate experiments.

MARV VP35 may be able to effectively compete with MDA5 and prevent such filament assembly, thus inhibiting important signaling events through MDA5 resulting in inhibition of IFN production. Because MARV VP35 does not bind short dsRNA ligands and cannot recognize the RNA ends, we hypothesize that MARV VP35 likely does not inhibit dsRNA mediated RIG-I activation. We have previously shown that ZEBOV VP35 interacts with the dsRNA backbone as well as the ends mimic the host receptor RIG-I's binding mode to dsRNA. Our structural and biochemical evidence suggests that MARV VP35 binds dsRNA in a manner that resembles MDA5 recognition of long dsRNA and poly I:C. This led us to hypothesize that MARV VP35 may be able to inhibit MDA5 activation and innate immune signaling by poly I:C. In order to test this hypothesis, we used thin layer chromatography assays to assess the ATPase activity of RIG-I and MDA5 proteins in the presence of activating ligands such as dsRNA and poly I:C. Our findings show that RIG-I ATPase activity is strongly activated by dsRNA, and this dsRNA mediated activation can be inhibited by ZEBOV VP35 IID in a dose dependent manner. In contrast, MARV VP35 IID is unable to inhibit dsRNA mediated RIG-I ATPase activity, which is consistent with our structural and biochemical data. Because MARV VP35 does not bind the blunt ends of the dsRNA, it is unable to compete with RIG-I, and hence unable to inhibit the ATPase activity. On the other hand, ZEBOV VP35 is able to outcompete RIG-I for dsRNA binding and thus inhibit ATPase activity. We tested the ATPase activity of MDA5 using the same assay. Consistent with previous findings, our studies show that poly I:C is able to activate the ATPase activity of MDA5. In contrast to RIG-I, both ZEBOV and MARV VP35 can inhibit poly I:C mediated activation of MDA5, validating our structural and biochemical data.

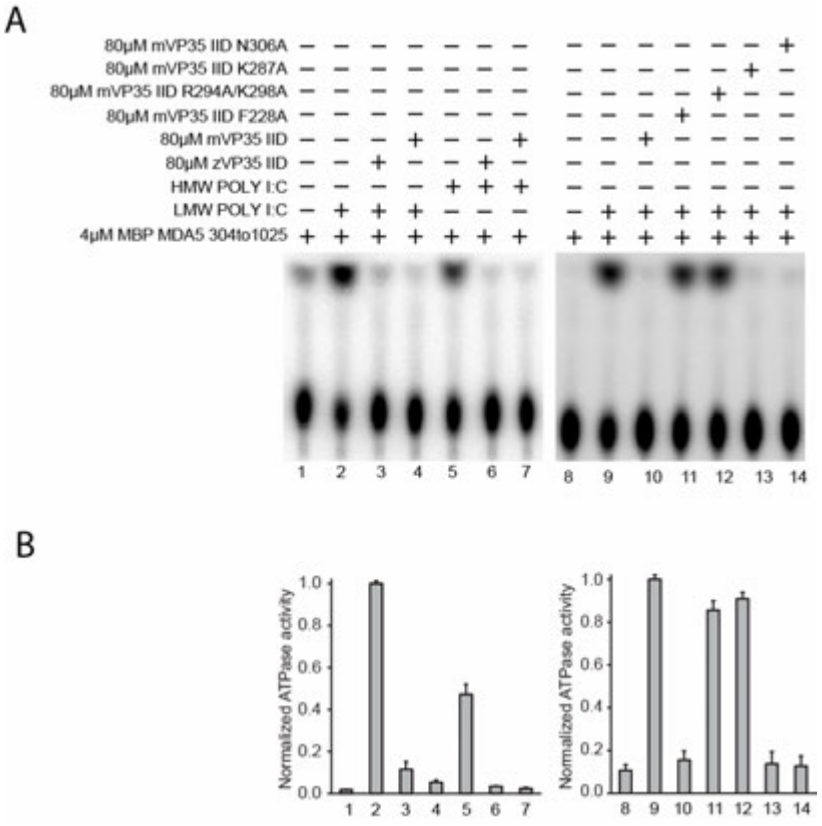

Figure 4-13. MARV VP35 is able to inhibit activation of MDA5 by poly I:C.

(A) ATPase activity of MDA5 was assessed by TLC using low-molecular weight (LMW) (lane 2) and high-molecular weight (HMW) (lane 5). Both Zaire EBOV VP35 IID (lanes 3 and 6) and MARV VP35 IID (lanes 4 and 7) were tested for their abilities to inhibit RIG-I ATPase activity by poly I:C. MARV VP35 IID mutants such as R924A/K298A (lane 11), F228A (lane 12),K287A (lane 13), and N306A (lane 14) were tested for their abilities to inhibit MDA5 activation by poly I:C. The quantitated ATPase activity, normalized to lane 2 is plotted in F. (B) The free inorganic phosphate in each lane was quantified, normalized to RIG-I activation by LMW poly I:C (lanes 2 and 9) and plotted as normalized ATPase activity. Error bars represent standard deviation from two separate experiments.

These results show that the mode of dsRNA binding by the filoviral VP35 proteins may play a role in differentially inhibition of the RIG-I like receptors. Together our data support a model in which ZEBOV and MARV VP35inhibit the production of type I IFN by hiding viral RNA from being recognized by these critical host pattern recognition receptors.

4.6 Disruption of VP35-dsRNA interactions in vitro results in attenuated IFN inhibition *in vivo*

We carried out filter binding assays to assess the RNA binding ability of wildtype and mutant MARV VP35 IID proteins. While WT MARV VP35 IID binds dsRNA with high affinity, filter binding data shows that alanine substitution of basic residues R301, K328, R294, K298 and S299 all resulted in diminished RNA binding (Figure 4-8), consistent with the interactions observed in the structure. Double mutations of residues R294/K298 and K298/S299 to alanine completely abolished dsRNA binding, suggesting a critical role for these residues (Figure 4-8). In addition, mutation of residues F228. N261 and Q263 to alanine, also resulted in diminished RNA binding. Poly I:C pulldowns of WT and mutant MARV VP35 proteins which were consistent with the filter binding assays and corroborated the role of these residues in dsRNA binding as observed in the structure.

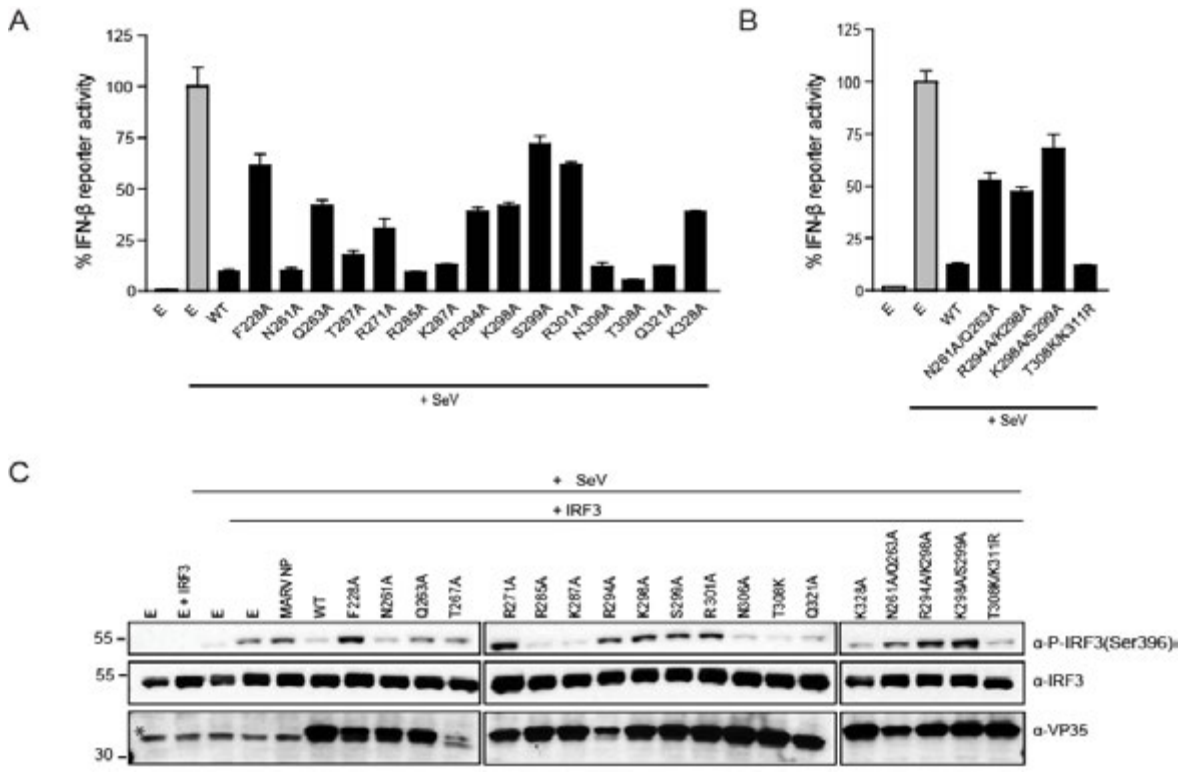

Figure 4-14. Mutations of residues involved in dsRNA binding in MARV VP35 IID attenuate IFN- β inhibition and IRF-3 phosphorylation.

(A) and (B) The IFN-β promoter activity induced by SeV infection of 293T cells transfected with either WT or mutant MARV VP35 proteins (black bars) were normalized relative to the empty vector control (gray bars). Error bars represent standard error of the mean for triplicate experiments. (C) Western blot analysis of the IRF3 phosphorylation state in 293T cells after SeV activation of the IFN-β promoter using anti-phospho IRF3 (top panel) and anti-IRF3 (middle panel) antibodies. The bottom panel is the expression of the different MARV VP35 mutants using monoclonal anti-MARV VP35 IID antibody. MARV NP was used as a negative control. E refers to empty vector transfection control. The * indicates a non-specific band.

In contrast, alanine substitutions of residues such as R285, K287, N306 and Q321 which are involved in protein-protein interactions in the crystal structure, did not have an impact on RNA binding in both the filter binding as well as the poly I:C pull-downexperiments (Figure 4-8), suggesting that these contacts are more likely formed in the context of crystal packing.

Previous studies with ZEBOV VP35 have shown that one of the key mechanisms underlying ZEBOV's ability to suppress IFN-β production is through inhibition of IRF-3 and IRF-7 phosphorylation by the IFN kinases IKK-ε and TBK-1. In order to test whether MARV VP35 employs a similar strategy, our collaborators tested the phosphorylation states of IRF-3 in 293T cells upon SeV activation. Similar to ZEBOV, MARV VP35 also inhibits IRF-3 phosphorylation. Mutations that result in loss of dsRNA binding also result in diminished ability to inhibit IRF-3 phosphorylation. In addition, MARV VP35 is also able to block IFN-β promoter activity upon overexpression of IKK-ε or TBK-1 in 293T cells. In contrast, when IRF-3 5D, a constitutively active form of IRF-3, is overexpressed in 293T cells, MARV VP35 is unable to inhibit the IFN-β promoter activity, suggesting that the inhibitory effect of MARV VP35 is upstream of IRF-3 phosphorylation and activation.

In order to assess the effect of these mutations on IFN inhibitory functions of VP35 *in vivo,* our collaborators used an IFN-β reporter assay, in which we transfected plasmids encoding either WT or mutant VP35 proteins into 293T cells, and monitored reporter activity induced by Sendai virus (SeV) infection. These results suggest that the mutation of residues that abrogate RNA binding *in vitro* also diminish VP35's role as an IFN antagonist *in vivo*.

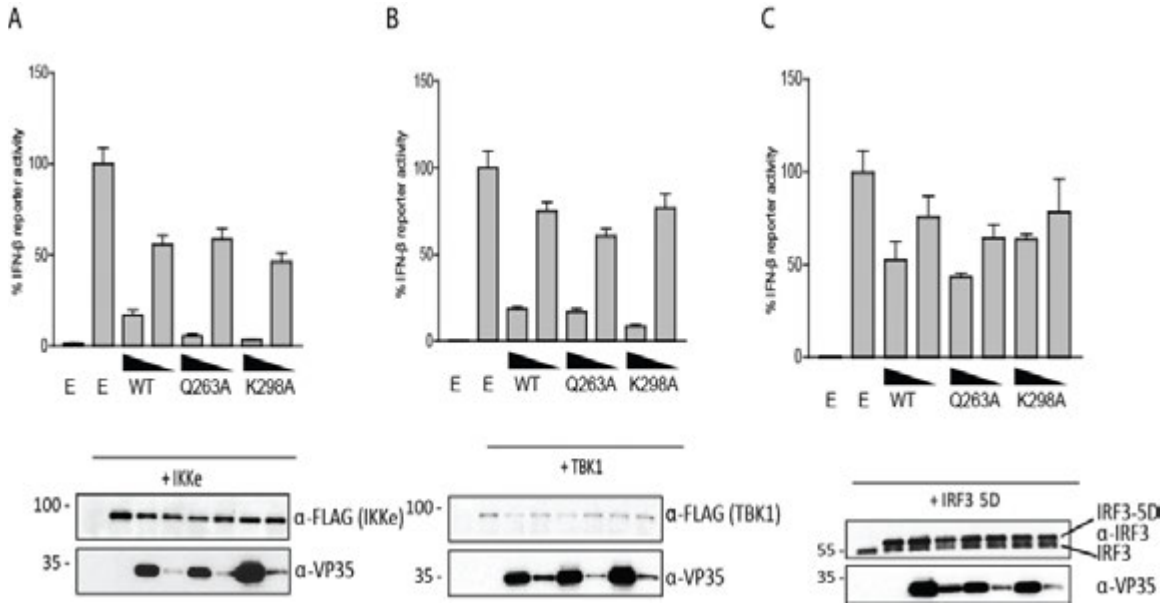

Figure 4-15. RNA-independent mechanism of immune evasion by MARV VP35.

IFN-β promoter activity of WT or mutant MARV VP35 proteins in 293T cells induced by overexpression of (A) FLAG-IKKe, (B) FLAG-TBK-1 or (C) constitutively active IRF3-5D constructs. The promoter activity was normalized to the empty vector control denoted as E. Error bars represent standard error of the mean for triplicate experiments. Western blot analysis of the protein expression levels were detected using anti-FLAG M2, anti-IRF3 and anti-MARV VP35 IID antibodies. Endogenous IRF-3 can be distinguished from IRF3-5D by the difference in migration on SDS gels (indicated by lines on lower panel of C).

In the case of ZEBOV VP35, mutations such as R312A, K339A, K319A/R322A were able to attenuate VP35's ability to inhibit SeV mediated IFN-β promoter activity, whereas mutation of residues in the FBP such as R222A, R225A, K248A and R251A do not have any effect on VP35 in this assay.

In the case of MARV VP35, the double-mutants R294A/K298A, K298A/S299A and N261/Q263 completely suppress VP35's ability to suppress IFN-β activation, followed by the point mutants R301A, K298A, K328A, S299A and F228A, which also show diminished IFN-β suppression relative to WT protein. In contrast R285A, K287A, N306A and Q321A mutants performed as well as WT in this assay, suggesting a strong correlation between dsRNA binding and IFN inhibitory functions of VP35.

4.7 Conclusions

Here we provide data to support a model that suggests that the dsRNA-binding mode of filoviral VP35 has a direct impact on its ability to antagonize the RIG-I like receptors. Using the ATPase activity of RIG-I and MDA5 (estimated by thin-layer chromatography) as an indicator of the functionally active state of the molecules, we tested the effect of both ZEBOV and MARV VP35 on RIG-I and MDA5. Our data show that short dsRNA is able to activate ATPase activity of RIG-I, while poly I:C activates MDA5. Only ZEBOV VP35 is able to inhibit dsRNA-mediated ATPase activity in a dose-dependent manner while MARV VP35 cannot. We show that this is directly correlated to the ability of ZEBOV VP35 to

compete with RIG-I for binding dsRNA backbone and blunt ends, because mutation of residues such as R312, F239, K319 and R322 abrogates ZEBOV VP35's ability to inhibit RIG-I. MARV VP35 does not interact with blunt ends of dsRNA; it is unable to inhibit RIG-I in this assay. In contrast, both MARV and ZEBOV VP35 can inhibit poly I:C mediated activation of MDA5, suggesting that while MARV cannot compete with RIG-I for dsRNA binding, it is able to compete with MDA5 (Table 4-2). This may be a key difference between the dsRNA-dependent immune evasion strategies employed by ZEBOV and MARV VP35. Our data provides a structural and functional basis for the observed lack of binding to short dsRNA binding by MARV VP35 and its inability to distinguish between blunt end and overhang containing dsRNA (Figure 4-16). It is interesting to note that although ZEBOV and MARV may exhibit the said differences in dsRNA-dependent mechanism of immune evasion, both proteins are able to inhibit the type I IFN pathway using a common RNA-independent mechanism by inhibiting TBK-1 and IKK-ε mediated phosphorylation of IRF-3/7 (Figure 4-16). This is another example of the structural plasticity of VP35 where the same fold results in distinct RNA binding modes but may mediate similar protein-protein interactions with the IFN kinases. Taken together our data have identified some potential differences and similarities in the immune evasion strategies of ZEBOV and MARV VP35. Further investigation is needed to evaluate the impact of these differences on pathogenesis and disease outcome. The identification of common and distinct structural features of filoviral immune antagonists is key for the rational design of therapeutics that can target both EBOV and MARV.

Table 4-2. Biochemical and structural differences between MARV and EBOV VP35 proteins, which are important for immune evasion mechanisms.

EBOV VP35 IID-dsRNA complex	MARV VP35 IID-dsRNA complex
STRUCUTAL DIFFERENCES	
Central basic patch residues such as R312, K319 and R322 are involved in dsRNA binding and protein-protein interactions	Central basic patch residues involved only in protein-dsRNA interactions. Protein-protein interactions are through distinct residues such as R285, K287, N306 and Q321.
Residues K319 and R322 in CBP are very important for both dsRNA binding and protein-protein interactions	Corresponding residues T308 and K311 are solvent exposed and don't make any contacts
F239, I340 and Q274 are involved in dsRNA end-capping interactions	Corresponding residues F228, I329 and Q263 are involved in dsRNA backbone contacts
BIOCHEMICAL DIFFERNCES	
Binds 8bp dsRNA.	Does not bind 8 bp dsRNA.
Binds to 18bp and 30bp dsRNA with similar affinities	Binds 30bp dsRNA with 3-fold higher affinity than 18bp dsRNA
Binds blunt-end dsRNA with 3-fold and 15-fold higher affinity than 5' and 3' overhang dsRNA	Binds blunt-end, 5'overhang and 3' overhang containing dsRNA with similar affinites
Can inhibit RIG-I ATPase activation by 8 and 30bp dsRNA by binding to blunt-end PAMPs	Cannot inhibit RIG-I ATPase activation by 8 and 30bp dsRNA since it cannot bind to blunt-end PAMPs
Can inhibit RIG-I ATPase activation by 5' and 3' overhang containing dsRNA by binding to dsRNA PAMPS	Can inhibit RIG-I ATPase activation by 5' and 3' overhang containing dsRNA by binding to dsRNA PAMPS
Can inhibit MDA5 ATPase activation by polyI:C, by binding to dsRNA PAMPs	Can inhibit MDA5 ATPase activation by polyI:C, by binding to dsRNA PAMPs
Inhibits IRF-3 phosphorylation by directly interacting with IKK-e and TBK-1 through CBP residues	Inhibits IRF-3 phosphorylation by unknown mechanism mediated by different set of residues from CBP.

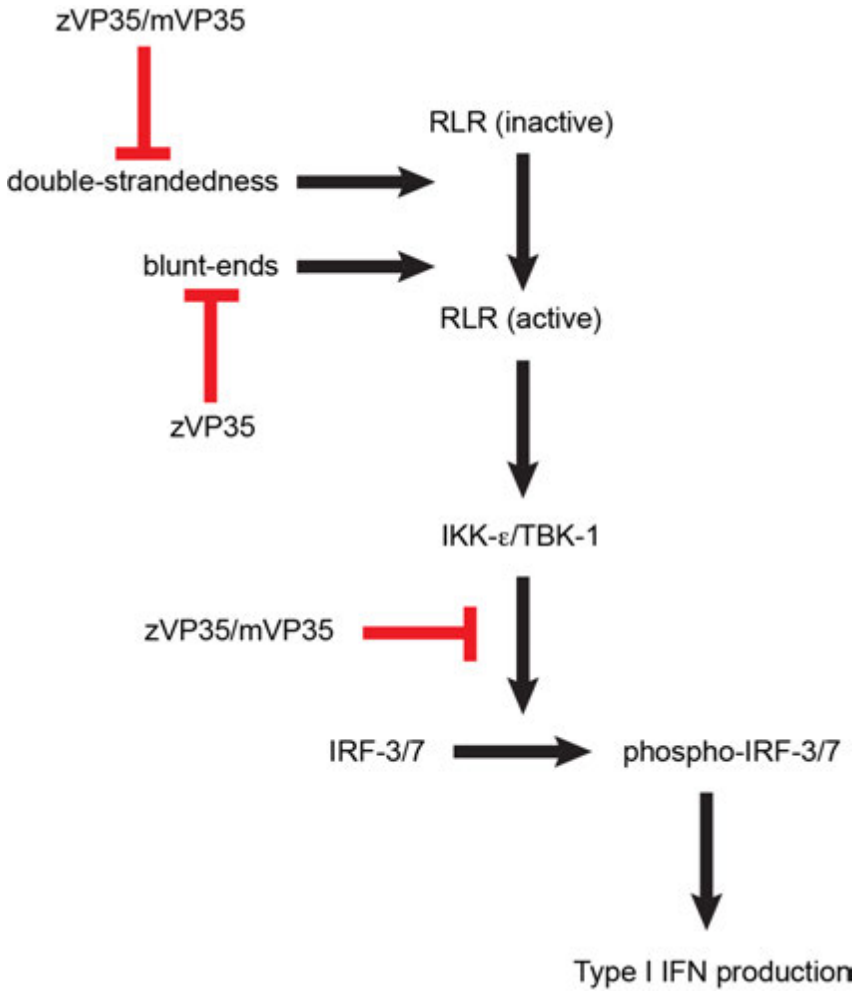

Figure 4-16. Model for filoviral VP35 mediated immune evasion.

Both ZEBOV and MARV VP35 inhibit recognition of double-strandedness PAMP by RIG-I like receptors by sequestration of RNA ligands. In contrast, only ZEBOV VP35 can inhibit blunt-end PAMP recognition by RIG-I like receptors. Both ZEBOV and MARV VP35 can inhibit type I IFN production in RNA-independent mechanism by inhibiting the IFN kinases from phosphorylation of downstream IRF-3/7 transcription factors.

4.8. References

Berke IC, Modis Y (2012) MDA5 cooperatively forms dimers and ATP-sensitive filaments upon binding double-stranded RNA. *EMBO Journal* **31:** 1714-1726

Enterlein S, Schmidt KM, Schumann M, Conrad D, Krahling V, Olejnik J, Muhlberger E (2009) The marburg virus 3' noncoding region structurally and functionally differs from that of ebola virus. *Journal of Virology* **83:** 4508-4519

Gear JS, Cassel GA, Gear AJ, Trappler B, Clausen L, Meyers AM, Kew MC, Bothwell TH, Sher R, Miller GB, Schneider J, Koornhof HJ, Gomperts ED, Isaacson M, Gear JH (1975) Outbreake of Marburg virus disease in Johannesburg. *British Medical Journal* **4:** 489-493

Kato H, Takeuchi O, Sato S, Yoneyama M, Yamamoto M, Matsui K, Uematsu S, Jung A, Kawai T, Ishii KJ, Yamaguchi O, Otsu K, Tsujimura T, Koh CS, Reis e Sousa C, Matsuura Y, Fujita T, Akira S (2006) Differential roles of MDA5 and RIG-I helicases in the recognition of RNA viruses. *Nature* **441:** 101-105

Kimberlin CR, Bornholdt ZA, Li S, Woods VL, Jr., MacRae IJ, Saphire EO (2010) Ebolavirus VP35 uses a bimodal strategy to bind dsRNA for innate immune suppression. *Proc Natl Acad Sci U S A* **107:** 314-319

Leung DW, Ginder ND, Fulton DB, Nix J, Basler CF, Honzatko RB, Amarasinghe GK (2009) Structure of the Ebola VP35 interferon inhibitory domain. *Proc Natl Acad Sci U S A* **106:** 411-416

Leung DW, Prins KC, Basler CF, Amarasinghe GK (2010a) Ebolavirus VP35 is a multifunctional virulence factor. *Virulence* **1:** 526-531

Leung DW, Prins KC, Borek DM, Farahbakhsh M, Tufariello JM, Ramanan P, Nix JC, Helgeson LA, Otwinowski Z, Honzatko RB, Basler CF, Amarasinghe GK (2010b) Structural basis for dsRNA recognition and interferon antagonism by Ebola VP35. *Nature Structural & Molecular Biology* **17:** 165-172

Leung DW, Shabman RS, Farahbakhsh M, Prins KC, Borek DM, Wang T, Muhlberger E, Basler CF, Amarasinghe GK (2010c) Structural and Functional Characterization of Reston Ebola Virus VP35 Interferon Inhibitory Domain. *J Mol Biol*

Moller P, Pariente N, Klenk HD, Becker S (2005) Homo-oligomerization of Marburgvirus VP35 is essential for its function in replication and transcription. *Journal of Virology* **79:** 14876-14886

Muhlberger E, Lotfering B, Klenk HD, Becker S (1998) Three of the four nucleocapsid proteins of Marburg virus, NP, VP35, and L, are sufficient to mediate replication and

transcription of Marburg virus-specific monocistronic minigenomes. *Journal of Virology* **72:** 8756-8764

Muhlberger E, Weik M, Volchkov VE, Klenk HD, Becker S (1999) Comparison of the transcription and replication strategies of marburg virus and Ebola virus by using artificial replication systems. *Journal of Virology* **73:** 2333-2342

Peisley A, Lin C, Wu B, Orme-Johnson M, Liu M, Walz T, Hur S (2011) Cooperative assembly and dynamic disassembly of MDA5 filaments for viral dsRNA recognition. *Proc Natl Acad Sci U S A* **108:** 21010-21015

Prins KC, Binning JM, Shabman RS, Leung DW, Amarasinghe GK, Basler CF (2010a) Basic residues within the ebolavirus VP35 protein are required for its viral polymerase cofactor function. *J Virol* **84:** 10581-10591

Prins KC, Cardenas WB, Basler CF (2009) Ebola virus protein VP35 impairs the function of interferon regulatory factor-activating kinases IKKepsilon and TBK-1. *J Virol* **83:** 3069-3077

Prins KC, Delpeut S, Leung DW, Reynard O, Volchkova VA, Reid SP, Ramanan P, Cardenas WB, Amarasinghe GK, Volchkov VE, Basler CF (2010b) Mutations abrogating VP35 interaction with double-stranded RNA render Ebola virus avirulent in guinea pigs. *J Virol* **84:** 3004-3015

Reid SP, Cardenas WB, Basler CF (2005) Homo-oligomerization facilitates the interferon-antagonist activity of the ebolavirus VP35 protein. *Virology* **341:** 179-189

Sanchez A, Kiley MP, Holloway BP, Auperin DD (1993) Sequence analysis of the Ebola virus genome: organization, genetic elements, and comparison with the genome of Marburg virus. *Virus Res* **29:** 215-240

Schumann M, Gantke T, Muhlberger E (2009) Ebola virus VP35 antagonizes PKR activity through its C-terminal interferon inhibitory domain. *J Virol* **83:** 8993-8997

Towner JS, Khristova ML, Sealy TK, Vincent MJ, Erickson BR, Bawiec DA, Hartman AL, Comer JA, Zaki SR, Stroher U, Gomes da Silva F, del Castillo F, Rollin PE, Ksiazek TG, Nichol ST (2006) Marburgvirus genomics and association with a large hemorrhagic fever outbreak in Angola. *Journal of Virology* **80:** 6497-6516

Valmas C, Grosch MN, Schumann M, Olejnik J, Martinez O, Best SM, Krahling V, Basler CF, Muhlberger E (2010) Marburg virus evades interferon responses by a mechanism distinct from ebola virus. *PLoS Pathog* **6:** e1000721

CHAPTER 5. CONCLUSIONS

Viruses are obligate parasites and are completely dependent on host cells for viral protein production and replication. A multitude of factors determine the outcome of viral infection. One of the important factors is the ability of the host cell to mount an effective and potent innate immune response, which is the first line of defense against any pathogen. Viruses encode proteins that hijack host cell machinery and reprogram cellular pathways to aid viral replication. To do this, viruses must first escape detection by the specialized proteins in the host cell, whose specific function is to detect and counter viruses and other pathogens. Viral proteins achieve this by multiple mechanisms that target various components of the host immune responses. Viral replication occurs at an extremely rapid pace compared to hosts, and viral polymerases are highly prone to errors during viral genome replication. The high frequency of mutations confers a probabilistic advantage in adapting to host immune defenses. Given this rapid rate of replication and mutation, viral proteins are more likely to sample beneficial mutations that allow it to evade host immune responses. Hence studying host-virus interactions is a challenging and interesting area of research due to the dynamic nature of the processes involved, in which viral components constantly evolve strategies to subvert the host defense mechanisms in order to successfully replicate, while immune components of host constantly adapt to the new challenges posed by pathogens in order to ensure the survival of the host and clear the virus.

Filoviruses are among the deadliest viruses that cause severe disease in humans, and currently there are no approved treatments for filoviral infections. The severe pathogenesis associated with filoviral infections has been attributed to the early and effective shut down of host innate immune responses, which also results in impaired adaptive immune responses. The fact that filoviruses encodes only seven proteins, which perform multiple functions can be taken advantage of, because it allows us to focus our attention on a few critical proteins that the virus is absolutely dependent on for survival in host cells. High-resolution structural information of viral proteins is absolutely critical for understanding the role of specific residues in immune evasion and other functions that aid viral replication. These studies can contribute to our fundamental understanding of protein structure and function, specifically how one protein fold has evolved to perform multiple, completely unrelated functions. This can be attributed to the plasticity of the protein structure and the conformational ensembles it can sample over time and space, based on the effect of external factors such as temperature, pH, ligands such as small molecules, other proteins and nucleic acids. Among the filoviral proteins that function as immune antagonists, VP35 is one of the key virulence factors that have been shown to inhibit host innate immune responses through its interactions with dsRNA and a variety of host proteins. Additionally VP35 plays a role as a structural protein and a co-factor in the viral polymerase complex. Recent studies focused on understanding VP35 mediated immune evasion have been predominantly done using EBOV VP35. Prior to this study, there was limited structural, biochemical or cell biological data showing the functions of MARV VP35.

In this study, we provide evidence to support a novel mechanism by which MARV VP35 protein mediates suppression of the host innate immune responses. We provide structural and biochemical evidence to highlight the differences between EBOV and MARV VP35 in their dsRNA binding characteristics. First, we show that MARV VP35 binds to dsRNA in a length dependent manner. Second, we show that MARV VP35 does not recognize the blunt-ends of dsRNA, unlike EBOV VP35. Using enzymatic assays, we show that MARV VP35 cannot prevent the dsRNA-mediated activation of RIG-I, the host receptor that recognizes both the double-strandedness and the blunt-end features of RNA. In contrast, MARV VP35 is able to inhibit poly I:C mediated activation of MDA5, another host receptor that recognizes only the double-strandedness of RNA. In contrast EBOV VP35 can inhibit both RIG-I and MDA5 due to its ability to bind both blunt-ends and double-stranded regions of RNA. Although the molecular details leading to the differences observed in the RNA binding characteristics of MARV and EBOV VP35 are still not completely understood, our work has identified differences in amino acids at key positions involved in both protein-protein and protein-dsRNA interactions that likely contribute to these differences. In addition to the RNA-dependent mechanism, we also provide evidence showing that both MARV and EBOV VP35 can also inhibit host innate immune responses using an RNA-independent mechanism, by inhibiting IRF-3 phosphorylation by the IFN kinases IKK-ε and TBK-1. In summary this work not only provides an additional structural target for development of antiviral therapies, but also gives new insights into the differences and similarities in mechanisms of MARV and EBOV VP35 mediated immune evasion.

ACKNOWLEDGEMENTS

I would like to thank my mentors Dr. Gaya Amarasinghe and Dr. Daisy Leung for the opportunity to conduct research in an exciting area of research and for creating a great learning environment in the lab. I will be always indebted to them for being approachable and available at all times to answer my every question with patience and understanding. I would like to thank them for challenging me constantly to become a better scientist and colleague. I would like to thank my undergraduate mentors Dr. T. Ramasami, Dr. B. Madhan and Dr. M.R.S. Sridharan for their kind support, guidance and for leading my way into graduate school. I would like to thank my mates in lab especially Mina Farahbakhsh, Craig Brown, Jennifer Binning, Dayna Peterson, Luke Helgeson, Alisha Stubbs, Dr. Tianjiao Wang, Juyoung Huh, Dr. Gai Liu and Dr. Wei Xu. They have all contributed to my research in many different ways and made the lab such a fun place to be. I would like to thank my parents Mr. K.S. Ramanan and Mrs. Suseela Ramanan, my sister Mrs. Chitra Sriram and my uncle Mr. K.S. Padmanabhan for being a constant source of love, strength and happiness. I would like to thank my wife Ms. Anusha Sethuraman for all the love and support during my graduate studies and for making me a better person. I would like to thank my dearest friends Mr. Karthik Thyagarajan, Mr. Arun Ravindran, Mr. Prasanna Sankaran, Mr. Suresh Kannan, Mr. Siddharth Sridhar, Mr. Aditya Ashok, Mr. Sethu Bharath, Mr. Dhanraj Selvaraj, Mr. Sriram Nagarajan, Mr. Aravind Balakrishnan, Mr. Karthik Babu, Miss. Nandini Ramaswamy, Miss. Suganthi Selvaraj, Mr. Bala Padmanabhan, Mr. Koushik Badri, and

Miss. Kavitha Padmanabhan for all the love and happiness they have given me and for making my experiences in graduate school infinitely more joyful and fun.